

## STATUS OF THESIS

Title of thesis

Experimental Investigation of Gas Diffusivity in Reservoir Fluid at Elevated Pressure for Malaysian Oilfield

I SUZALINA BINTI ZAINAL

hereby allow my thesis to be placed at the Information Resource Center (IRC) of Universiti Teknologi PETRONAS (UTP) with the following conditions:

1. The thesis becomes the property of UTP
2. The IRC of UTP may make copies of the thesis for academic purposes only
3. This thesis is classified as

Confidential

Non-confidential

If the thesis is confidential, please state the reason:

---

---

---

The contents of the thesis will remain confidential for \_\_\_\_\_ years.

Remarks on disclosure:

The contents or any part of the thesis should not be copied or published by anyone without the written permission by the author.

Endorsed by

\_\_\_\_\_  
Signature of Author

\_\_\_\_\_  
Signature of Supervisor

Permanent address:

No. 22, Jalan SM5,  
Taman Sunway Batu Caves,  
68100 Batu Caves, Selangor

Name of Supervisor

Assoc. Prof. Dr. Ismail M. Saaid

Date: \_\_\_\_\_

Date: \_\_\_\_\_

UNIVERSITI TEKNOLOGI PETRONAS

EXPERIMENTAL INVESTIGATION OF GAS DIFFUSIVITY IN RESERVOIR

FLUID AT ELEVATED PRESSURE FOR MALAYSIAN OILFIELD

by

SUZALINA BINTI ZAINAL

The undersigned certify that they have read, and recommend to the Postgraduate Studies Programme for acceptance this thesis for the fulfillment of the requirements for the degree stated.

Signature: \_\_\_\_\_

Main Supervisor: Assoc. Prof. Dr Ismail M. Saaid \_\_\_\_\_

Signature: \_\_\_\_\_

Co-Supervisor: \_\_\_\_\_

Signature: \_\_\_\_\_

Head of Department: Assoc. Prof. Dr Ismail M. Saaid \_\_\_\_\_

Date: \_\_\_\_\_

EXPERIMENTAL INVESTIGATION OF GAS DIFFUSIVITY IN RESERVOIR  
FLUID AT ELEVATED PRESSURE FOR MALAYSIAN OILFIELD

by

SUZALINA BINTI ZAINAL

A Thesis

Submitted to the Postgraduate Studies Programme

as a Requirement for the Degree of

MASTER OF SCIENCE

DEPARTMENT OF GEOSCIENCE & PETROLEUM ENGINEERING

UNIVERSITI TEKNOLOGI PETRONAS

BANDAR SERI ISKANDAR,

PERAK

SEPTEMBER 2014

## DECLARATION OF THESIS

Title of thesis

Experimental Investigation of Gas Diffusivity in Reservoir Fluid  
at Elevated Pressure for Malaysian Oilfield

I SUZALINA BINTI ZAINAL

hereby declare that the thesis is based on my original work except for quotations and citations which have been duly acknowledge. I also declare that it has not been previously or concurrently submitted for any other degree at UTP or other institutions.

Witnessed by

\_\_\_\_\_  
Signature of Author

\_\_\_\_\_  
Signature of Supervisor

Permanent address:

No.22, Jalan SM5,

Taman Sunway Batu Caves,

68100 Batu Caves, Selangor.

Name of Supervisor

Assoc. Prof. Dr. Ismail M. Saaid

Date: \_\_\_\_\_

Date: \_\_\_\_\_

## DEDICATIONS

I would like to dedicate this effort to my husband, Mohd Hafiz for his love, care, patience, encouragement and support; and also to my son, Haris Imran and daughter, Adeena Shahira, for their love and understanding without which this work could not have been accomplished. I am also especially indebted to my parents, Hjh Sopiah Idris and Hj Zainal Rahmat for their love and support.

## ACKNOWLEDGEMENTS

First of all, I thank Allah, by whose constant supply of grace I was able to labor. I would like to take this opportunity to express my deepest gratitude and appreciation to the people who have given me their assistance throughout my studies and during the preparation of this thesis. I would like to thank my supervisor, Dr Ismail M Saaid for his guidance and support and my ex-Program Head Mr Jamil Jelani for his nomination to pursue my MSc Program.

I would also like to express my sincere thanks to my mentor Puan Pauziyah Abd Hamid for her kindness, constant encouragement and support. I am also grateful to my team members, Khor, Luqman and Hon who guide and help in solving many laboratory technical challenges. I wish to also take the opportunity to thank and acknowledge the PVT technicians, Abdul Hadi, Tajudin and Asmadi; and practical student Nurul Hidayah for their continuous support and great assistance.

Acknowledgements are also extended to PETRONAS Research for approval to include some of the technical information in this research work.

## ABSTRACT

This experimental work was conducted to evaluate the suitability of a diffusion coefficient equation to describe the diffusivity of gas-liquid hydrocarbon systems for the Malaysian fluid system at elevated temperature and pressure.

Test temperature up to 90°C and test pressure up to 1719 psi was used. A high pressure PVT cell was utilized in the experiment and a number of fluid combinations including gas and crude oil samples from Malaysian oilfields were used to evaluate the correlation by Zhang *et al.* (2000).

This correlation was evaluated through the design of an experimental set-up and results validation with published values for the studies of diffusion coefficient of pure gas-water and pure gas-crude oil systems. Then, the correlation was extended to the study of gas-liquid diffusion of an actual produced gas and actual crude oil system which dealt with multicomponent gas-liquid properties. The effect of different fluid compositions, pressures and temperatures to the gas-liquid diffusivity were also investigated.

The bulk diffusion coefficients of methane-oil systems for Sumandak and Angsi were in the same order of magnitude as reported by quoted literatures. Large differences can be seen due to different oil properties, test conditions and methods used. The bulk diffusion coefficients of the produced gas (multicomponent)-oil systems for Sumandak and Angsi fluid were also in the same order of magnitude as its respective pure gas-oil systems.

The mathematical model adopted from Zhang *et al.* (2000) which was developed originally for a pure gas-oil system was found to be relevant for Malaysian light oil systems at elevated temperature and pressure test conditions. For multicomponent gas-oil system, gas resembling a pure gas state was found to be more suitable.

## ABSTRAK

Penyelidikan ini dijalankan untuk menilai kesesuaian korelasi pekali resapan untuk menggambarkan kemeresapan sistem hidrokarbon gas-cecair untuk sistem bendalir Malaysia pada suhu dan tekanan tinggi .

Suhu ujian sehingga 90°C dan tekanan ujian sehingga 1719 psi telah digunakan. Sel PVT bertekanan tinggi digunakan dalam eksperimen dan beberapa kombinasi bendalir dari sampel gas and minyak mentah dari telaga minyak Malaysia telah diuji untuk menilai korelasi oleh Zhang *et al.* (2000).

Korelasi ini telah dinilai melalui reka bentuk ujikaji dan keputusan eksperimen disahkan dengan keputusan yang telah pun diterbitkan khusus untuk penilaian pekali resapan sistem gas tulen-air dan sistem gas tulen-minyak mentah. Kemudian, korelasi telah dilanjutkan kepada kajian penyebaran sistem gas-minyak mentah di mana sampel gas dan minyak terdiri dari ciri-ciri gas dan minyak berbilang. Dalam ujikaji ini, penilaian telah dibuat mengenai kesan yang berbeza terhadap komposisi cecair, tekanan dan suhu terhadap kemeresapan gas -cecair.

Pekali resapan untuk sistem metana-minyak untuk Sumandak dan Angsi berada dalam magnitud yang sama seperti yang dilaporkan oleh kajian terdahulu. Perbezaan yang besar dapat dilihat kerana sifat minyak yang berbeza, keadaan ujian dan kaedah yang digunakan. Pekali resapan untuk sistem gas-minyak berbilang dari sampel cecair telaga minyak Sumandak dan Angsi juga berada dalam magnitud yang sama sepertimana sistem gas- minyak tulen mereka.

Model matematik yang diguna pakai dari Zhang *et al.* (2000) yang telah dibangunkan asalnya untuk sistem gas- minyak tulen didapati relevan untuk sistem gas dan minyak dari telaga minyak Malaysia pada suhu dan ujian tekanan. Bagi sistem berbilang gas-minyak, kerelevanannya terhad kepada tahap kekotoran sampel gas.



In compliance with the terms of the Copyright Act 1987 and the IP Policy of the university, the copyright of this thesis has been reassigned by the author to the legal entity of the university,

Institute of Technology PETRONAS Sdn Bhd.

Due acknowledgement shall always be made of the use of any material contained in, or derived from, this thesis.

© Suzalina Zainal, 2014

Institute of Technology PETRONAS Sdn Bhd

All rights reserved.

## TABLE OF CONTENTS

DECLARATION OF THESIS .....	iv
DEDICATIONS.....	v
ACKNOWLEDGEMENTS.....	vi
ABSTRACT .....	vii
ABSTRAK.....	viii
LIST OF TABLES .....	xiii
LIST OF FIGURES .....	xiv
LIST OF ABBREVIATIONS.....	xvii
1. INTRODUCTION.....	1
1.1 Background .....	1
1.2 Objectives of Research .....	4
1.3 Scope of Study .....	5
1.4 Thesis Organization.....	5
2. LITERATURE REVIEW .....	7
2.1 Diffusivity and Its Applications .....	7
2.1.1 Gas Injection.....	8
2.1.2 Solvent Injection and Heavy Oil Recovery .....	8
2.1.3 Gas Hydrates.....	9
2.1.4 Phase Redistribution Process.....	9
2.1.5 Transient Shut-in Model.....	10
2.2 Theories on Diffusivity .....	11
2.2.1 Mass Transfer .....	11
2.2.2 Molecular Diffusion.....	13
2.2.3 Diffusion Coefficient .....	15
2.2.4 Effect of Pressure, Temperature and Compositions .....	17
2.3 Importance of Molecular Diffusion Measurement.....	18
2.3.1 Input Parameter for Compositional Modeling .....	19
2.3.2 Input Parameter for Transient Shut-in Modeling.....	20
2.4 Reported Mathematical Model and Analysis.....	20
2.4.1 Pressure-time Profile Using PVT Cell by Riazi (1996) .....	21
2.4.2 Pressure-time Profile Using PVT Cell by Zhang <i>et al.</i> (2000).....	24
2.4.3 Volume-time Profile Using Diffusion Cell in Temperature Controlled Water Bath by Jamialahmadi <i>et al.</i> (2006).....	26

2.5	Reported Experimental Set-up.....	28
2.5.1	Diffusion Coefficient Determination from Pressure-time Data.....	28
2.5.1.1	Experimental Set-up by Riazi (1996).....	28
2.5.1.2	Experimental Set-up by Zhang <i>et al.</i> (2000) .....	30
2.5.2	Diffusion Coefficient Determination from Volume-time Data .....	31
2.5.2.1	Experimental Set-up by Jamialahmadi <i>et al.</i> (2006).....	31
2.6	Other Studies on Gas Diffusivity in Hydrocarbon Liquid .....	33
2.7	Comparison on Diffusion Coefficient for Various Binary Systems .....	33
2.8	Literature Summary .....	35
3.	RESEARCH METHODOLOGY .....	37
3.1	Experimental Approach.....	37
3.2	Test Apparatus .....	38
3.3	Test Samples.....	43
3.3.1	Types of Fluids .....	43
3.3.2	Sampling Methods.....	43
3.4	Sample Preparation .....	44
3.5	Equipment preparation .....	44
3.6	Test Procedure .....	45
3.7	Data Measurement and Acquisition .....	46
3.8	Mathematical Analysis .....	49
3.8.1	Fundamental Mathematical Model .....	49
3.8.2	Graphical Method.....	51
3.8.3	Numerical Method.....	52
3.9	Validation Methods.....	53
4.	RESULTS AND DISCUSSION.....	54
4.1	Phase 1: Diffusivity of Pure Gas-Water System.....	54
4.1.1	Carbon Dioxide -Water System .....	55
4.1.2	Methane -Water System.....	57
4.2	Phase 2: Diffusivity of Pure Gas-Actual Oil System.....	58
4.2.1	Methane-Sumandak Oil System .....	61
4.2.2	Methane-Angsi Oil System.....	66
4.2.3	Effect of Pressure .....	70
4.2.4	Effect of Temperature.....	73
4.2.5	Effect of Composition .....	74
4.3	Phase 3: Diffusivity of Multicomponent Gas-Oil System .....	76
4.3.1	Sumandak Gas – Sumandak Oil System .....	77
4.3.2	Angsi Gas – Angsi Oil System .....	81
5.	CONCLUSIONS AND RECOMMENDATIONS .....	85
5.1	Conclusions .....	85
5.2	Recommendations.....	86
	REFERENCES.....	87

APPENDIX A: SAMPLE PREPARATION, TEST PROCEDURES AND EQUIPMENT DESCRIPTION.....	92
APPENDIX B: FINDGRAPH SOFTWARE AND SAMPLE CALCULATIONS	100
APPENDIX C: DERIVATION OF MATHEMATICAL MODEL.....	107
APPENDIX D: GAS AND CRUDE OIL COMPOSITIONAL ANALYSIS .....	110

## LIST OF TABLES

Table 1.1: Comparison of results from various investigators for methane-oil system..	4
Table 2.1 : Fick’s Law equivalent forms .....	14
Table 2.2: Findings from different investigators on relationship of diffusion coefficient with pressure, temperature and viscosity .....	18
Table 2.3 : Comparison of diffusion coefficients of published studies .....	34
Table 4.1 : Published diffusion coefficients for various gas-oil systems .....	55
Table 4.2 : Comparison of CO <sub>2</sub> – water system with published values (using graphical method).....	56
Table 4.3: Comparison of CH <sub>4</sub> – water system with published values (using graphical method).....	58
Table 4.4: Comparison of equilibrium pressure for methane-Sumandak Oil System.	63
Table 4.5: Diffusion coefficient values for methane-Sumandak oil system at different pressures .....	65
Table 4.6: Comparison of equilibrium pressure for methane-Angsi oil system .....	69
Table 4.7: Diffusion coefficient values for methane-Angsi oil system at different pressures .....	69
Table 4.8: Effect of pressure on diffusion coefficient values of methane-Malaysian oil system.....	71
Table 4.9: Effect of temperature on diffusion coefficient values of methane-Sumandak oil system.....	74
Table 4.10: Effect of oil viscosity on diffusion coefficient values of methane-oil system .....	75
Table 4.11: Diffusion coefficient values for Sumandak gas-Sumandak oil system at different pressures .....	80
Table 4.12: Diffusion coefficient values for Angsi gas-oil system at different pressures .....	84

## LIST OF FIGURES

Figure 2.1: Phase redistribution after well is shut in.....	10
Figure 2.2 : Schematic of simple Nitrogen-Air diffusion process.....	13
Figure 2.3 : Schematic of a constant volume cell (Riazi, 1996).....	23
Figure 2.4 : Schematic and dimensions of diffusion process (Zhang <i>et al.</i> , 2000).....	25
Figure 2.5 : Schematic and dimensions of a constant-volume cell (Riazi, 1996) .....	29
Figure 2.6 : Schematic of a constant-volume cell (Zhang <i>et al.</i> , 2000).....	31
Figure 2.7: Schematic of a constant-volume cell (Jamialahmadi <i>et al.</i> , 2006).....	32
Figure 3.1: An overview of the PVT unit.....	38
Figure 3.2: Schematic diagram of the diffusivity test set-up.....	39
Figure 3.3: Schematic diagram of long windowed PVT cell (left) and the actual PVT window cell (right).....	40
Figure 3.4: Video camera at the back of the PVT unit.....	40
Figure 3.5: PVT cell.....	41
Figure 3.6: Gas chamber .....	42
Figure 3.7: Hand pump.....	42
Figure 3.8: Data acquisition system.....	46
Figure 3.9 : Screen shot of the pressure plot .....	47
Figure 3.10: Raw data selection using Visual Basic program.....	48
Figure 3.11: Code in Visual Basic program .....	48
Figure 3.12 : Schematic and dimension of the diffusion process model.....	49
Figure 4.1: HTGC spectrum for Sumandak crude oil (wellhead sample).....	60
Figure 4.2: Interpreted compositions of Sumandak crude oil (wellhead sample) .....	60
Figure 4.3: HTGC spectrum for Angsi crude oil (separator sample).....	60
Figure 4.4 : Interpreted compositions of Angsi crude oil (wellhead sample) .....	61
Figure 4.5: Methane-Sumandak oil pressure decay profile at different initial pressures .....	62
Figure 4.6: Semi-logarithmic plot of methane-Sumandak oil at initial pressure of 797 psi (Test 1).....	63

Figure 4.7: Semi-logarithmic plot of methane-Sumandak oil at initial pressure of 1035 psi (Test 2) .....	63
Figure 4.8: Non-linear exponential plot of methane-Sumandak oil at initial pressure of 797 psi (Test 1) ( <i>extracted from FindGraph software</i> ) .....	64
Figure 4.9: Non-linear exponential plot of methane-Sumandak oil at initial pressure of 1035 psi (Test 2) ( <i>extracted from FindGraph software</i> ) .....	64
Figure 4.10: Comparison of the diffusion coefficients of methane-Sumandak oil to published reports in terms of oil viscosity difference .....	65
Figure 4.11: Methane-Angsi oil pressure decay profile at different initial pressures .	66
Figure 4.12: Semi-logarithmic plot of methane-Angsi oil at initial pressure of 967 psi (Test 1) .....	67
Figure 4.13: Semi-logarithmic plot of methane-Angsi oil at initial pressure of 1289 psi (Test 2) .....	67
Figure 4.14: Non-linear exponential plot of methane-Angsi oil at initial pressure of 967 psi (Test 1) ( <i>extracted from FindGraph software</i> ).....	68
Figure 4.15: Non-linear exponential plot of methane-Angsi oil at initial pressure of 1289 psi (Test 2) ( <i>extracted from FindGraph software</i> ).....	68
Figure 4.16: Comparison of the diffusion coefficients of methane-Angsi oil to published reports in terms of viscosity difference .....	70
Figure 4.17: Pressure-diffusivity plot extracted from published report by Riazi (1996) on methane-n-pentane system at 37.8°C .....	72
Figure 4.18: Pressure-diffusivity plot extracted from published report by Nguyen and Farouq Ali (1995) for carbon dioxide-oil and methane-oil systems at 57.1°C.....	72
Figure 4.19: Pressure-diffusivity plot extracted from published report by Jamialahmadi <i>et al.</i> (2006) for methane-dodecane systems at 45°C, 65°C and 81°C .....	73
Figure 4.20: Viscosity-Diffusivity relationship of Sumandak and Angsi methane-oil systems .....	75
Figure 4.21: Compositions of Sumandak gas (wellhead sample) .....	76
Figure 4.22: Compositions of Angsi gas (separator sample) .....	76
Figure 4.23: Sumandak gas-Sumandak oil pressure decay profile at different initial pressures .....	77

Figure 4.24: Semi-logarithmic plot of Sumandak gas-Sumandak oil at initial pressure of 868 psi (Test 1).....	78
Figure 4.25: Semi-logarithmic plot of Sumandak gas-Sumandak oil at initial pressure of 1092 psi (Test 2).....	78
Figure 4.26: Non-linear exponential plot of Sumandak gas-Sumandak oil at initial pressure of 868 psi (Test 1) ( <i>extracted from FindGraph software</i> ) .....	79
Figure 4.27: Non-linear exponential plot of Sumandak gas-Sumandak oil at initial pressure of 1092 psi (Test 2) ( <i>extracted from FindGraph software</i> ) .....	79
Figure 4.28: Effect of gas molecular weight to diffusivity on Sumandak gas-oil system .....	80
Figure 4.29: Angsi gas-Angsi oil pressure decay profile at different initial pressures	82
Figure 4.30: Semi-logarithmic plot of Angsi gas-Angsi oil at initial pressure of 1571 psi (Test 1) .....	82
Figure 4.31: Semi-logarithmic plot of Angsi gas-Angsi oil at initial pressure of 1719 psi (Test 2) .....	82
Figure 4.32: Non-linear exponential plot of Angsi gas-Angsi oil at initial pressure of 1571 psi (Test 1) ( <i>extracted from FindGraph software</i> ) .....	83
Figure 4.33: Non-linear exponential plot of Angsi gas-Angsi oil at initial pressure of 1719 psi (Test 2) ( <i>extracted from FindGraph software</i> ) .....	83



## LIST OF ABBREVIATIONS

$A$	Cross-sectional area of the cell ( $\text{cm}^2$ )
AAPE	Average Absolute Percentage Error
$\text{CO}_2$	Carbon dioxide
$\text{CH}_4$	Methane
Cr	Chromium
$D_{AB}$	diffusion coefficient ( $\text{m}^2/\text{s}$ )
HTGC	High Temperature Gas Chromatograph
Ni	Nickel
NMR	Nuclear Magnetic Resonance
$P_{eq}$	Equilibrium pressure
$P_1$	Pressure of gas chamber
$P_2$	Initial pressure of gas in test cell
PVT	Pressure Volume Temperature
$P$	Pressure
$R$	Gas constant ( $8314 \text{ kPa}\cdot\text{cm}^3/\text{mol}\cdot\text{K}$ )
$T$	Temperature ( $^{\circ}\text{C}$ )
$t$	Time (s)
$V_1$	Volume of gas chamber
$V_I$	Volume of gas chamber and gas in test cell
$V$	Volume of gas in cell ( $\text{cm}^3$ )
Vapex	Vapor Extraction
$x_I$	initial molar concentration of gas in the oil phase (component 1) ( $\text{mol}/\text{cm}^3$ )

$z$	liquid position along the diffusion cell (cm)
$z_0$	height of the liquid in the cell (cm)
$Z_g$	Gas compressibility factor
$\mu$	Viscosity of liquid phase

# CHAPTER 1

## INTRODUCTION

### 1.1 Background

The diffusivity and molecular diffusion of gases in liquids has mostly been studied for various purposes in the chemical industry. For example, in the removal of pollutants from plant discharge streams by adsorption, the stripping of gases from wastewater, the diffusion of adsorbed substances within the pores of activated carbon and rate of catalyzed chemical and biological reactions, among others (Welty *et al.*, 1984). In contrast, limited information is available on diffusivity of gases in the oil recovery studies, especially in heavy oil system (Zhang *et al.*, 2000). Evidently there is also a lack of experimental data on diffusion coefficient for lighter oil systems at high pressures especially in multicomponent mixtures and reservoir fluids (Riazi, 1996; Jamialahmadi *et al.*, 2006; Ping *et al.*, 2009).

Some of the Malaysian oilfields are currently pursuing enhanced oil recovery (EOR) in an effort to have higher recovery factor and ultimately, an increase in oil reserves. The two main methods are by injection of gas and chemical. Petroliam Nasional Berhad (PETRONAS) which is a Malaysian Oil and Gas Company, has embarked pilot projects on a water-alternating-gas (WAG) and chemical EOR at Dulang and Angsi fields respectively (Nadeson *et al.*, 2004; Zainal *et al.*, 2008; Abd. Manap *et al.*, 2011). However, long term research and development work is a necessity to assess the true potential of an identified EOR process. Incremental oil gained need to be balanced with the investment of capital and operational expenditure as an EOR process is not cheap and the oil are not ‘easy oil’ anymore. As such, a lot of data is gathered from the laboratory studies and these data is scaled-up via numerical simulation. The goal is to be able to evaluate each EOR process performance and its potential in recovering more oil under actual reservoir conditions.

The gas diffusivity study is contributing to the efforts in providing more accurate data specifically in a gas injection process. In enhanced oil recovery projects, it is necessary to understand the diffusion process when different gas is injected into the reservoir when designing and planning for gas injection projects in oil reservoirs. Diffusion also plays an important role in heterogeneous or fractured reservoirs and gas diffusion through cap rock processes (Halbaek *et al.*, 1996). In this application, diffusion coefficient becomes one of the design parameters in which it is required to assist in optimizing the gas injection rate. Overall, in both heavy and light-medium oil applications, diffusion of gas into oil has contributed possibly in reducing the oil viscosity, density and surface tension (Jamialahmadi *et al.*, 2006); all of which increases the oil recovery.

In detail reservoir studies, diffusivity data provides better knowledge of the transport properties in the gas and liquid systems. The diffusivity or diffusion coefficient occurred due to molecular diffusion and difference in concentration gradient (Hines and Maddox, 1985). It is the fundamental quantity in calculating the rate of transport caused by concentration gradient (Sachs, 1998). The higher the diffusion coefficient, the faster one species diffuse or disperse to the other. Similarly, this is the rate of mass transfer. At reservoir conditions, the most important property required for determining the rate of mass transfer between the gas and oil phase is the molecular diffusion (Jamialahmadi *et al.*, 2006).

In reservoir studies, molecular diffusion is being highlighted as compared to other transport properties such as dispersion, advection and forced convection. Molecular diffusion involves concentration gradient and occurs in a free convection system. This parameter is more prominent in a subsurface system due to the low rate of fluid mobility and the molecular level by which the fluid is transported in the porous media.

For many years, a number of experimental methods have been developed for measurement of diffusivity or diffusion coefficients in gases and liquids. This includes an experimental measurement by Riazi (1996) that developed a method to determine diffusion coefficient of gas in liquid at constant volume and temperature using PVT cell. Zhang *et al.* (2000) adopted Riazi's method but the study is focused towards a heavy oil system. Contrary to Riazi's technique, Zhang *et al.* (2000) simplified the method by eliminating the need of recording the interface position with time.

In terms of actual gas and liquid samples studied, there appears to be no reported work on experimental diffusion coefficient determination on Malaysian oilfields. Riazi (1996) studied methane and normal pentane as its binary system while Zhang *et al.* (2000) experimented with methane and carbon dioxide using Hamaca Oil by INVETEP from Venezuela. The study by Jamialahmadi *et al.* (2006) was conducted using Iranian crude. Other studies involving oil samples in other parts of the world includes analysis by Nguyen and Farouq Ali (1995) which measured the diffusivity of carbon dioxide in Aberfeldy (Scotland) heavy oil and Upreti and Mehrotra (2002) which measured the diffusivity of carbon dioxide, methane, ethane and nitrogen in Athabasca (Canada) bitumen.

The diffusivity results from these earlier studies vary depending on the type of fluids and test conditions. Table 1.1 shows that different investigators produced different results even for the same binary system such as methane and oil. Diffusivity is a function of pressure, temperature and composition. Hence, there is a need to measure it experimentally for a specific gas-oil system. Moreover, according to Jamialahmadi *et al.* (2006) Zhang *et al.* (2000) and Riazi (1996), diffusion coefficient predictions at high pressure, high temperature and multicomponent system are still lacking and experimental data is scarce due to the tediousness of diffusivity measurement.

In order to achieve this, it is important to have a good and reliable experimental set-up to conduct an accurate diffusivity determination of each gas-liquid system. In particular, actual gas and oil samples from the reservoirs. The actual fluid samples are unique and the diffusion coefficient of their gas-liquid systems need to be measured experimentally.

Table 1.1: Comparison of results from various investigators for methane-oil system

Reference	Gas	Liquid	Temperature (°C)	Pressure		Diffusivity (10 <sup>-9</sup> m <sup>2</sup> /s)
				(kPa)	(psi)	
Riazi (1996)	Methane	n-Pentane	37.8	10,200	1,480	15.1
Zhang et al (2000)	Methane	Solvent oil (5000 cP)	21.0	3,510	509	8.6
Jamialahmadi et al (2006)	Methane	Dodecane (1.34 cP)	45.0	up to 30,000	up to 4351	8.0- 12.5
			65.0	up to 30,000	up to 4351	10.5 - 15.0
			81.0	up to 30,000	up to 4351	11.5 - 17.0
	Methane	Iranian crude (0.16-0.29 cP)	25.0	up to 30,001	up to 4352	8.0 - 13.6
			50.0	up to 30,001	up to 4352	9.8 - 16.4
Schmidt (1989)	Methane	Solvent oil (8360 cP)	50.0	5,000	725	0.4 - 0.75

In this study, the focus of analysis is towards molecular diffusion at reservoir conditions. The diffusion coefficient values specific to fluid samples from Malaysian oilfields were generated from selected correlation. The effects of pressure, temperature and fluid compositions were examined in detail.

## 1.2 Objectives of Research

The objectives of this research are described as the following:

1. To identify a diffusion coefficient equation that is suitable to describe a gas-liquid hydrocarbon system.
2. To design a laboratory set-up to measure the diffusion coefficient parameters of a gas-crude oil system.
3. To generate a set of diffusion coefficients of actual hydrocarbon gas-crude oil system of pre-determined fields in Malaysia under various pressures and temperatures.
4. To validate the experimental results against published reports

### **1.3 Scope of Study**

The experimental methods will generate values of diffusion coefficients of actual gas in a crude oil system under various pressures and temperatures to simulate pre-determined Malaysian reservoir conditions. The approach is to test a simplified diffusion coefficient correlation by means of laboratory experiment.

The scopes of this study are:

1. To evaluate published diffusion coefficient measurement methods and related correlations and select a suitable test method and correlation for assessment of diffusivity of the Malaysian gas-crude oil systems.
2. To gather hydrocarbon gas and crude oil samples from candidate oilfields.
3. To design experimental set-up and run preliminary analysis using a pure gas-crude oil system and validate results to published values.
4. To run experiments using actual hydrocarbon gas and crude oil sample from candidate oilfields and validate results according to its pressure, temperature and compositions relativity.

### **1.4 Thesis Organization**

This thesis comprised of five chapters including introduction, literature review, methodology, results and discussions, and conclusions and recommendations.

Chapter 1 provides a brief introduction to the importance of the gas-liquid diffusivity studies, objectives and scope of the research.

Chapter 2 reviews the application of the gas-liquid diffusivity studies to the oil and gas industry, related theories, mathematical models and experimental approaches.

Chapter 3 deals with the methods of experiments and analysis which include the fluid samples, experimental set-up and procedures, data analysis and method of results evaluation.

Chapter 4 details the results obtained from the study and deals with the discussions on the validation of the mathematical model, suitability of the model to the gas-liquid systems and effect of pressure, temperature and compositions.

Chapter 5 summarizes the main conclusions of the thesis and provides recommendations for further work.



## CHAPTER 2

### LITERATURE REVIEW

This chapter reviews the background literature that is relevant to diffusivity or diffusion coefficient applications and the related investigations. Section 2.1 covers the applications of diffusion coefficient in the oil recovery. Section 2.2 comprises of related theories on diffusion coefficients which include its relation to mass transfer and molecular diffusion. Section 2.3 covers the specific importance of the molecular diffusion in relation to its overall diffusion coefficient concept. Section 2.4 contains related model and experimental methods.

#### **2.1 Diffusivity and Its Applications**

Gas diffusivity has numerous roles in petroleum engineering applications. For one, diffusion of gas into oil has contributed possibly in reducing the oil viscosity, density and surface tension when the gas is injected into the reservoir (Jamialahmadi *et al.*, 2006). In this outlook for heavy oil application, gas diffusion into oil greatly assists in reducing the oil viscosity and density, therefore improving oil mobility for production and increases oil recovery. In another, diffusion influenced the oil recovery for solution gas drive reservoir where diffusion controls the bubble growth (Sheng, 1996). This growth of gas bubbles which formed when pressure is reduced below bubble point pressure helps to push the oil out of the pores.

In enhanced oil recovery (EOR) projects, diffusion coefficient becomes one of the design parameters. Some of the EOR processes that commonly require diffusion coefficient data are gas and solvent injection (Riazi *et al.*, 1994; Riazi, 1996; Zhang *et al.*, 2000; Jamialahmadi *et al.*, 2006). Other processes include the studies of gas hydrates formation and phase distribution process in a shut-in well. Overall, knowledge on diffusivity has become important in order to understand the degree of

its contribution in assisting specific oil recovery processes. In reservoir condition, molecular diffusion is the focus of study.

### **2.1.1 Gas Injection**

The understanding of the diffusion process when different gas is injected into the reservoir is necessary in the design and planning of gas injection projects in oil reservoirs. Different gas compositions injected at various pressure and temperature conditions possess different diffusion rate and time of equilibration which is needed for an effective process.

In gas injection projects, it is necessary to know the rate of mass transfer contributed by molecular diffusion in order to determine the amount of gas diffusing into oil (Riazi *et al.*, 1994). For instance, in vertical miscible floods, it is vital to understand the effect of molecular diffusion on the total amount and rate of gas dissolution (Riazi, 1996). The molecular diffusion assists gases to penetrate the oil that results in inhibiting viscous fingering, delaying gas breakthrough and increasing oil production rate (Bardon and Denoyelle, 1984). In carbon dioxide (CO<sub>2</sub>) flooding for fractured carbonate oil reservoirs, molecular diffusion of CO<sub>2</sub> from the fracture to the oil in the matrix is found to have an effect on the oil production rate from this matrix to the fracture (Fjelde *et al.*, 2008). Regardless of the type of gas injection projects, molecular diffusion is a prominent subject. Moreover, Jamialahmadi *et al.* (2006) highlighted claims by Burger and Mohanty (1995) and LeGallo *et al.* (1997) that problem of mass transfer by molecular diffusion in oil reservoirs has become important when a non-equilibrium gas is injected into the reservoirs.

### **2.1.2 Solvent Injection and Heavy Oil Recovery**

In non-thermal heavy oil recovery using solvent injection, the diffusivity of the solvent determined the rate of solvent adsorption by the oil. The diffusivity here often becomes the rate controlling mechanism (Zhang *et al.*, 2000). In this application, the solvent diffuses into the heavy oil, reducing its viscosity. When produced, the solvent-oil mixture is withdrawn and recovered. It is important to evaluate the diffusion coefficients of miscible solvents in heavy oil where mass transfer is a crucial

mechanism affecting the oil recovery rates in all solvent-based processes, like warm VAPEX (Vapor Extraction) (Luo *et al.*, 2007).

In heavy oil recovery generally, molecular diffusion is considered important in supercritical fluid extraction of heavy oils where the gas diffusion coefficient has a direct impact on the amount of gas that is released and the level of supersaturation that presents during pressure depletion (Zhang *et al.*, 2000).

### **2.1.3 Gas Hydrates**

In relation to gas hydrates formation, an experimental method by Sach (1998) investigated the diffusional transport of gas molecules in the water phase, especially at reservoir conditions. The results indicated that diffusion coefficient of methane in water increases with temperature and hence, possibilities of high methane transport rates in water at reservoir temperatures. Sach (1998) also found that in the study of methane hydrates, the analysis on diffusion process may provide better understanding in the mechanism of gas hydrate formation.

### **2.1.4 Phase Redistribution Process**

In phase redistribution process when a well is shut in, fluid equilibration and transient rearrangement of different phases are due to mass transfer by molecular diffusion. Diffusion takes place at the interface between these different phases. In particular, during the transient process when the less dense phase propagates to the top and the denser phase settles at the bottom. This phenomenon is clearly indicated by Jamialahmadi *et.al.* (2006) which stated that mechanism of molecular diffusion causes transfer of one or more components from the gas phase to the liquid (or vice versa) when a gas and a liquid phase which are not thermodynamically in equilibrium are brought into close contact. The time it takes to reach equilibrium depends on the diffusion rate of the gas-liquid system. This diffusion rate or diffusion coefficient is one of the most important transport properties in the calculation of mass transfer rates (Riazi and Whitson, 1993).

The scenario on phase redistribution is illustrated in Figure 2.1:

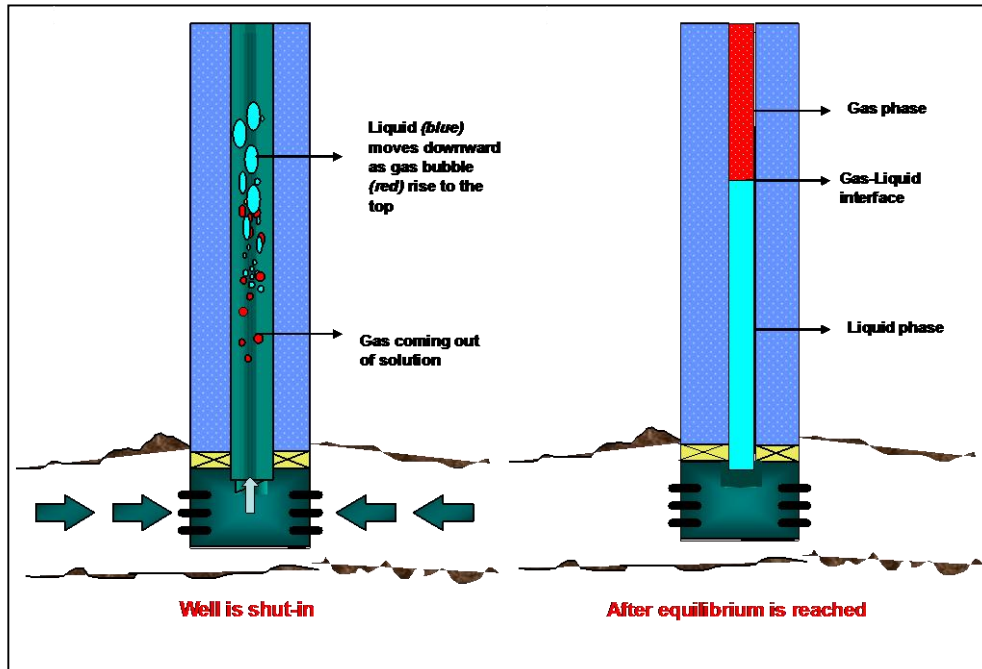


Figure 2.1: Phase redistribution after well is shut in

### 2.1.5 Transient Shut-in Model

The time element in a transient shut-in model is considered essential to properly model the mass transfer phenomena. This time factor is contributed by diffusion coefficient, which is a parameter in a mass transfer correlation. Equation 2.1 describes the mass transfer coefficient for a mass transport processes called ‘film theory’. In the film theory, the mass transfer coefficient  $k_L^o$  is directly proportional to the diffusion coefficient  $D_{AL}$  and inversely proportional to the film thickness  $\delta$ . The unit of diffusion coefficient is  $m^2/sec$  in which is expressed as diffusional area over time.

$$k_L^o = \frac{D_{AL}}{\delta} \quad (2.1)$$

In the modeling of a transient shut-in process in a well, mass transfer rate is one of the important parameters (Morgenroth and Wallman, 2005). The time element (i.e.: rate) provides a more realistic prediction as to when an equilibrium condition is reached and estimation on the correct fluid gradients which is important for reservoir pressure measurement. This is related to the transient period of mass transfer between the gas and liquid phases before the two phases equilibrate when a well is shut-in.

This includes fluid segregation, fluid ingress from the reservoir as bottom hole pressure builds up to reservoir pressure and gas/oil compression. If mass transfer is assumed instantaneous, all produced gas is assumed to dissolve immediately into the oil, neglecting the time element in mass transfer. This assumption may result in larger liquid column in the well due to higher solution gas in the liquid. Consequently, higher gas-liquid contact level in the tubing may be estimated. This may lead to incorrect estimation of the fluid gradients which is important for reservoir pressure measurement.

Likewise, the same principle of mass transfer rate is applicable to a gas lifted well. The rate of mass transfer provides a more accurate prediction of the actual phenomena when gas is injected into the well. If the rate or time is not considered in the well performance model, all the injected gas is assumed to dissolve instantaneously into the oil. Contrary, if mass transfer rate is involved, the gas bubbles actually travel a certain distance before it dissolves into the oil. Hence, a well performance model requires that the time element in mass transfer be incorporated for better prediction of the actual occurrence.

## **2.2 Theories on Diffusivity**

### **2.2.1 Mass Transfer**

Mass transfer is the physical process that involves molecular and convective transport of atoms and molecules within physical systems (Welty *et al.*, 1984). Mass transfer includes both fluid flow and separation unit operations. Some common examples of mass transfer processes are the evaporation of water from a pond to the atmosphere and during the diffusion of chemical impurities in lakes, rivers, and oceans from natural or artificial point sources. Mass transfer is also responsible for the separation of components in an apparatus such as a distillation column. Mass transfer and diffusion occur in liquids and solids as well as in gas in many circumstances. For example, a cup of water left in a room eventually evaporates as a result of water molecules diffusing into the air (liquid-to-gas mass transfer). A piece of solid CO<sub>2</sub> (dry ice) will get smaller and smaller in time as the CO<sub>2</sub> molecules diffuse into the air (solid-to-gas mass transfer). Spoons of sugar in a cup of tea will eventually moves up

and sweeten the tea even though the molecules of sugar are higher than the water molecules (solid-to-liquid mass transfer) (Incropera and DeWitt, 1996).

Mass transfer is a subject of interest when describing fluid flow and phase segregation process. The driving force for mass transfer is a difference in concentration where the random motion of molecules causes a net transfer of mass from an area of high concentration to an area of low concentration (Incropera and DeWitt, 1996). The process can take place in a gas, vapor or liquid. It can result from the random velocities of the molecules (molecular diffusion) or from the circulating or eddy currents present in a turbulent fluid (eddy diffusion) (Coulson and Richardson, 1990).

The amount of mass transfer can be quantified through the calculation and application of mass transfer coefficients or diffusion coefficient. The rate of diffusion is governed by Fick's Law which expresses the mass transfer rate as a linear function of the molar concentration (Welty *et al.*, 1984). In a mixture of two gases A and B, assumed ideal, Fick's Law may be written for a steady state diffusion as:

$$N_A = -D_{AB} \frac{dC_A}{dy} \quad (2.2)$$

Where  $N_A$  is the molar flux of A (moles per unit area at unit time),  $C_A$  is the concentration of A (moles of A per unit volume),  $D_{AB}$  is the diffusivity or diffusion coefficient for A and B and  $y$  is the distance in the direction of transfer (Coulson and Richardson, 1990).

An exactly similar equation may be written for B; where  $N_B$  is the molar flux of B,  $C_B$  is the concentration of B.

$$N_B = -D_{AB} \frac{dC_B}{dy} \quad (2.3)$$

To illustrate the mass transfer diffusion process, consider a tank that is divided into two equal parts by a partition (Figure 2.2).

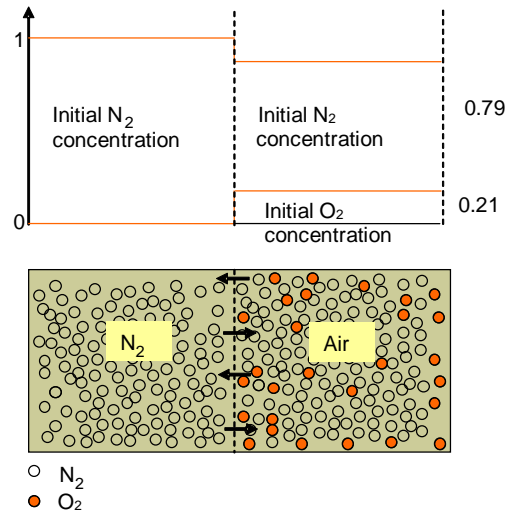


Figure 2.2 : Schematic of simple Nitrogen-Air diffusion process

Initially, the left section of the tank contains nitrogen  $N_2$  gas while the right section contains air (about 21 %  $O_2$  and 79 %  $N_2$ ) at the same temperature and pressure. The  $O_2$  and  $N_2$  molecules are indicated by the red and white circles respectively. When the partition is removed the nitrogen molecules will start diffusing into the air while the oxygen molecules diffuse into the nitrogen. If waited long enough, a homogenous mixture of nitrogen and oxygen in the tank is achieved.

### 2.2.2 Molecular Diffusion

Molecular diffusion is also called molecular mass transfer where it describes the macroscopic transport of mass which is independent of any convection within the system (Welty *et al.*, 1984). In a gaseous mixture, this kind of transport phenomena can be illustrated from the kinetic theory of gases. At temperature above absolute zero, individual molecules are in a continual yet random motion. Collisions between the solute and the solvent molecules are continually occurring. As a result of this collision, the solute molecules move along a zigzag path, sometimes toward regions of higher concentration, sometimes toward a lower concentration (Welty *et al.*, 1984).

The basic relation for molecular diffusion defines the molar flux relative to the molar-average velocity,  $J_A$ . An empirical relation for this molar flux, called Fick's Law (as in Equation 2.2 and 2.3) defines the diffusion of component A in an

isothermal, isobaric system (Welty *et al.*, 1984). For simplification, for diffusion in only the z-direction, the Fick's law can be written as:

$$J_{A,Z} = -D_{AB} \frac{dc_A}{dz} \quad (2.4)$$

Where  $J_{A,Z}$  is the molar flux in the z-direction,  $dc_A/dz$  is the concentration gradient in z-direction and  $D_{AB}$  is the diffusion coefficient for component A diffusing into component B. Equation 2.4 is in similar form as in the molar flux as per Equation 2.2 and 2.3 earlier.

Table 2.1 below summarizes the equivalent forms of the Fick's Law or Fick's rate equation (Welty *et al.*, 1984):

Table 2.1 : Fick's Law equivalent forms

Flux	Gradient	Fick's rate equation	Restrictions
$n_A$	$\nabla \omega_A$ $\nabla \rho_A$	$n_A = -\rho D_{AB} \nabla \omega_A + \omega_A (n_A + n_B)$ $n_A = -D_{AB} \nabla \rho_A + \omega_A (n_A + n_B)$	Constant $\rho$
$N_A$	$\nabla y_A$ $\nabla c_A$	$N_A = -c D_{AB} \nabla y_A + y_A (N_A + N_B)$ $N_A = -D_{AB} \nabla c_A + y_A (N_A + N_B)$	Constant $c$
$j_A$	$\nabla \omega_A$ $\nabla \rho_A$	$j_A = -\rho D_{AB} \nabla \omega_A$ $j_A = -D_{AB} \nabla \rho_A$	Constant $\rho$
$J_A$	$\nabla y_A$ $\nabla c_A$	$J_A = -c D_{AB} \nabla y_A$ $J_A = -D_{AB} \nabla c_A$	Constant $c$

From the table above, any one of the equations can be used to describe molecular diffusion, however, certain fluxes are more suitable for specific cases as described below (Welty *et al.*, 1984):

- i. Mass fluxes,  $n_A$  and  $j_A$ : used when the Navier-Stokes equations are required to describe the process
- ii. Molar fluxes,  $J_A$  and  $N_A$ : used to describe mass transfer when involved chemical reaction



- iii. Fluxes,  $n_A$  and  $N_A$ : used to describe engineering operations within process equipment
- iv. Fluxes,  $j_A$  and  $J_A$ : used to describe mass transfer in diffusion cells for measuring diffusion coefficient.

Molecular diffusion is a free convection system (Riazi, 1996). In the measurement of gas-liquid diffusion in an isothermal system as per the test set-up by Riazi (1996) and Zhang *et al.* (2000), a free convection system is assured to ensure results reliability and correct application of the related correlations. It is also to note that a chemically reactive gas-liquid system does not represent a molecular diffusion condition.

### 2.2.3 Diffusion Coefficient

Diffusion coefficient is a parameter to describe molecular diffusion process. This parameter,  $D_{AB}$  is proportionality in Fick's Law as in Equation 2.2, 2.3 and 2.4 above.

Diffusion coefficient is a function of pressure, temperature and composition of the system (Welty *et al.*, 1984). Diffusion coefficient or  $D_{AB}$  has been reported in units length squared over time;  $\text{cm}^2/\text{s}$ ,  $\text{m}^2/\text{s}$  (SI unit) and  $\text{ft}^2/\text{s}$  (English system). Due to mobility of the molecules, the diffusion coefficients are higher for gases (in the range of  $5 \times 10^{-6}$  to  $1 \times 10^{-5} \text{ m}^2/\text{s}$ ) compared to liquids (in the range of  $10^{-10}$  to  $10^{-9} \text{ m}^2/\text{s}$ ) and solids (in the range  $10^{-14}$  to  $10^{-10} \text{ m}^2/\text{s}$ ) (Welty *et al.*, 1984).

Fick's 1<sup>st</sup> Law as expressed in Equation 2.4 is used in steady state diffusion in which the concentration volume does not change with time (Wikipedia "Fick's Law of Diffusion", 2008). Fick's 2<sup>nd</sup> Law as expressed in Equation 2.5 and 2.6 is used in non-steady or continually changing state diffusion where the concentration within the diffusion volume changes with time.

$$\frac{\partial \phi}{\partial t} = D \frac{\partial^2 \phi}{\partial x^2} \quad (2.5)$$

Where:

- $\phi \equiv$  concentration in dimensions of; amount of substance (length<sup>-3</sup>, mol m<sup>3</sup>)
- $t \equiv$  time (sec)
- $D \equiv$  diffusion coefficient in dimensions of; (length<sup>2</sup> time<sup>-1</sup>, m<sup>2</sup> s<sup>-1</sup>)
- $x \equiv$  position; (length, m)

The 2<sup>nd</sup> Fick's Law can be derived from the 1<sup>st</sup> Fick's Law and the mass balance is per follows:

$$\frac{\partial \phi}{\partial t} = -\frac{\partial}{\partial x} J = \frac{\partial}{\partial x} \left( D \frac{\partial \phi}{\partial x} \right) \quad (2.6)$$

This 2<sup>nd</sup> Fick's Law is further derived by many investigators (Riazi, 1996; Zhang *et al.*, 2000; Ping *et al.*, 2009) to devise correlations for molecular diffusion measurements involving gas-liquid systems. Below are the reported correlations:

- Riazi (1996) on measurement of methane in n-pentane system

$$\frac{\partial C_{oi}}{\partial t} - u_o \frac{\partial C_{oi}}{\partial z_o} = \frac{\partial}{\partial z_o} \left[ D_{oi} \frac{\partial C_{oi}}{\partial z_o} \right] \quad (2.7)$$

Where:  $C_{oi}$  is the molar concentration of component  $i$  in oil,  $z_o$  is axis for diffusion in the cell,  $D_{oi}$  is Maxwell-Stefan diffusion coefficient of component  $i$  in oil and  $t$  is time.

- Zhang *et al.*, (2000) on measurement of methane in multicomponent oil system.

$$\frac{dx_1}{dt} + v^* \frac{dx_1}{dz} = D_{AB} \frac{d^2 x_1}{dz^2} \quad (2.8)$$

Where  $x_1$  is the molar concentration of the gas,  $z$  is position along diffusion vessel,  $v^*$  is molar average velocity,  $D_{AB}$  is the diffusion coefficient and  $t$  is time.

- Ping *et al.*, (2009) on multicomponent gas-oil system. Equation 2.9 is for the oil phase and Equation 2.10 is for the gas phase.

$$\frac{\partial C_{oi}}{\partial t} = \frac{\partial}{\partial z_o} \left[ D_{oi} \frac{\partial C_{oi}}{\partial z_o} \right] \quad (2.9)$$

$$\frac{\partial C_{gi}}{\partial t} = \frac{\partial}{\partial z_g} \left[ D_{gi} \frac{\partial C_{gi}}{\partial z_g} \right] \quad (2.10)$$

Where:  $C_{oi}$  is the  $i$ -component mass concentration of the oil phase,  $C_{gi}$  is the  $i$ -component mass concentration of the gas phase,  $z_o$  and  $z_g$  are the coordinate axes respectively for the oil and gas,  $D_{oi}$  and  $D_{gi}$  are the diffusion coefficient in the oil and gas phase respectively and  $t$  is time.

#### 2.2.4 Effect of Pressure, Temperature and Compositions

Welty *et al.* (1984) stated that diffusion coefficient is a function of pressure, temperature and composition of the system. Viscosity is a parameter that is closely related to compositions. This relates to the crude oil compositions, its hydrocarbon number, its molecular weight and its proportional relationship to crude oil viscosity. Compositional analysis on crude oil showed that crude oil with higher number of the heavier hydrocarbon components and molecular weight, has higher viscosity. Hence, a number of published studies reported viscosity effect on diffusion coefficient values. For a gas-liquid system, the liquid viscosity plays major influence on the system's gas-liquid diffusivity. According to Jamialahmadi *et al.* (2006), almost all correlations available for the prediction of diffusion coefficients of gases in liquids show that at a given temperature, the diffusion coefficient depends primarily on the liquid phase viscosity. For this reason, several other investigators (Riazi and Whitson, 1993; Nyugen and Farouq Ali, 1995) also correlated their experimental data to liquid phase viscosity.

Table 2.2 demonstrates that there is a consistent finding on diffusion coefficient with viscosity. It shows that diffusion coefficient values are lower with increasing

viscosity. The same consistency was observed with diffusion coefficient-temperature relationship. It shows that diffusion coefficient increases with increasing temperature. However, pressure appeared to have different effect on diffusion coefficient between these investigators. Among all these investigators, Riazi (1996) is the only one that observed an inverse relationship between pressure and diffusion coefficient. It may be attributed to the test conditions of each gas-liquid system. As for Nguyen and Farouq Ali (1995), it explained that pressure has different effect to diffusion coefficient in their study on carbon dioxide-oil system. They found that the diffusivity depends on the state of carbon dioxide in the gas-liquid system. Carbon dioxide is in gas phase when the system pressure is low and in liquid phase at higher pressure. This change of state is subject to the carbon dioxide pressure-temperature phase diagram. When carbon dioxide is in gas phase, the molecules move freely and hence, it diffuses faster to the liquid phase. However, when carbon dioxide is in the liquid phase, its molecular speed is lower than the strong molecular forces hence its diffusivity is slowed down (Nguyen and Farouq Ali, 1995).

Table 2.2: Findings from different investigators on relationship of diffusion coefficient with pressure, temperature and viscosity

Reference	Temperature (T) vs. $D_{AB}$	Pressure (P) vs. $D_{AB}$	Viscosity ( $\mu$ ) vs. $D_{AB}$
Book: Hines & Maddox (1985)	Proportional ( $T$ high, $D_{AB}$ high)	- not reported -	- not reported -
Riazi (1996)	- not reported -	Inverse ( $P$ high, $D_{AB}$ low)	Inverse ( $\mu$ high, $D_{AB}$ low)
Zhang et al. (2000)	- not reported -	- not reported -	- not reported -
Jamialahmadi et al. (2006)	Proportional ( $T$ high, $D_{AB}$ high)	Proportional ( $P$ high, $D_{AB}$ high)	Inverse ( $\mu$ high, $D_{AB}$ low)
Upreti & Mehrotra (2002)	Proportional ( $T$ high, $D_{AB}$ high)	Proportional ( $P$ high, $D_{AB}$ high)	-
Nguyen & Farouq-Ali (1995)	Proportional ( $T$ high, $D_{AB}$ high)	Proportional ( $P$ high, $D_{AB}$ high)	Inverse ( $\mu$ high, $D_{AB}$ low)

### 2.3 Importance of Molecular Diffusion Measurement

Molecular diffusion coefficient at reservoir condition is the most important property in determining the mass transfer rate between gas and oil phase (Jamialahmadi *et al.*, 2006). Theory based correlation can be used to predict molecular diffusion for low pressure system. For example, for low pressure gas system, kinetic theory such as

Chapman-Enskog theory is adequate to estimate the molecular diffusion (Riazi and Whitson, 1993). For liquid system however, most developed correlations are based on the Stokes-Einstein equation in which diffusion coefficient is inversely related to liquid viscosity (Jamialahmadi *et al.*, 2006).

However, at high pressure system, this theory based correlations failed to perform properly and thus, empirical correlations were developed (Jamialahmadi *et al.*, 2006; Riazi and Whitson, 1993). For high pressure system, even though empirical correlation seemed to be more accurate than theory based correlation, the current available correlations are found not suitable for the prediction of diffusion coefficient of gas in hydrocarbon liquids at high pressure and temperature. For example, Riazi and Whitson (1993) described that Sigmund correlation predicts gas diffusivity of gases dissolved in liquid hydrocarbons at high pressure which are 80% – 100% higher than reported experimental values. Jamialahmadi *et al.* (2006) reported that inaccuracy was also observed by Denoyelle and Bardon (1983). This study reported that diffusion coefficients for carbon dioxide in oil at reservoir conditions which are 5 – 10 times higher than those measured at atmospheric conditions. According to Jamialahmadi *et al.* (2006), inaccuracy of diffusion coefficient prediction at high pressure system is due to lack of reliable high pressure and temperature molecular diffusion experimental data. This is supported by Zhang *et al.* (2000) in their evaluation of gas diffusion coefficient in heavy oil. They found that its experimental data is relatively scarce due to the tedious nature of diffusivity measurement. According to Riazi (1996), sufficient experimental data on diffusion coefficients at high pressures for multicomponent mixtures and reservoir fluids is still lacking.

### **2.3.1 Input Parameter for Compositional Modeling**

Molecular diffusion acts as input parameter, particularly in compositional modeling for gas flooding applications. The gas diffusivity and interface mass transfer are important in evaluating the rate of dissolution of the injected gas in oil during secondary recovery such as a gas flooding project. Hence, for proper gas injection strategies, accurate values of these parameters are required for reservoir simulation and prediction of oil recovery by miscible gas flooding (Civan and Rasmussen, 2006).

In Eclipse 300 compositional modeling software, the related input functions are called DIFFCGAS and DIFFCOIL which represent the diffusion components in the gas and oil respectively. These functions are particularly relevant when observing the effect of gas diffusivity at small scale such as in micro model or core scale as diffusivity of gas in oil happens at very slow rate.

### **2.3.2 Input Parameter for Transient Shut-in Modeling**

A more downstream application of gas-liquid molecular diffusivity measurement is its application in transient shut-in modeling. The interest is at the production tubing, primarily in describing the phase redistribution process in a shut-in well. Gas-liquid diffusivity has been suggested to account for the molecular interactions and distribution between the gas and oil phase in a producing well during transient flow (Zainal *et al.*, 2011).

In the transient shut-in modeling, the diffusion coefficient data is used to calculate the mass transfer rate. The time element embedded in diffusion coefficient is a vital part of the calculation as it represents a non-instantaneous transfer of gas into liquid therefore giving a much more representative gas-liquid phase distribution when a well is shut-in. This improved assumption on gas-liquid contact level provides better accuracy in estimating the gas and liquid gradient. A much accurate data on gas and liquid gradient coupled with reliable data on PVT characteristics and reservoir fluid influx allow the transient shut-in model to have better preciseness in calculating the near wellbore bottomhole reservoir pressure.

### **2.4 Reported Mathematical Model and Analysis**

One of the most important properties in the calculation of mass transfer rates is diffusion coefficient (Riazi, 1996). It is an important transport property in mass transfer calculations (Riazi and Whitson, 1993). For example, when a non-equilibrium gas is brought into contact with a liquid in a constant-temperature, constant-volume vessel, the system will approach its equilibrium state. The time required for the system to reach its final equilibrium state depends on the diffusion coefficient of the components in the system (Riazi, 1996).

Zhang *et al.* (2000) stated that experimental tests to determine gas diffusivity in oil are necessary since there is no universal theory to calculate diffusion coefficient from other known properties of the system. Moreover, most conventional methods need compositional analysis which is tedious and time consuming.

Various methods have been used to measure diffusion coefficients in hydrocarbon systems. According to Riazi (1996), there are two general categories. In the first category, during experiment, fluids are sampled at various times and analyzed using gas chromatography or other analytical tools. This method was used by Berry and Koeller (1960), Sigmund (1976) and Dickson and Johnson (1988). In the second category, there is no samples being analyzed, instead, equipment such as NMR measures self diffusion coefficient and then correlations were used to calculate binary diffusion coefficients. Riazi (1996) reported that this method was used by Dawson *et al.* (1970) and Woessner *et al.* (1969). There is also another method besides these two categories which measures volume of gas dissolved in oil over time at constant pressure which are: studies by Denoyelle and Bardon (1984) and Renner (1988).

Below are some of the recent methods in predicting diffusion coefficients of reservoir fluids. From these three methods, Zhang *et al.* (2000) method was used in this study for the calculation of diffusion coefficient as it is a reliable yet simplified model where compositional analysis and interface position measurement are not necessary. Moreover, the experimental set-up using high pressure and high temperature PVT cell is available in the existing laboratory with only minor modification required.

#### **2.4.1 Pressure-time Profile Using PVT Cell by Riazi (1996)**

Riazi (1996) developed the first method to determine diffusion coefficient using a constant volume, constant temperature PVT cell.

The binary systems by Riazi (1996) were methane (gas) and normal pentane (nC<sub>5</sub>) at temperature of 37.8°C and initial pressure of 102 bar (1480 psia). The objective of Riazi's (1996) study was to develop a model that can predict the gas-liquid interface position and pressure in a constant-volume cell via a time period. The idea was to

obtain a correct value of diffusion coefficient from the model using the measured pressure or interface position.

The experiment analyzed the rate of pressure and interface position as a function of time in a constant volume, constant temperature cell. The initial compositions of the liquid were measured. This experiment is based on the concept that when a non-equilibrium gas is brought into contact with a liquid in constant volume, constant temperature vessel, the system approaches its equilibrium state. However, the time required for this system to reach its final equilibrium depends on the diffusion coefficient of components in the system.

This concept is based on some major assumptions. First assumption is; equilibrium exists between the liquid and gas phase at the interface at all times. Secondly, velocity of interface movement and the rate of pressure change in the system depend on the rate of diffusion in each phase. If correct values for diffusion coefficients of all components are used in the proposed model, then the predicted rate of interface movement should be consistent with the experimental results. In this case, no compositional measurement is necessary. This is an advantage over conventional methods where it eliminated the need to measure compositional analysis over time. In order to validate the proposed model, the diffusion coefficient of methane in n-pentane was measured at 70 bar and compared with the literature value.

Riazi (1996) used 2<sup>nd</sup> Fick's Law in Equation 2.11 to evaluate his experimental method and to describe the diffusion process. The concept of the test set-up is per Figure 2.3 which is described with more detail in section 2.5.1.1.

$$\frac{\partial C_{oi}}{\partial t} - u_o \frac{\partial C_{oi}}{\partial z_o} = \frac{\partial}{\partial z_o} \left[ D_{oi} \frac{\partial C_{oi}}{\partial z_o} \right] \quad (2.11)$$

Where:

$C_{oi} \equiv$  Molar concentration of component  $i$  in oil

$t \equiv$  Time

$z_o \equiv$  Axis for diffusion in the cell as defined in Figure 2.3

$D_{oi} \equiv$  Maxwell-Stefan diffusion coefficient of component  $i$  in oil



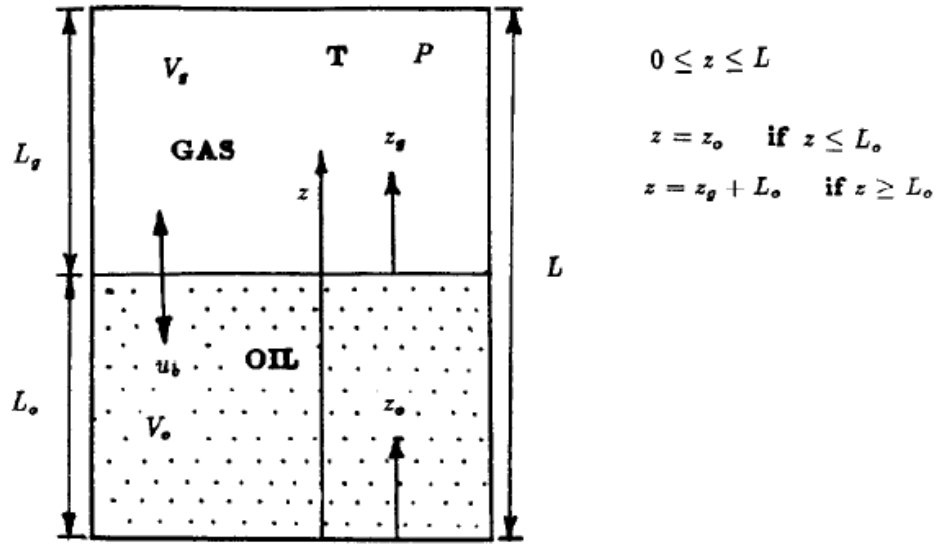


Figure 2.3 : Schematic of a constant volume cell (Riazi, 1996)

To further determine the diffusion coefficient, there are three selected correlations used to simulate the experiment. As reported in Riazi (1996), the first one is from Sigmund (1976) which is one of the simplest correlations. It is in the form of a reduced density-diffusivity product as a function of mixture reduced density. Secondly is the Wilke's method (Wilke, 1950) and thirdly, the Riazi and Whitson (1993) correlation.

Riazi and Whitson (1993) correlation which is expressed in terms of viscosity is as below:

$$\frac{\rho D_{AB}}{(\rho D_{AB})^o} = a \left( \frac{\mu}{\mu^o} \right)^{b+cP_x} \quad (2.12)$$

Where:

$$a = 1.0$$

$$b = -0.27 - 0.38\omega$$

$$c = -0.05 + 0.1\omega$$

$$P_x = P/P_c$$

$$P_c = x_A P_{c,A} + x_B P_{c,B}$$

$$\omega = x_A \omega_A + x_B \omega_B$$

$x_A$	$\equiv$	mole fraction of components A
$x_B$	$\equiv$	mole fraction of components B
$\rho$	$\equiv$	molar density of fluid, kmol/m <sup>3</sup>
$\mu$	$\equiv$	viscosity of fluid, mPa.s (cP)
$\mu^o$	$\equiv$	low pressure viscosity, mPa.s (cP)

The Riazi and Whitson (1993) correlation (Equation 2.12) is a simple and generalized correlation in terms of viscosity and molar-density to estimate diffusion coefficients for both binary and multicomponent hydrocarbon systems. They claimed that the correlation could be used for both gases and liquids up to 400 bar (6000 psia) pressure. Moreover, it is based on experimental data in hydrocarbon system. Its input parameters are molecular weight, critical properties, and acentric factor of components in the system. Other input parameters are predicted from appropriate correlation which includes mixture molar density, low pressure gas viscosity and actual viscosity (Riazi and Whitson, 1993).

#### **2.4.2 Pressure-time Profile Using PVT Cell by Zhang *et al.* (2000)**

Zhang *et al.* (2000) evaluated the feasibility of determining diffusion coefficients of gases in heavy oils by monitoring pressure in a closed volume containing a column of the oil below a gas cap. The study involved binary systems consist of methane–oil and carbon dioxide–oil. The technique used is adopted from Riazi’s (1996) technique but is developed for a heavy oil system. Compositional analysis is therefore, not required. However, Zhang *et al.* (2000) simplified Riazi’s method where it does not require recording of the interface position with time. This study claimed that the position of the interface did not change significantly with time. For this experiment, test temperature was 21°C while initial pressure was 3471 kPa (503psi) for the methane-oil system and 3510 kPa (509psi) for the carbon dioxide-oil system. The temperature is assumed constant during the test.

The experiment analyzed the pressure change inside the cell. The diffusion coefficient was determined from pressure-time profiles and was based on a mathematical analysis using Fick’s Law. The analysis is based on the concept that the amount of gas eventually transferred into the liquid phase depends on the gas

solubility. However, the rate of gas transfer into the liquid phase is controlled by the diffusion coefficient of the gas. This experiment assumed that diffusion coefficient,  $D_{AB}$  did not change significantly with concentration over the concentration difference during the test period (Zhang *et al.*, 2000).

Zhang *et al.* (2000) used the Fick's Law equation as in Equation 2.13 to describe the molar flux of a gas diffusing into liquid.

$$\frac{dx_1}{dt} + v^* \frac{dx_1}{dz} = D_{AB} \frac{d^2 x_1}{dz^2} \quad (2.13)$$

Where:  $x_1$  is the molar concentration of the gas,  $v^*$  is the molar average viscosity,  $z$  is the position along the diffusion cell and  $t$  is time.

The mathematical analysis is based on a pressure-time profile from the diffusion process as below:

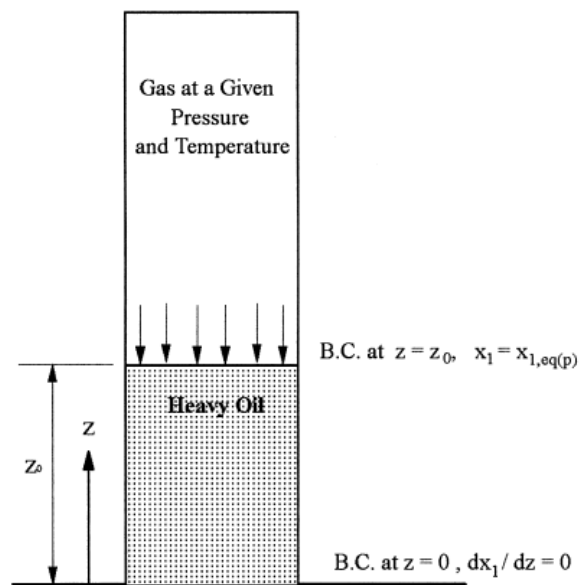


Figure 2.4 : Schematic and dimensions of diffusion process (Zhang *et al.*, 2000)

From the above, the oil-gas interface is located at  $z = z_0$  and bottom of the test cell is at  $z = 0$ . B.C is the respective 'Boundary Condition'. Based on the above diffusion process, the relationship between pressure and time is expressed as in Equation 2.14 below:

$$\ln[P(t) - P_{eq}] = \ln\left(\frac{8Bz_o x_{1,eq(p)}}{\pi^2}\right) - \frac{\pi^2 D_{AB} t}{4z_o^2} \quad (2.14)$$

Where:  $P(t)$  and  $P_{eq}$  are the measured and equilibrium pressure respectively,  $B$  is constant defined as per Appendix C,  $x_{1,eq(p)}$  is the oil-gas interface molar concentration at a given time,  $z_o$  is the height of the oil in the vessel and  $t$  is time.

A straight line fit is obtained by plotting the experimental data according to the above equation. The slope and intercept of this line corresponds to the diffusion coefficient,  $D_{AB}$  and the equilibrium molar concentration,  $x_{1,eq(p)}$ , respectively. However, this method is heavily dependent on the  $P_{eq}$  chosen since the  $D_{AB}$  values are sensitive to this assumed value. It can be used to calculate the  $D_{AB}$  but with low reliability.

Another method is the numerical method which results in simple  $D_{AB}$  equation as the following:

$$D_{AB} = \frac{4z_o^2}{k_1 \pi^2} \quad (2.15)$$

Where:  $z_o$  is the length of the liquid column in the cell and  $k_l$  is the constant determined by regression. The diffusion coefficient calculated using this method as published by Zhang *et al.*, 2000 (Equation 2.15) is  $8.6 \times 10^{-9}$  m<sup>2</sup>/s for the CH<sub>4</sub>-oil system and  $4.8 \times 10^{-9}$  m<sup>2</sup>/s for the CO<sub>2</sub>-oil system.

#### **2.4.3 Volume-time Profile Using Diffusion Cell in Temperature Controlled Water Bath by Jamialahmadi *et al.* (2006)**

Jamialahmadi *et al.* (2006) studied the diffusion coefficient of methane in liquid hydrocarbons at high pressure and high temperature conditions. It highlights that accurate prediction of methane in liquid hydrocarbon is important for: 1) improving the prediction of compositional oil reservoir simulators, 2) designing surface facilities, and 3) in high gas/liquid mass transfer operations.

The method employed the usage of a precision high pressure and temperature diffusion cell apparatus to measure diffusion coefficients of methane in dodecane and methane in a typical Iranian crude oil at high pressures and temperatures. Experiments were conducted at pressures up to 40MPa (5,801psi) at different temperatures.

The experiment analyzed the mechanism of mass transfer during the incubation period by solving the equation of continuity for diffusion cell numerically and considering that diffusion coefficient is changing with time and concentration. The measuring technique used accurate high-pressure diffusion cell with “finite-domain” moving boundary behavior to demonstrate the effect of solute concentration and viscosity on diffusion coefficient. The system is based on the assumption that gas dissolved in the liquid phase is released when the pressure is decreased and the temperature of the system is increased. The findings by this study are more applicable to Iranian crudes under a high pressure and temperature condition.

Jamialahmadi *et al.* (2006) used 2<sup>nd</sup> Fick’s Law as in Equation 2.16 below to determine the diffusion coefficient for one dimensional diffusion cell. The assumptions include the movement of the interface at the boundary conditions of the system in the absence of chemical reaction.

$$\frac{\partial C_A}{\partial t} = D \frac{\partial^2 C_A}{\partial x^2} \quad (2.16)$$

Equation 2.16 is simplified from the equation of continuity for solute component. This equation is used to develop a number of mathematical models in determining the diffusion coefficients from experimental volume-time profiles (Civan and Rasmussen, 2002).

The study used a “finite-domain moving boundary” model. Jamialahmadi *et al.* (2006) stated that experimentally, finite systems provide conditions for more precise estimates of diffusion coefficients. This kind of system allows the design or construction of small and compact apparatus, which is an advantage when working with high pressure and temperature conditions. The concept is that, when liquid in the diffusion cell contacts the gas phase, diffusion starts to take place. However, no mass transfer occurs across the ends of the cell since the cell is sealed and is of finite length.

Jamialahmadi *et al.*'s method in determining diffusion coefficients is different from that of Riazi (1996) and Zhang *et al.* (2000). The experiment was conducted at constant pressure and temperature. Then, volume of dissolved methane in liquid phase as a function of time is determined from the movement of the interface and the position of the piston rod of the displacement pump. Here, diffusion coefficient is calculated from the volume – time data whereas Riazi (1996) and Zhang *et al.* (2000)'s calculations are from pressure – time data.

This study also investigates the effect of liquid viscosity and temperature to diffusion coefficient determination. It found that at test temperatures range from 25°C to 81°C, the diffusion coefficient decreases steadily as the liquid phase viscosity increases. Liquid phase viscosity also decreases with increasing liquid phase temperature. As such, the diffusion coefficient also increases as liquid phase temperature increases. The relationship between diffusion coefficients on liquid phase viscosity is as follows:

$$D(T, P) = a_o \mu^{a_1} \quad (2.17)$$

Where:  $a_o$  and  $a_1$  are coefficients which can be obtained from the experimental data. Jamialahmadi *et al.* (2006) found that reported values for coefficient  $a_o$  vary from  $0.5 \times 10^{-10}$  to  $0.4 \times 10^{-11}$ . Conversely, almost all investigators reported that coefficient  $a_1$  is negative and varies from -0.45 to -0.12. This has shown that diffusion coefficient has an inverse relationship with liquid phase viscosity.

## 2.5 Reported Experimental Set-up

### 2.5.1 Diffusion Coefficient Determination from Pressure-time Data

#### 2.5.1.1 Experimental Set-up by Riazi (1996)

Riazi (1996) experiment involved pure methane (gas) and normal pentane (liquid) at temperature of 37.8°C (100°F) and initial pressure of 102 bar (1480 psia). The experimental set-up used a visual sapphire PVT cell. The height of the cell is 21.943 cm and its diameter is 2.56 cm.

The test used a constant-volume cell containing non-equilibrium gas and liquid (oil) mixture with known initial compositions. The temperature of system was maintained constant throughout the experiment as it approaches the equilibrium state. The test set-up is as below:

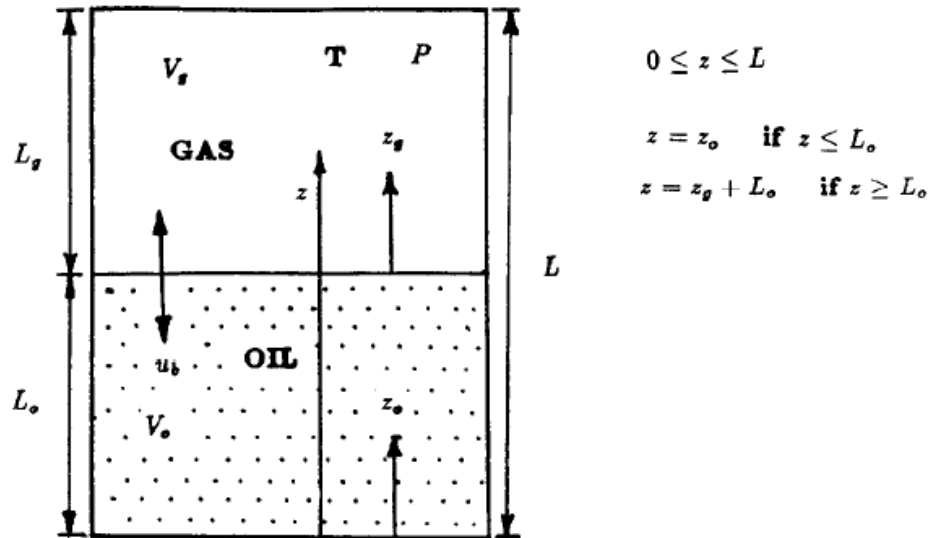


Figure 2.5 : Schematic and dimensions of a constant-volume cell (Riazi, 1996)

In Figure 2.5, the  $L_o$  and  $L_g$  represent the heights of the oil and gas respectively while  $V_o$  and  $V_g$  represent the volume of each oil and gas. The axis for diffusion in the cell is defined by  $z$  where  $z_o$  and  $z_g$  are the respective axis for the oil and gas.

The experimental started by partially filling in the cell (35% by volume) with normal pentane. The liquid is then vacuumed and liquid volume at saturated conditions was made in order to determine the moles of n-pentane initially. Then, high pressure methane was introduced slowly until the pressure reached 102 bar. At this point, the experiment began and the pressure, temperature and liquid level were recorded over time. During the test, pressures were recorded manually at selected times and continuously on a strip chart. The liquid level was measured manually with a precision of  $\pm 0.02$  mm.

Some calculations were done prior to this diffusion experiment. PVT behavior of the initial pure components and final equilibrium mixture were calculated with Peng Robinson EOS. Volume shift parameters of -0.2044 and -0.045 were used for methane & n-pentane respectively. Binary interaction coefficient of 0.054 was used. Pure

compound densities at initial conditions were used to determine volume translation coefficients & the interaction coefficient was modified to match the final liquid volume fraction (Riazi, 1996). Using this method, calculated final equilibrium gas compositions were:  $y_1 = 95.43\%$ ,  $y_2 = 4.57\%$ , compared with measured values of  $y_1 = 94.92\%$ ,  $y_2 = 5.08\%$ , confirming the validity of EOS used for phase equilibrium calculations.

#### ***2.5.1.2 Experimental Set-up by Zhang et al. (2000)***

Zhang *et al.* (2000) experiment studied 2 types of binary systems which are methane-heavy oil and carbon dioxide-heavy oil at temperature of 21°C. The oil used was Hamaca oil, supplied by INVETEP of Venezuela. The initial pressure for the methane-oil system was 3471 kPa (503.4 psi) while the carbon dioxide-oil system was 3510 kPa (509.1 psi). The experimental set-up is an adaptation from Riazi's (1996) but it was simplified where it did not include measurement of interface position with time.

The experimental set-up, illustrated by Figure 2.6 consists of a constant volume stainless steel cylinder fitted with 2 flanges and a window. The internal cross section of cell is 4.94 cm<sup>2</sup> while cell height is 25.0 cm. The cell was placed in vertical position and the top flange of cell was connected to a high pressure gas cylinder. A high accuracy digital pressure gauge was also connected to the top flange and was used to measure the pressure change inside the cell during the experiment. The bottom flange was equipped with a valve which permits injection of oil into the cell.



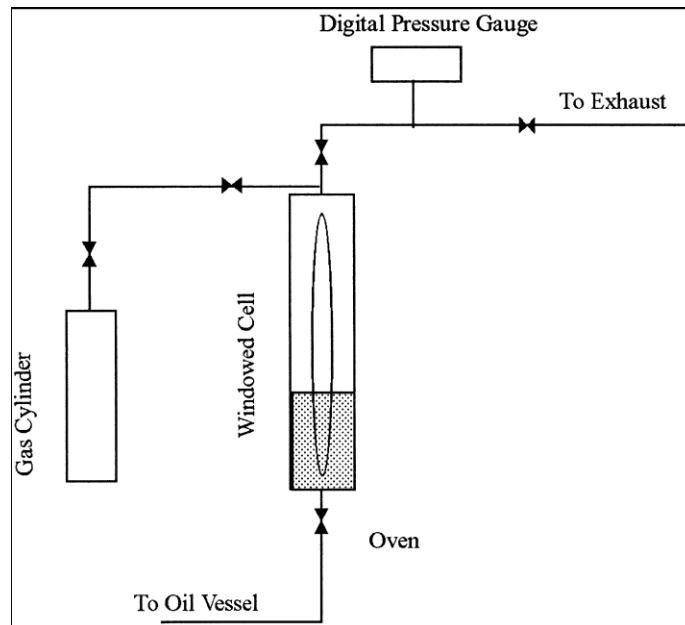


Figure 2.6 : Schematic of a constant-volume cell (Zhang *et al.*, 2000)

The experiment was conducted at room temperature. Firstly, oil was injected into the cell to obtain an oil column of desired height. Then high pressure gas was injected slowly into the cell from top of flange until the pressure reached the desired test pressure (for example, 3471 kPa was used in a methane-oil system). Then, the PVT cell and pressure gauge were isolated and the test began. As time passes, the gas diffuses into the oil and pressure tends to drop very slowly in the gas phase. The gas diffusivity was determined from the recorded pressure history.

It is important to note that unlike Riazi (1996) that measured interface position with time, Zhang *et al.*'s (2000) experiment above assumed  $z_o$ , (height of the liquid column or the interface position) constant during the test.

## 2.5.2 Diffusion Coefficient Determination from Volume-time Data

### 2.5.2.1 Experimental Set-up by Jamialahmadi *et al.* (2006)

Jamialahmadi *et al.* (2006) experiment studied 2 types of binary systems which are methane-dodecane and methane-Iranian crude at various temperatures up to 180°C and pressures up to 40 MPa (5801 psi). All tests were performed in an accurate high-pressure diffusion cell with “finite-domain” moving boundary behavior. Based on this finite-domain method, it is assumed that diffusion coefficient is either: 1) independent

or 2) dependent, on solute concentration in the liquid phase. As such, diffusivity may be constant over the diffusion process or may change as diffusion time increases as the solution becomes more concentrated with the solute.

The experimental set-up for this study consists of diffusion cell surrounded by a temperature-controlled air bath (temperature from ambient to 180<sup>0</sup>C was controlled by electrical heaters installed). The methane gas was stored in a 500 cm<sup>3</sup> high pressure stainless steel cylinder. The diffusion cell which is a 400 cm<sup>3</sup> cylinder had three glass windows. The liquid level was not directly observed due to safety reason but a mirror image was provided by the reading from a precise cathetometer, which is equipped with a sliding scope and illumination system. The cell bore was designed such that 1 mm fluid level change corresponds to a volume change of 1 cm<sup>3</sup>. The diffusion cell permits examination of gas and liquids samples for pressures up to 70MPa (10,000psi) and temperature up to 180<sup>0</sup>C. The injection of gas and liquid at the desired pressure used fully automatic mercury pumps.

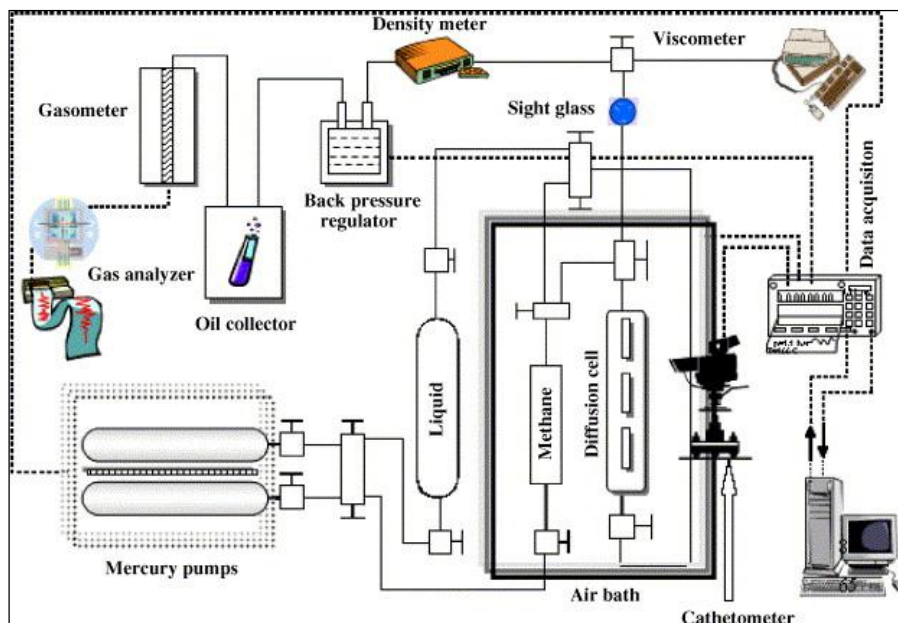


Figure 2.7: Schematic of a constant-volume cell (Jamialahmadi *et al.*, 2006)

Prior to the diffusion experiment, the cell was cleaned and dried. Air or any other gases was vacuumed out from the system. Then the cell was pressurized until it reached 0.025 kPa (0.004 psi). The liquid was then injected from the bottom upward and filled up to about 35% of cell volume. The pure methane was injected into the reservoir cylinder at the desired pressure. The heaters were then switched on until the

desired temperature is reached. The cell was then degassed and left for about 10 hours at the desired pressure and temperature to ensure homogeneous condition throughout the system. When the pressure in the cell reached the desired value, the top valve was closed and liquid level recorded. As time passes, methane diffuses into liquid phase, liquid level rises and its volume increases. Pressure was kept constant by continuous injection of mercury to the bottom of cell. Volume of dissolved methane in the liquid phase was determined as a function of time from: a) the movement of the interface, and b) position of the piston rod of the mercury pump. The diffusion coefficient was then determined from the volume-time data.

## **2.6 Other Studies on Gas Diffusivity in Hydrocarbon Liquid**

The interest on diffusion coefficient measurement was initiated long before the Riazi (1996), Zhang *et al.* (2000) and Jamialahmadi *et al.* (2006). Many earlier experimental methods have been developed for measurement of diffusion coefficient in gases and liquids as quoted by these three published reports. This includes Hill and Lacey (1934), Reamer *et al.* (1958), Gavalas *et al.* (1968), Woesner *et al.* (1969), McKay (1971), Lo (1974), Sigmund (1976), Schmidt *et al.* (1982), Denoyelle and Bardon (1984), Renner (1988) and Nguyen and Farouq Ali (1995). All these experiments studied various gas-liquid systems at various test conditions (temperature and pressure). Some of these earlier studies (Hill and Lacey, 1934; Reamer *et al.*, 1958; Woessner *et al.*, 1969; McKay, 1971; Lo, 1974; Sigmund, 1976; Denoyelle and Bardon, 1984; Renner, 1988) reported experimental measurements for hydrocarbon and petroleum systems at high pressures.

However, Riazi (1996) reported that most of the data gathered by these investigators are limited to pressures much lower than actual pressures in petroleum reservoirs due to equipment limitation. Zhang *et al.* (2000) highlighted that experimental tests are necessary due to the fact that there is no universal theory to calculate diffusion coefficients from other known properties of the gas-liquid system.

## **2.7 Comparison on Diffusion Coefficient for Various Binary Systems**

The results from various studies were compared as per Table 2.3.

Table 2.3: Comparison of diffusion coefficients of published studies

Reference	Gas	Liquid	Temperature (°C)	Pressure		Diffusion coefficient (m <sup>2</sup> /s)	Ref. for Results
				(kPa)	(psi)		
Riazi (1996)	Methane	n-Pentane	37.8	10,200	1,480	15.1 x 10E-9	Table 4 - Zhang et al (2000)
Zhang et al (2000)	Methane	Solvent oil (5.00 Pa.s)	21.0	3,510	509	8.6 x 10E-9	Table 4 - Zhang et al (2000)
	CO <sub>2</sub>	Solvent oil (5.00 Pa.s)	21.0	3,471	503	4.8 x 10E-9	Table 4 - Zhang et al (2000)
Jamialahmadi et al (2006)	Methane	Dodecane	45.0	up to 35,000	up to 5000	0.8 - 1.25 x 10E-8	Fig. 10 (a)- Jamialahmadi et al (2006)
			65.0	up to 35,000	up to 5000	1.05 - 1.5 x 10E-8	Fig. 10 (a)- Jamialahmadi et al (2006)
			81.0	up to 35,000	up to 5000	1.15 - 1.7 x 10E-8	Fig. 10 (a)- Jamialahmadi et al (2006)
	Methane	Iranian crude	25.0	up to 30,000	up to 4351	0.8 - 1.36 x 10E-8	Fig. 10 (b)- Jamialahmadi et al (2006)
			50.0	up to 30,000	up to 4351	0.98 0 1.64 x 10E-8	Fig. 10 (b)- Jamialahmadi et al (2006)
Nguyen & Farouq-Ali (1982)	CO <sub>2</sub>	Solvent oil (1.842 Pa.s)	21.15	3,450	500	3.2544 x 10E-9	Table 4 - Zhang et al (2000)
	Methane	Solvent oil (1.842 Pa.s)	57.11	3,450	500	6.9301 x 10E-11	Table 3 - Nguyen & Farouq Ali (1995)
			57.11	6,890	999	8.4217 x 10E-11	Table 3 - Nguyen & Farouq Ali (1995)
Schmidt (1989)	Methane	Solvent oil (8.36 Pa.s)	50.0	5,000	725	0.4 - 0.75 x 10E-9	Table 4 - Zhang et al (2000)
	CO <sub>2</sub>	Solvent oil (8.36 Pa.s)	50.0	5,000	725	0.5 x 10E-9	Table 4 - Zhang et al (2000)
Svrcek and Mehrotra (1982)	Methane	Solvent oil (4.46 Pa.s)	45.8	3,180	461		Table 4 - Zhang et al (2000)
	CO <sub>2</sub>	Solvent oil (6.43 Pa.s)	25.6	3,010	437		Table 4 - Zhang et al (2000)

The table has shown that the diffusion coefficients are different for each gas-liquid system. Since diffusion coefficient is a function of pressure, temperature and compositions, the diffusion coefficient would change when any of these conditions changed. Other factors that may contribute to the different diffusion coefficients results are the different test set-up and methods of analysis. However, a relationship between pressure and temperature to  $D_{AB}$  could be derived.

Hines and Maddox (1985) stated that temperature and  $D_{AB}$  has proportional relationship which means,  $D_{AB}$  increases at higher temperature. The same relationship is also observed from studies conducted by Jamialahmadi *et al.* (2006) and Nguyen and Farouq Ali (1995). In terms of  $D_{AB}$ 's relationship with pressure, Hines and Maddox (1985) stated that  $D_{AB}$  increases at lower pressure. Study by Riazi (1996) showed the same observation. However, findings by Jamialahmadi *et al.* (2006) and Nyugen and Farouq Ali (1995) showed the contrary. Other studies did not specifically study these relationships; as such no further comparisons could be made. These pressure and temperature relationships to diffusivity have also been discussed in relation to the earlier Table 2.2.

## 2.8 Literature Summary

From all the studies shown in Table 2.3 and earlier investigations described in section 2.6, there seemed to have no evidence of diffusion coefficient measurement of gas diffusivity in oil using gas-liquid samples from Malaysia or even the Malay basins. Hence, there is good potential for this research project to develop and evaluate the diffusion coefficient of the gas-liquid from Malaysian oilfields. It would benefit any oil recovery projects and provide better understanding on the transport properties of the gas-liquid systems.

In summary, all the reported experiments showed slightly different results when compared as they were performed at different binary systems, pressure and temperature conditions. Nonetheless, the reported diffusion coefficients are still within  $10^{-8}$  and  $10^{-9}$  m<sup>2</sup>/s for gas-liquid systems. This has at least given some indications on the expected results and its relationship at different pressures and temperatures.

For this project, mathematical model by Zhang *et al.* (2000) was adopted as it is simple yet very reliable for pure gas-liquid diffusivity measurement. The results shown in their study are comparable to other published values. According to Ping *et al.* (2009), the pressure draw-down method by Zhang *et al.* (2000) is one of the methods most widely used for gas-oil at static condition. In terms of its application at light oil system (i.e: < 10 cP), Fjelde *et al.* (2008) has also adopted this mathematical model in their CO<sub>2</sub>-synthetic seawater and CO<sub>2</sub>-oil systems in which the oil viscosity was 5.2 cP at 25°C. Hence, the correlation introduced by Zhang *et al.* (2000) and its method is likely to be suitable for gas-liquid diffusivity measurement for the Malaysian light oil systems.

In terms of the laboratory experiments, Zhang *et al.* (2000) utilized a stainless steel cylinder for the gas-liquid diffusion evaluation which is equipped with the necessary pressure gauges to monitor the pressure reading inside the mentioned stainless steel test cell. Moreover, they have simplified the measurement method from Riazi (1996) where interface measurement was not required. The same concept of laboratory set-up was adopted in this research but a high pressure PVT glass cell was used instead. In addition to that, some minor modifications to the existing normal PVT test set-up were made which include additional installation of high pressure gas cylinders and a new pressure transducer with an automated data acquisition system. A more detailed description of the associated equipment is described in Chapter 3: Methodology.

The practicality of the test method and its associated correlation, coupled with references made by other published reports (Ping *et al.*, 2009; Fjelde *et al.*, 2008; Jamialahmadi *et al.*, 2006) supported the choice for Zhang *et al.* (2000) as the selected reference for this current research.. Both diffusivity of pure gas-oil and multicomponent gas-oil systems were evaluated.

## CHAPTER 3

### RESEARCH METHODOLOGY

This chapter describes the experimental procedures, mathematical model and analysis to determine the gas diffusivity or also called diffusion coefficient of gas-liquid systems. The experiments were designed to run at preset pressure and temperature with regards to specific gas and oil compositions.

#### **3.1 Experimental Approach**

##### ***Phase 1: Preliminary experiments using pure gases (CO<sub>2</sub>, CH<sub>4</sub>) and water system.***

An experimental set-up based on published report by Zhang *et al.* (2000) with its relevant mathematical model was selected. Simple pure gas-water systems were used. Pure gases used were CO<sub>2</sub> and CH<sub>4</sub>. The diffusion coefficient values obtained were compared to published values at the specified initial pressures and test temperatures. The objectives of this phase are to establish the correct experimental set-up, test procedures and apparatus for gas-liquid diffusivity measurement and, to understand molecular diffusion concept.

##### ***Phase 2: Experiments using pure gases (CH<sub>4</sub>) and actual oil system.***

The experiment was extended to a pure gas-oil system. CH<sub>4</sub> was chosen as the pure gas based on findings in Phase 1. The same published correlation by Zhang *et al.* (2000) and its associated experimental set-up was used to determine the diffusion coefficient of the pure gas-oil system. The objectives of this phase are to establish that the chosen correlation and method of analysis is suitable for the measurement of diffusivity for a pure gas-oil system for the Malaysian oilfield and, to generate a simple relationship of diffusion coefficient to the oil properties of the Malaysian crude oil system.

**Phase 3: Experiments using multicomponent gases (actual produced gas) and actual oil system.**

The test is aimed to measure the diffusivity of actual gas and oil system under reservoir conditions for predetermined oil fields. This test is aimed to test if the chosen correlation by Zhang *et al.* (2000) is also applicable to a multicomponent gas-oil system for the Malaysian oilfield.

### 3.2 Test Apparatus

A Pressure Volume Temperature (PVT) unit available in Petronas Research Sdn Bhd's petroleum engineering lab's facility was utilized in the experiments. The test apparatus is shown in Figure 3.1.

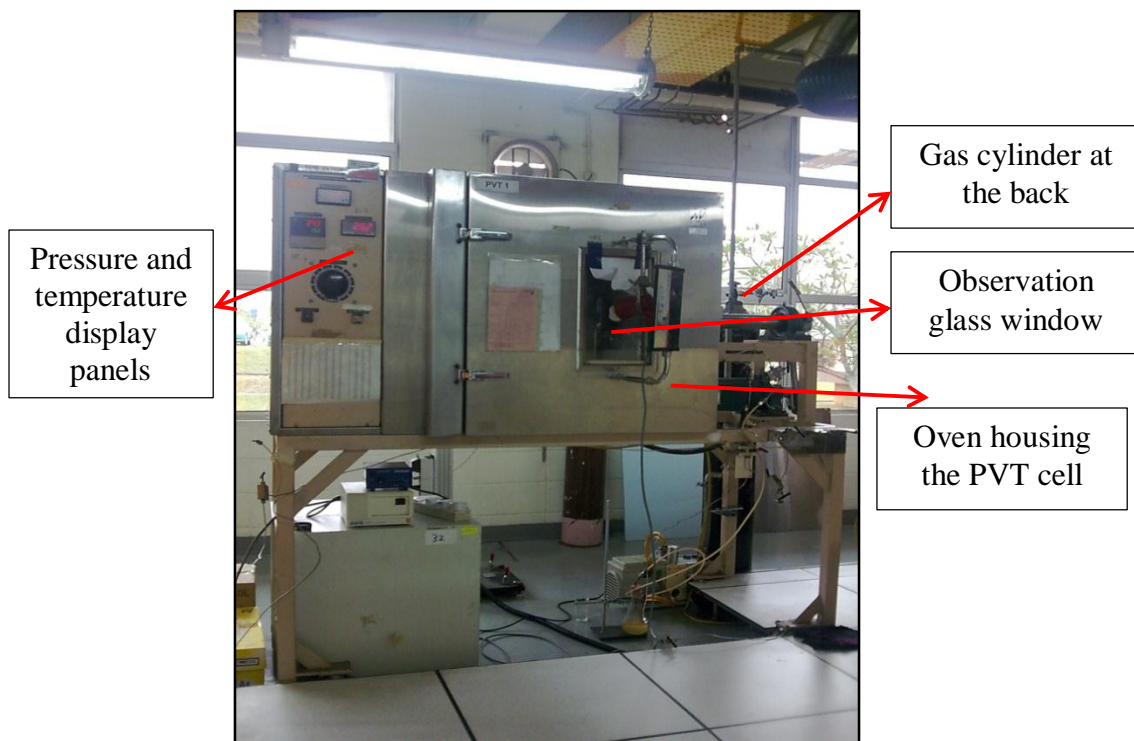


Figure 3.1: An overview of the PVT unit

The PVT unit is normally run for analysis of constant composition expansion, differential vaporization tests and other PVT analysis. It allows evaluation of actual gas and oil systems under the reservoir's high temperature, high pressure conditions. All the diffusivity experiments were conducted using the same PVT unit to ensure



consistency of the results. The schematic diagram of the diffusivity test set-up is presented in Figure 3.2.

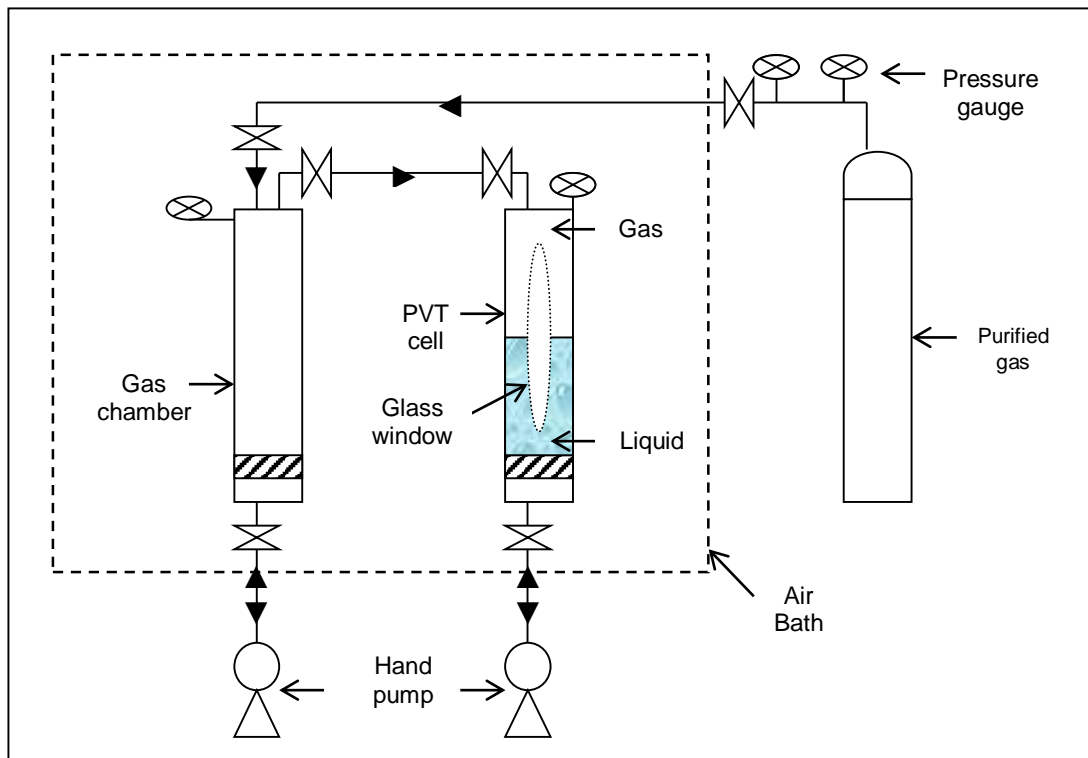


Figure 3.2: Schematic diagram of the diffusivity test set-up

The main component of the diffusivity test set-up is the PVT cell. It consists of a constant-volume PVT cell with long observation glass window. This window enables the monitoring of the gas-oil interface movement during the test. This movement can be captured via the video camera placed at the back of the PVT cell unit. This video camera moves vertically to constantly capture the image in the cell throughout the experiment. This image can be directly monitored via a monitor in which the interface level and piston position can be recorded

A high accuracy pressure gauge is mounted on top of the long windowed PVT cell to monitor the pressure change inside the cell throughout the experiment. The accuracy of this gauge is critical to enable measurement of very small pressure changes up to 0.001 psi unit.

The diffusion/PVT cell is surrounded by a temperature controlled air bath. The bath is partitioned such that a duct is separated from the area provided for the cell. The

duct houses the heaters, the thermostat and the blower, which provides forced air circulation through the bath.

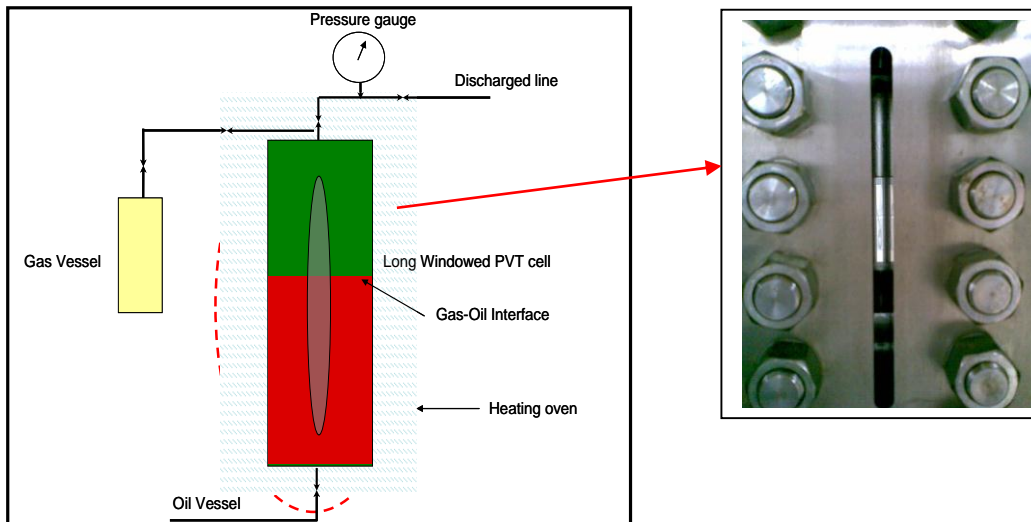


Figure 3.3: Schematic diagram of long windowed PVT cell (left) and the actual PVT window cell (right)



Figure 3.4: Video camera at the back of the PVT unit

The details of the main components in the diffusivity test set-up are below. The detail descriptions of the laboratory apparatus which include the type, model number and related information are presented in Appendix A.

- PVT Cell

The gas and oil samples are placed in the PVT pyrex glass cell and enclosed in A-286 stainless steel and hardened alloy steel (15% Ni and 15% Cr precipitation) PVT cell. The cross-sectional area of the glass cell is 1.23 in<sup>2</sup> (7.92 cm<sup>2</sup>) and the height is 6.52 in (16.56 cm). The PVT cell allows a maximum working pressure of 10,000 psia with safe working pressure of 8,000 psia. The samples in the cell can be examined up to maximum temperature of 200°C. The top flange of this cell is connected to the gas chamber while the bottom flange is equipped with a valve which permits the injection of oil into the glass cell. This cell is placed in a vertical position with two long glass windows each placed at the front and back sides permitting the interface level and piston position to be determined visually.

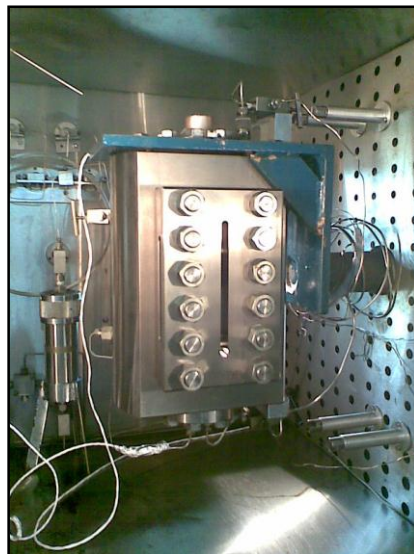


Figure 3.5: PVT cell

- Gas Chamber

The purified gas for the preliminary laboratory test (i.e.: CO<sub>2</sub> and CH<sub>4</sub>) and the actual dry gas samples are placed in this gas chamber before gas is injected into the PVT cell. The gas in this chamber is pressurized using the hand pump. This chamber can store gas volume up to 630 cc at maximum pressure of 15,000 psi and is connected to the top of the diffusion cell.



Figure 3.6: Gas chamber

- Hand Pump

Two (2) units of high pressure positive displacement pumps (referred as hand pump) using mineral oil as overburden liquid are utilized for the test. First hand pump is used to pressurize the gas sample in the gas chamber up to accuracy of 10 psi unit. Initial test pressure is set using this hand pump. Another hand pump is connected to the bottom piston of the PVT cell.



Figure 3.7: Hand pump

In this research, the basic principle of gas-liquid diffusivity measurement and test procedure is an adaptation of the method by Zhang *et al.* (2000). However, a number of improvements were made in terms of equipment used. This was done to enable the measurement of diffusion coefficient at elevated pressure and temperature systems. One major improvement is the utilization of a high pressure, high temperature PVT cell. Zhang *et al.* (2000) used a stainless steel cylinder which did not allow measurement at high pressure and temperature conditions. In addition, the monitoring

and measurement of the gas-liquid interface level were done automatically. A video camera was put in place which enable better monitoring of the gas-liquid diffusion scenario and interface conditions during the test. The image from this video was displayed to a monitor and automatically measured as shown in Figures 3.8 and 3.9. A highly accurate pressure acquisition system was also installed specially for this research to enable close monitoring of the pressure changes throughout the experiment which also include establishing the equilibrium condition.

### **3.3 Test Samples**

#### **3.3.1 Types of Fluids**

For Phase 1, experiments were conducted using highly purified carbon dioxide (99.95%) and highly purified methane (99.8%) as the gas phase, and deionized water as the liquid phase. For Phase 2, highly purified methane gas (99.8%) and actual crude oil (wellhead and separator samples) from selected candidate oil wells in Malaysia were tested. Finally, for Phase 3, experiments were performed using actual produced gas and crude oil samples (wellhead and separator samples) from the selected candidate oil wells.

#### **3.3.2 Sampling Methods**

This is applicable to the collection of the actual gas and liquid samples from the candidate wells. Minimum 500cc sampling bottles/cylinders are required. Sampling points for the gas and crude oil samples depend on the availability of the sampling equipment at each well. First option would be the separator oil and gas samples. Second option would be the wellhead samples, collected using PVT sampling cylinder.

If the gas and oil samples are collected from the test separator, the sampling pressure, temperature, gas flow rate, oil flow rate and gas-oil-ratio (GOR) data are recorded. If wellhead samples are gathered, the tubing head pressure and temperature are recorded.

Angsi fluid samples were the oil and gas separator samples gathered via high pressure sampling cylinders. At Sumandak oilfield, it is not possible to collect

separator fluid samples since the test separator unit was not available. Instead, the flowrate and volume of the produced fluid were measured using the Multiphase Flow Meter (MPFM) which does not allow any physical separation of the gas, oil and water. Therefore, the best collection method is via the sampling point at the wellhead. Detailed collection methods are described in Appendix A.

### **3.4 Sample Preparation**

The fluid samples gathered either from the wellhead or separator was sent for quality check at PETRONAS Research's PVT laboratory facility. This is to ensure free contamination and representative samples were gathered for the purpose of gas diffusivity analysis. Special quality check procedures were followed for the separator gas and oil samples. These samples, contained in stainless steel pressurized test cylinders underwent standard PVT fluid quality check before the respective gas and oil samples were flashed (i.e.: separated) for further analysis. These flashed fluid samples were sent for compositional analysis. Detail procedures on quality checking are explained in Appendix A.

For the liquid samples, only oil samples from the candidate oilfield were sent for compositional analysis using the High Temperature Gas Chromatograph (HTGC) unit (Hewlett Packard, Model No. HP 5890 series II plus). The purpose is to determine the respective hydrocarbon components for each oil sample. Other additional tests include viscosity and density tests.

For the gas samples, only compositional analysis is required. If the produced gas gathered from either the wellhead or separator is used, the gas samples would be sent for compositional analysis using the Natural Gas Analyzer unit (Agilent Technologies, Model No. 6890N). However, if pure gas such as methane and carbon dioxide is used, no compositional analysis is necessary since the fluid properties are known.

### **3.5 Equipment preparation**

Before initiating the diffusion experiment, the oven encapsulating the PVT unit and the gas chamber was heated up to the test temperature. Once this temperature had

stabilized, the sample gas was filled into the gas chamber. This pressurized gas sample was then transferred to the PVT glass cell until reaching a 100cc volume. This total volume (100cc) was marked and the gas-liquid interface and piston bottom positions were recorded. This is important for ensuring a constant volume condition throughout the experiment. Leak test was performed to ensure no leakage at the tubing and joints. This is especially critical when flammable gas such as methane is used. After this step was done, the entire transferred gas sample was vacuumed and the PVT glass cell was left empty.

The liquid sample was then filled into the PVT glass cell while the gas sample was re-filled into the gas chamber and pressurized. The liquid sample was then de-gassed (if water is used). At this point, it is necessary to maintain a constant temperature for the experiment.

### 3.6 Test Procedure

This experiment involved constant volume and constant temperature test conditions. A 100 cc total gas and liquid volume was used at the desired gas-liquid volume ratios. The initial test pressure was estimated using pressure-volume relationship from the ideal gas law per below:

$$P_1V_1 = P_2V_2 \quad (3.1)$$

Where:

$P_1 \equiv$  Set pressure in the gas chamber

$V_1 \equiv$  Volume of gas in the gas chamber

$P_2 \equiv$  Desired initial test pressure in the gas chamber

$V_2 \equiv$  Volume of gas in the PVT test cell

Before the gas diffusivity experiment began, it is important to ensure that the desired test pressure in the high pressure gas chamber and also the test temperature has stabilized. Once this is achieved, the pressurized test gas sample was slowly transferred from the gas chamber into the long windowed PVT glass cell until the total

fluid reached the 100cc total volume marked earlier. The PVT glass cell was immediately isolated and the cell's initial pressure, temperature and the gas-liquid interface level were recorded. At this point, there would be a decrease in pressure until equilibrium condition is reached. During this time, the pressure, temperature, interface level and piston bottom level were recorded. Test was then stopped when no significant pressure change is observed ( $< 2$  psi change). This shall indicate an equilibrium condition. Throughout the experiment, the temperature was kept constant as much as possible. Temperature changes affect pressure. A detailed test procedure is explained as per Appendix A.

### 3.7 Data Measurement and Acquisition

An automated pressure and temperature data acquisition system are linked to the PVT unit. This is an additional upgrade of the current PVT unit set-up to enable more accurate data capturing and analysis for diffusion coefficient measurement. This automated data acquisition system has the ability to record the PVT glass cell's temperature and pressure and generated respective plots. Users can choose the desired frequency of data capture (i.e.: every 10 seconds). Besides giving a substantial monitoring of the test, it also allows better determination of the equilibrium condition. The automated pressure and temperature data acquisition system is illustrated in Figures 3.8 and 3.9.

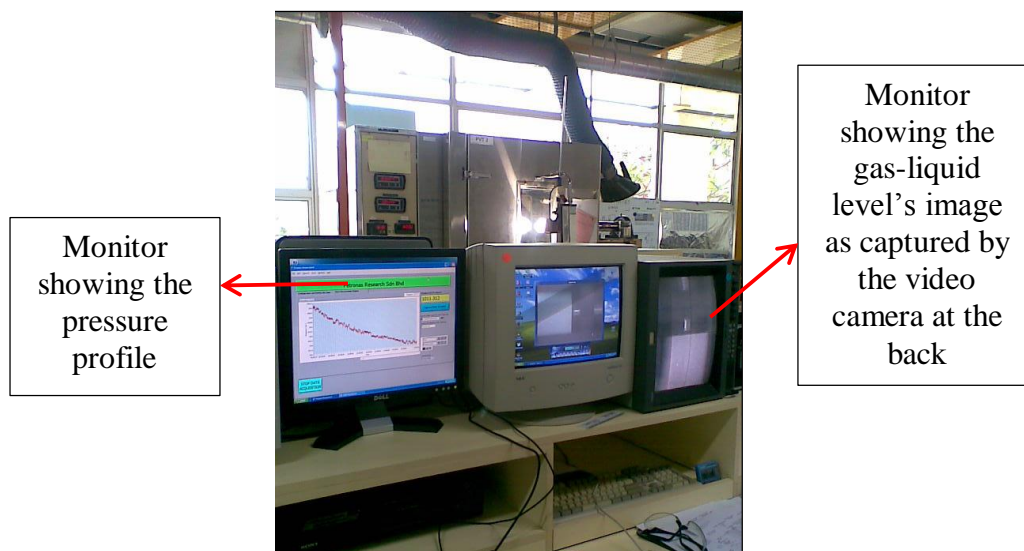


Figure 3.8: Data acquisition system



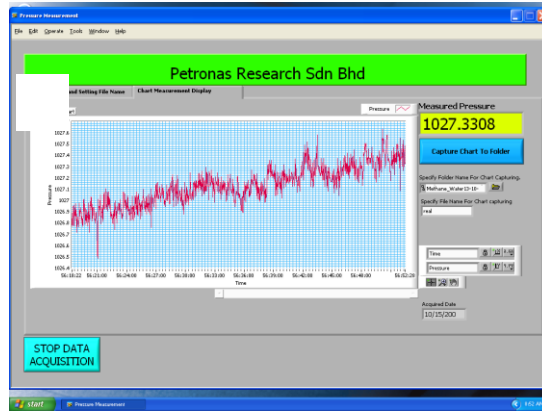


Figure 3.9 : Screen shot of the pressure plot

The pressure-time measurement is important for the purpose of diffusion coefficient analysis. The first data is read on the first maximum pressure after all the gas has been released. It is also called the initial pressure which the highest pressure observed after the gas is fully released. Molecular diffusion starts at this point.

All the pressure-time data captured is saved under a Microsoft Excel file. The trend of the data was analyzed and for efficient data analysis, a simple Visual Basic program was used in which pressure data captured every second by the data acquisition software was sampled at every 1000 second interval. Figures 3.10 and 3.11 show the snapshots of the data capturing and related Visual Basic program.

D2779		f <sub>c</sub> 1266.3894														
	A	B	C	D	E	F	G	H	I	J	K	L	M	N		
1	Date	Time	Time (sec)	Pressure (psi)	Pt - Peq (psi)	Pt - Peq (kPa)	ln(Pt - Peq)						0	6.8269726		
2					Assumed Peq	TIS	psi @ 482000 sec						1000	6.8437939		
3	5/20/2009	10:16:00		107.7221									2000	6.8021877		
4													3000	6.5684726		
5	5/20/2009	10:16:02		107.6461									4000	6.5368255		
6													5000	6.5157996		
7	5/20/2009	10:16:07		107.4239									6000	6.4668656		
8													7000	6.4661444		
9	5/20/2009	10:16:12		107.4371									8000	6.4370426		
10													9000	6.4102814		
11	5/20/2009	10:16:17		107.3765									10000	6.3863722		
12													11000	6.3688213		
13	5/20/2009	10:16:22		107.4379									12000	6.3459124		
14													13000	6.3231965		
15	5/20/2009	10:16:27		107.6004									14000	6.2985994		
16													15000	6.2861466		
17	5/20/2009	10:16:32		107.5811									16000	6.2693784		
18													17000	6.2652577		
19	5/20/2009	10:16:37		107.4771									18000	6.2492813		
20													19000	6.2404784		
21	5/20/2009	10:16:42		107.3772									20000	6.2290099		
22													21000	6.1771089		
23	5/20/2009	10:16:47		107.3594									22000	6.1639925		
24													23000	6.1555525		
25	5/20/2009	10:16:52		107.3759									24000	6.137643		
26													25000	6.1276598		
27	5/20/2009	10:16:57		107.3925									26000	6.1184539		
28													27000	6.1103523		
29	5/20/2009	10:17:02		107.4399									28000	6.0805126		
30													29000	6.0651952		
31	5/20/2009	10:17:07		107.4297									30000	6.0587361		
32													31000	6.027894		
33	5/20/2009	10:17:12		107.4385									32000	6.0166338		
34													33000	6.0045072		
35	5/20/2009	10:17:17		107.4441									34000	5.9746337		
36													35000	5.9617581		
37	5/20/2009	10:17:22		107.3645									36000	5.9507652		
38													37000	5.9271479		
39	5/20/2009	10:17:27		107.4118									38000	5.913109		
40													39000	5.8974812		
41	5/20/2009	10:17:32		107.2592									40000	5.8706061		
42													41000	5.8586659		
43	5/20/2009	10:17:37		107.2138									42000	5.8333281		
44													43000	5.8125007		
45	5/20/2009	10:17:42		107.3472									44000	5.8130984		
46													45000	5.7881722		
47	5/20/2009	10:17:47		107.209									46000	5.7619477		
48													47000	5.7522077		
49	5/20/2009	10:17:52		107.2009									48000	5.7455621		
50													49000	5.7290604		

Figure 3.10: Raw data selection using Visual Basic program

```

CommandButton1 Click
Private Sub CommandButton1_Click()

Dim R1TMP(250) As Double, R2TMP(250) As Double, R3TMP(250) As Double, Dev As Double
Dev = 2

For I = 1 To 80

' I = (I - 1) * 400 + 2379
' Note: '2379' is the row no. in the formula -is the 1st point to calculate based on every 1000 interval

R1TMP(I) = Sheets("1").Range("C" & (I - 1) * 400 + 2379).Value

R3TMP(I) = Sheets("1").Range("F" & (I - 1) * 400 + 2379).Value

If R3TMP(I) > 0 Then

R2TMP(I) = Sheets("1").Range("G" & (I - 1) * 400 + 2379).Value

End If

If R2TMP(I) > Dev Then
Sheets("1").Range("M" & I).Value = R2TMP(I)
End If

Sheets("1").Range("L" & I).Value = R1TMP(I)

Next I

End Sub

```

Figure 3.11: Code in Visual Basic program

### 3.8 Mathematical Analysis

#### 3.8.1 Fundamental Mathematical Model

The determination of the diffusion coefficient from pressure-time profiles in the experiment is based on a mathematical analysis from Zhang *et al.* (2000). The diffusion model is shown schematically as per Figure 3.12 below:

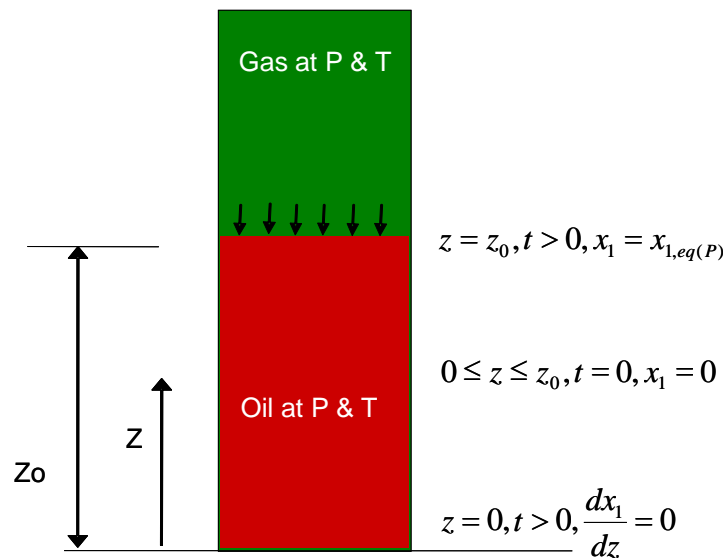


Figure 3.12 : Schematic and dimension of the diffusion process model

Based on the schematic above;

- $z$        ≡       liquid position along the diffusion cell (cm)
- $z_o$      ≡       height of the liquid in the cell (cm)
- $x_1$      ≡       initial molar concentration of gas in the liquid phase (component 1)  
(mol/cm<sup>3</sup>)
- $x_{1,eq(P)}$  ≡       gas-liquid interface molar concentration (component 1) at a  
given time (mol/cm<sup>3</sup>)
- $t$        ≡       time (s)
- $P$        ≡       pressure (psi)
- $T$        ≡       temperature (°C)

The gas-liquid interface is located at  $z = z_o$  and bottom of cell is  $z = 0$ . The initial molar concentration ( $x_1$ ) is assumed zero while  $x_{1,eq(P)}$  varies with temperature and

pressure. However, since temperature is constant,  $x_{1,eq(P)}$  is therefore, varies only with pressure.

The diffusion process model as in Figure 3.12 above is possible with some assumptions as reported in the study by Zhang *et al.* (2000). First assumption is that the swelling of the liquid phase is negligible. Therefore,  $z_o$  remains constant in the experiment. Secondly is that the concentration at the gas-liquid interface is the equilibrium concentration. Thirdly, the temperature remains constant throughout the test. Fourthly is that the diffusion coefficient,  $D_{AB}$ , does not change significantly with concentration during the range of concentration difference in the experiment. Finally, is that the oil is non-volatile.

Based on 2<sup>nd</sup> Fick's Law, the molar flux of gas diffusing into oil can be expressed as:

$$\frac{dx_1}{dt} + v \frac{dx_1}{dz} = D_{AB} \frac{d^2 x_1}{dz^2} \quad (3.2)$$

Where:

- $x_1$      ≡     initial molar concentration of gas in the oil phase (component 1)  
                  (mol/cm<sup>3</sup>)
- $D_{AB}$    ≡     diffusion coefficient (m<sup>2</sup>/s)
- $z$        ≡     liquid position along the diffusion cell (cm)
- $t$        ≡     time (s)
- $v$        ≡     molar average velocity

The diffusion model has considered that when gas is injected, the pressure varies with position but at later times, the pressure is assumed independent of position and varies only with time. Therefore;

$$\frac{dp}{dz} = 0 \quad (3.3)$$

From Equation 3.2 above, the liquid is assumed to be at rest throughout the experiment. Thus;

$$v \frac{dx_1}{dz} = 0 \quad (3.4)$$

The boundary and initial conditions are as follows:

$$z = z_o, t > 0, x_1 = x_{1,eq(P)} \quad (3.5)$$

$$z = 0, t > 0, \frac{dx_1}{dz} = 0 \quad (3.6)$$

$$0 \leq z \leq z_o, t = 0, x_1 = 0 \quad (3.7)$$

From Equation 3.2 and considering the above assumptions (Equations 3.3 to 3.7), the diffusion model is simplified to an unsteady state one dimensional diffusion expression as below:

$$\frac{dx_1}{dt} = D_{AB} \frac{d^2 x_1}{dz^2} \quad (3.8)$$

This diffusion equation is later derived as per Zhang *et al.* (2000) to get a simplified diffusion coefficient equation that relates to the pressure-time profiles from the diffusion experiment. The derivation approach is described in Appendix C.

### 3.8.2 Graphical Method

In order to determine the diffusion coefficient value from a pressure-time profile, Equation 3.9 below is used. This equation was derived as described in Appendix C. It can be expressed in a linear plot of  $y = mx + c$ . This is known as the graphical method.

$$\ln[P(t) - P_{eq}] = \ln\left(\frac{8Bz_o x_{1,eq(P)}}{\pi^2}\right) - \frac{\pi^2 D_{AB} t}{4z_o^2} \quad (3.9)$$

Therefore, this plot yields:

$$\begin{aligned} \text{y-axis} &\equiv \ln[P(t) - P_{eq}] \\ \text{x-axis} &\equiv t \\ \text{Slope} &\equiv -\frac{\pi^2 D_{AB}}{4z_o^2} \\ \text{Intercept} &\equiv \ln\left(\frac{8Bz_o x_{1,eq(P)}}{\pi^2}\right) \end{aligned}$$

By plotting the log pressure versus time of the experiment data, a straight line fit can be obtained. From this straight line fit, the  $D_{AB}$  can be calculated from the slope. In this method however, a value of  $P_{eq}$  need to be estimated.  $P_{eq}$  would be the equilibrium pressure at which the pressure has no significant change and at the stagnant stage (< 2 psi change) from the pressure profile.

### 3.8.3 Numerical Method

An alternate method in determining the  $D_{AB}$  value is using a non-linear regression data analysis called numerical method. It involves a numerical expression that agrees with below equation (described as Equation C1.7 in Appendix C) to the pressure-time data relationship.

$$P(t) - P_{eq} = \frac{8Bz_o x_{1,eq(p)}}{\pi^2} \sum_{n=0}^{\infty} \frac{1}{(2n+1)^2} \exp\left(-\frac{(2n+1)^2 \pi^2 D_{AB} t}{4z_o^2}\right) \quad (3.10)$$

The equation above is simplified and expressed as in Equation 3.11 (Zhang *et al.*, 2000):

$$P(t) = m_1 \exp\left(-\frac{t}{k_1}\right) + m_2 \exp\left(-\frac{t}{k_2}\right) + P_{eq} \quad (3.11)$$

Non-linear regression of the experimental data has to be performed to determine the values of  $m_1$ ,  $m_2$ ,  $k_1$ ,  $k_2$  and  $P_{eq}$ . A simplified  $D_{AB}$  equation is then obtained as follows:

$$D_{AB} = \frac{4z_o^2}{k_1\pi^2} \quad (3.12)$$

Where:

- $z_o$      ≡     length of the liquid column in the cell
- $k_1$      ≡     constant determined by regression

The numerical method used the FindGraph software to enable the data being expressed as per Equation 3.11. The advantage of this method is that the equilibrium pressure is automatically calculated by the software and not estimated from the pressure profile. A comparison of the equilibrium pressure ( $P_{eq}$ ) between the graphical and numerical method is discussed in the next chapter.

The detailed method on transferring the raw pressure-time data to FindGraph software and related analysis are described in Appendix B.

### 3.9 Validation Methods

For the purified gas-water systems and the methane-actual oil systems, published gas-liquid diffusion coefficients were used to validate the results at the closest temperature and pressure conditions. As for the actual gas-actual oil system, the diffusion coefficient results were compared to its methane-actual oil systems and relationship towards the pressure, temperature and compositional properties were evaluated.

## CHAPTER 4

### RESULTS AND DISCUSSION

This chapter has been organized into three main sections. The diffusion study on pure gas-water system is reported and evaluated in section 4.1. The study on pure gas-crude oil system is presented in section 4.2 which also include the analysis of the effect of pressure, temperature and composition to gas-liquid diffusion. Finally, the diffusion on actual multicomponent gas-crude oil system is discussed in section 4.3.

#### **4.1 Phase 1: Diffusivity of Pure Gas-Water System**

The objective of the preliminary experiments was to gauge the reliability and repeatability of the experimental procedure as well as equipment integrity. The correct approaches were evaluated by comparing the measured and published data. Experiments were conducted at different temperature, pressure and gas-liquid volume ratios and to establish relationships of diffusion coefficient within the various test conditions. The tuning of the experimental procedure was carried out with a series of preliminary experiments. The results from the experiments were compared to published diffusion coefficient as per Table 4.1.



Table 4.1 : Published diffusion coefficients for various gas-oil systems

Reference	Gas	Liquid (viscosity)	Temperature (°C)	Pressure		Diffusion coefficient (10 <sup>-9</sup> m <sup>2</sup> /s)
				(kPa)	(psi)	
<b>CH<sub>4</sub> - oil</b>						
Riazi (1996)	CH <sub>4</sub>	n-Pentane (0.23 cP)	37.8	10,200	1,480	15.1
Zhang <i>et al.</i> (2000)	CH <sub>4</sub>	Solvent oil (5,000 cP)	21.0	3,510	509	8.6
Jamialahmadi <i>et al.</i> (2006)	CH <sub>4</sub>	Iranian crude (0.16 - 0.29 cP)	25.0	3,500 - 27,500	508 - 3,989	8.0 to 13.8
			50.0	3,500 - 27,500	508 - 3,989	9.8 to 16.4
	CH <sub>4</sub>	Dodecane (1.34 cP)	45.0	4,000 - 35,000	580 - 5,076	8.0 to 12.5
			65.0	4,000 - 35,000	580 - 5,076	10.5 to 15.0
			81.0	4,000 - 32,000	580 - 4,641	11.5 to 17.0
Schmidt (1989)	CH <sub>4</sub>	Solvent oil (8,360 cP)	50.0	5,000	725	0.40 to 0.75
<b>CH<sub>4</sub> - water</b>						
Sach (1998)	CH <sub>4</sub>	Water (liquid)	25.0	8,200	1,189	1.40
	CH <sub>4</sub>	Water (liquid)	40.0	8,000	1,160	2.60
	CH <sub>4</sub>	Water (liquid)	50.0	7,600	1,102	3.57
	CH <sub>4</sub>	Water (liquid)	50.0	32,500	4,713	3.25
<b>CO<sub>2</sub> - oil</b>						
Zhang <i>et al.</i> (2000)	CO <sub>2</sub>	Solvent oil (5,000 cP)	21.0	3,471	503	4.80
Nguyen & Farouq-Ali (1982)	CO <sub>2</sub>	Solvent oil (1,842 cP)	21.15	3,450	500	3.25
Schmidt (1989)	CO <sub>2</sub>	Solvent oil (8,360 cP)	50.0	5,000	725	5.00
Hill and Lacey (1934)	CO <sub>2</sub>	Oil (25 - 12000 μ <sup>2</sup> /μ <sup>2</sup> )	30 - 60	2,070	300	0.7 to 13.3
<b>CO<sub>2</sub> - water</b>						
Welty <i>et al.</i> (1984)	CO <sub>2</sub>	Water (liquid)	9.85	101.35	14.7	1.46
	CO <sub>2</sub>	Water (liquid)	19.85	101.35	14.7	1.77

#### 4.1.1 Carbon Dioxide -Water System

Tests were conducted using highly purified CO<sub>2</sub> (99.8%) as the gas phase and deionized water as the liquid phase at temperature of 50°C and different pressures. The measured diffusion coefficients were then compared to the published values shown in Table 4.2.

Table 4.2 shows that at constant temperature, diffusion coefficient of CO<sub>2</sub> in water slightly increases at higher pressure. The same trend of observation has also been reported by Jamialahmadi *et al.* (2006) and Nguyen and Farouq Ali (1995) which investigated gas-liquid diffusion coefficients at different pressures and temperatures. However, there are no studies conducted at the same test conditions that can be used to compare with. Under similar gas-liquid system but different laboratory set-up, the reference study, Welty *et al.* (1984) also produced lower diffusion coefficients at lower pressure and temperature.

Table 4.2 : Comparison of CO<sub>2</sub> – water system with published values (using graphical method)

Reference	Gas	Liquid	Gas-oil ratio	Initial pressure (psi)	Temperature (°C)	Diffusion coefficient (m <sup>2</sup> /s)
Test 1	CO <sub>2</sub>	Water	50:50	844	60.0	7.16E-07
Test 2	CO <sub>2</sub>	Water	50:50	430	60.0	6.49E-07
Welty <i>et al.</i> (1984)	CO <sub>2</sub>	Water	-	14.7	19.9	1.77E-09

During the experiment, it was observed that there were turbulence at the gas-liquid interface, which was largely due to chemical reaction between CO<sub>2</sub> and water at the operated temperature and pressure. Carbon dioxide reacts chemically with water to form carbonic acid. It potentially has massive effect on the concentration profile that may cause the diffusivity to be erroneous. Relatively, this also produces fluxes on the gas-liquid interface and distorts molecular diffusion measurement. Even if the trend of the diffusion coefficient with pressure and temperature follows the expected relationship based on the reported results (Jamialahmadi *et al.*, 2006; Upreti and Mehrotra, 2002; Nguyen and Farouq Ali, 1995), validation of the experimental set-up using CO<sub>2</sub>-water system could not be used. It was noted that this turbulence was not caused by fast injection rate of the gas stream since proper measures were taken to ensure that the gas was slowly transferred from the gas chamber into the long windowed PVT glass cell.

According to Riazi (1996), molecular diffusion is applicable when there is no convection taking place in the system. Following this, Zhang *et al.* (2000) assumed zero convection in their mathematical model in which the oil was at rest during the experiment. Similarly, the concentration of the gas and liquid at its interface is the equilibrium condition. As such, there should not be concentration difference at the interface and apparently, no influx and assures no free convection. In the CO<sub>2</sub>-water system, fluxes at the interface resulting from the gas-water chemical reaction are against the molecular diffusion concept. Chemical reaction may falsify the diffusivity measurement as it creates an unstable condition at the gas-liquid interface.

For future molecular diffusion experiments, non-chemically reactive gas-liquid systems should be selected. Even so, turbulence at the gas-liquid interface should also be avoided to ensure no free convection. Much attention and care are required when

releasing the high pressure sample gas into the PVT cell. The sample gas needs to be released slowly into the cell to avoid any turbulence condition.

#### **4.1.2 Methane -Water System**

Further tests were performed using CH<sub>4</sub> – water systems. Highly purified CH<sub>4</sub> gas (99.95%) and deionized water were used. A number of tests were conducted to evaluate results at different pressure, temperature and gas-liquid volume ratios. These relationship need to be established in order to understand the anticipated trend of diffusivity for the actual gas-oil samples.

In order to validate the experimental set up, CH<sub>4</sub>-water diffusion tests were run and similar test conditions as per published study by Sach (1998) were adopted. However, in the actual tests, an exactly similar initial pressures per Sach (1998) could not be achieved due to limitations of the laboratory set-up. The control systems (i.e.: valves) were all manually operated rather than automated and hence, it was quite difficult to achieve the targeted test pressure as desired. Nonetheless, the difference between the set and actual is < 10% and was therefore, acceptable.

Table 4.3 shows that diffusion coefficient value from Test 4 agrees with the study by Sach (1998). Slight difference in the results may be due to different experimental set-up and gas-oil ratio used. It was observed that gas-oil ratio of 75:25 produced a closer match with the published values as compared with others. This suggested that higher gas volume is needed to compensate for the low solubility of methane gas in water, which is 0.4 ml/100ml of water at 20°C (Perry *et al.*, 1997).

Solubility affects the rate of absorption and diffusivity. Low solubility means lower driving force and rate of mass transfer. This may contribute to the longer time in reaching an equilibrium condition. Knowledge on gas-liquid solubility is required to plan for diffusion test.

Table 4.3: Comparison of CH<sub>4</sub> – water system with published values (using graphical method)

Reference	Gas	Liquid	Gas-oil ratio	Initial pressure (psi)	Temperature (°C)	Diffusion coefficient (m <sup>2</sup> /s)
Test 1	CH <sub>4</sub>	Water	50:50	1035	50.0	8.31E-06
Test 2	CH <sub>4</sub>	Water	50:50	1052	50.0	7.42E-06
Test 3	CH <sub>4</sub>	Water	50:50	1078	50.0	1.58E-08
Test 4	CH <sub>4</sub>	Water	75:25	994	50.0	4.06E-09
Sach (1998)	CH <sub>4</sub>	Water	(Not reported)	1102	50.0	3.57E-09

From all the four tests listed in Table 4.3, it is learned that more data points are required to analyze small pressure changes. A more sensitive, accurate and automatic data acquisition system is needed to generate reliable pressure profile for diffusivity analysis. It is especially important to enable future diffusion coefficient analysis using numerical method by Zhang *et al.* (2000). The numerical method is a non-linear regression analysis which needs a reasonable pressure history to enable correct computation of the regression parameters in determining diffusion coefficient values. For these preliminary experiments, only graphical analysis method by Zhang *et al.* (2000) was used for diffusion coefficient measurement. The numerical analysis was performed to a more complex gas-oil system in later tests.

The successful results from the CH<sub>4</sub>-water system suggested that the proposed laboratory set-up and mathematical model used might be valid, repeatable and capable of handling other binary gas-liquid or even more complex systems.

#### 4.2 Phase 2: Diffusivity of Pure Gas-Actual Oil System

In Phase 1, tests were conducted using pure gas and water systems to validate the experimental set-up, test procedure and method of analysis for diffusion coefficient measurement. In this preliminary phase, pure gas and water system were chosen since they were considered to represent a simple binary system consisting of a single component gas and known water system and does not require offshore sampling work.

In Phase 2, the study focused more towards the actual hydrocarbon system. The principle calculation approach by Zhang *et al.* (2000) is again adopted. This time, both

graphical and numerical methods were utilized in the diffusion coefficient calculation for comparison purpose. Zhang *et al.* (2000) mathematical model was designed for pure gas-heavy oil system. However, Fjelde *et al.*, (2008) has also adopted the same mathematical model in their CO<sub>2</sub>-synthetic seawater and CO<sub>2</sub>-oil systems in which the oil viscosity was 5.2 cP at 25°C. Based on this reported study, diffusion coefficients obtained using this approach has suggested that the same model may be also applicable for other pure gas in light oil system.

Temperatures of the tests were set at 60°C for Sumandak and 90°C for Angsi while pressures were varied. These temperatures were selected based on each field's estimated bottomhole reservoir temperature. Compositional analysis of the oil samples were performed using the High Temperature Gas Chromatograph (HTGC) unit. Figures 4.1 to 4.4 show the different hydrocarbon components in each oil sample. The HTGC spectrum per Figures 4.1 and 4.3 were obtained directly from the gas chromatograph's calculated area versus retention time of each specific hydrocarbon component. The interpreted compositions (Figures 4.2 and 4.4) however, were the selected hydrocarbon components which are simplified for the purpose of this study. The areas of peaks in between the n-paraffins are added to the higher carbon number (i.e.: peaks in between nC<sub>6</sub>-nC<sub>7</sub> are summed as C<sub>7</sub>). The molecular weight and density used for this summation are according to Firoozabadi & Katz's typical values (Firoozabadi *et al.*, 1978). This interpretation is used for both Angsi and Sumandak crude oil even when Sumandak's oil is naturally a biodegraded oil type. As observed, there is no distinct hydrocarbon peak in Sumandak (as in Figure 4.1) as compared to Angsi's as presented in Figure 4.3.

Detail compositions for the crude oil samples are presented in Appendix D. From the tables presented in Appendix D, Sumandak crude oil has higher compositions of the heavier components (i.e.: C<sub>7</sub>+) which is 99.89 wt% as compared to Angsi which has 97.65 wt%. This contributed to a higher crude oil viscosity for Sumandak which is 10.40 cP as compared to Angsi's viscosity which is 4.73 cP.

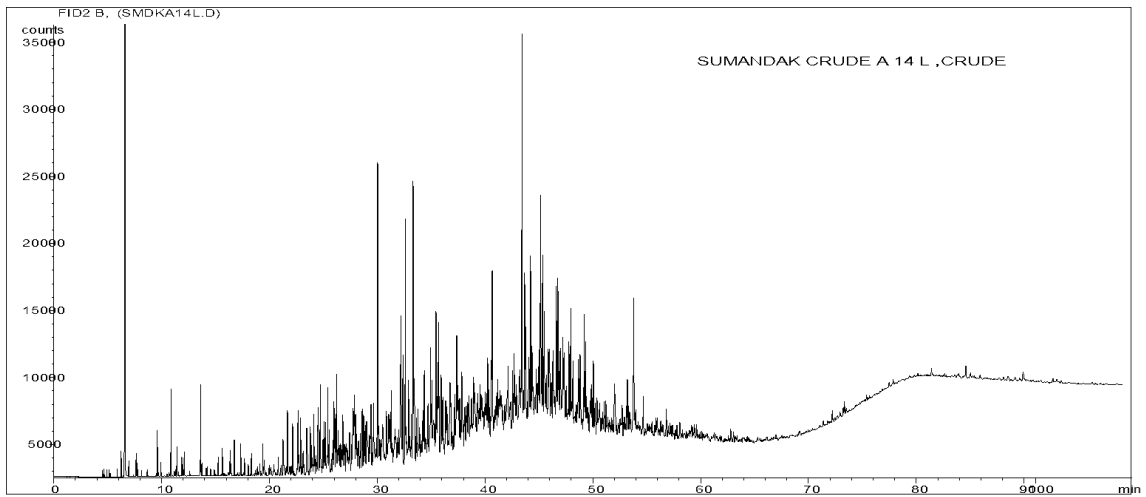


Figure 4.1: HTGC spectrum for Sumandak crude oil (wellhead sample)

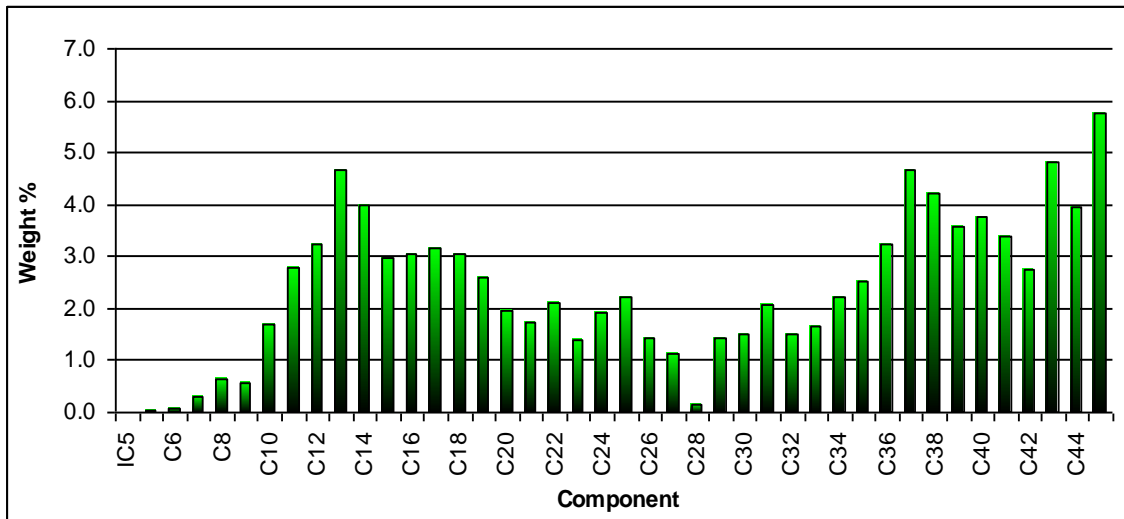


Figure 4.2: Interpreted compositions of Sumandak crude oil (wellhead sample)

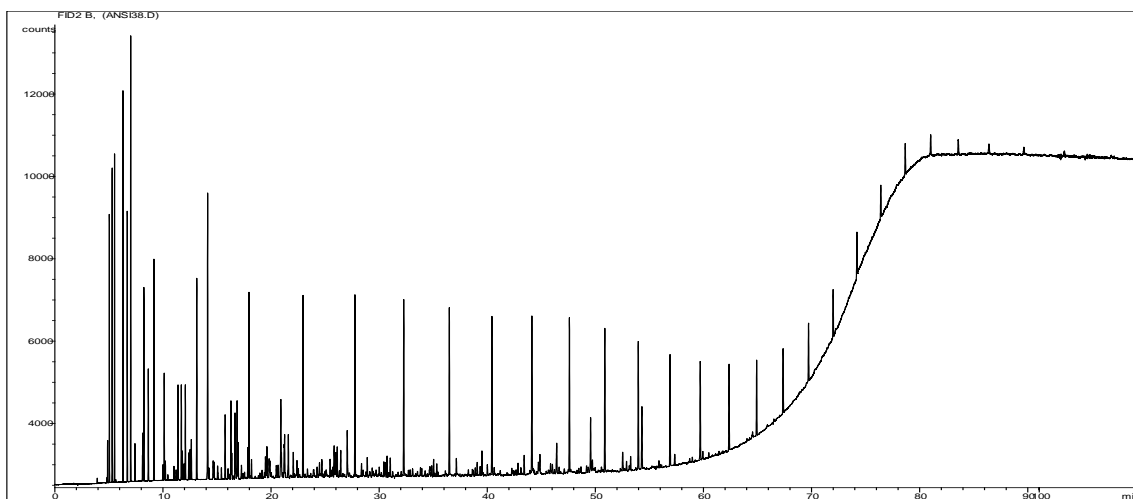


Figure 4.3: HTGC spectrum for Angsi crude oil (separator sample)

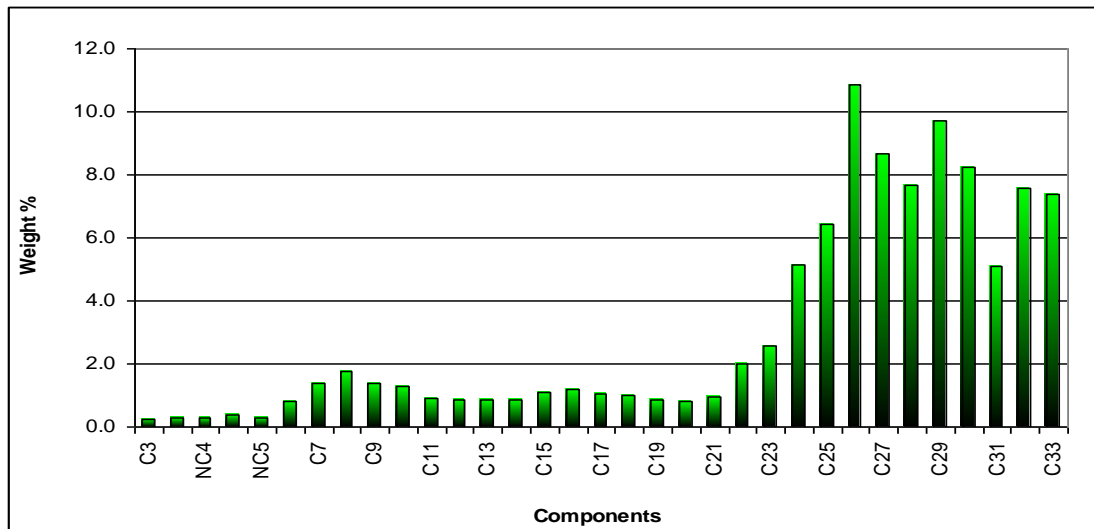


Figure 4.4 : Interpreted compositions of Angsi crude oil (wellhead sample)

#### 4.2.1 Methane-Sumandak Oil System

Figure 4.5 shows the experimental pressure-time profile for the methane-Sumandak oil system. The rapidly decreasing pressure at the initial period is called “incubation period” (Renner, 1988). This is when the gas dissolved in the oil at the early stage. Then, the pressure slowly decreased until it reached equilibrium, a state where the differential pressure is assumingly zero. The pressure decay profile and estimated equilibrium pressure for each of the methane-oil system was different owing to the respective pressure conditions. As observed, higher initial test pressure required shorter time to reach equilibrium. In the PVT test cell, the oil was at atmospheric condition while the test gas to be released was at higher pressure. At higher test pressure, there was larger pressure difference between the two phases. It seemed that higher test pressure gave an earlier equilibrium condition.

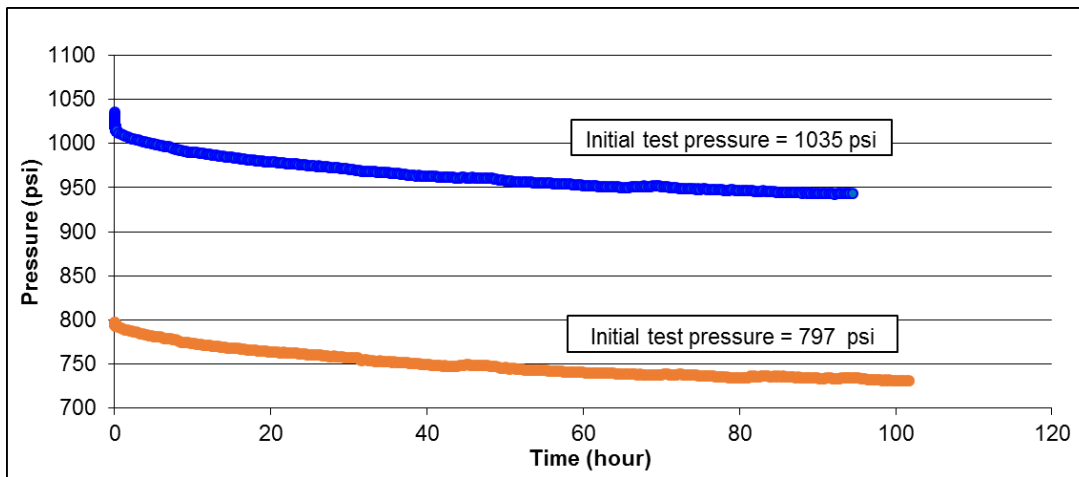


Figure 4.5: Methane-Sumandak oil pressure decay profile at different initial pressures

The pressure-time data were further translated into semi logarithmic pressure-time plot (graphical method) and non-linear exponential pressure-time plot (numerical methods). The diffusion coefficient results calculated from both methods were then compared.

Figures 4.6 and 4.7 are the semi logarithmic plots (graphical method) for the methane-Sumandak oil systems while Figures 4.8 and 4.9 are the non-linear exponential plots (numerical method) of the same gas-oil system at initial pressures of 797 psi and 1035 psi respectively. In constructing the semi logarithmic plots for Figures 4.6 and 4.7, equilibrium pressure values were estimated based on the experimental pressure decay profile. Then, based on the straight line linear fit, the slope was estimated and the diffusion coefficient was calculated. On the other hand, with the non-linear exponential plot, equilibrium pressure was not estimated but calculated by numerically fitting an analytical expression based on the pressure history. The equilibrium pressures obtained from both methods were compared as per Table 4.4. The values are very close regardless of the method of analysis. It may be due to the many pressure-data points used in the graphical method, hence giving good estimation of the equilibrium pressure.



Table 4.4: Comparison of equilibrium pressure for methane-Sumandak Oil System

Initial test pressure (psi)	Time to equilibrium		Equilibrium pressure, $P_{eq}$ (psi)	
	(sec)	(hour)	Graphical method	Numerical method
797	366,840	101.9	731.0	732.9
1035	340,560	94.6	943.0	945.0

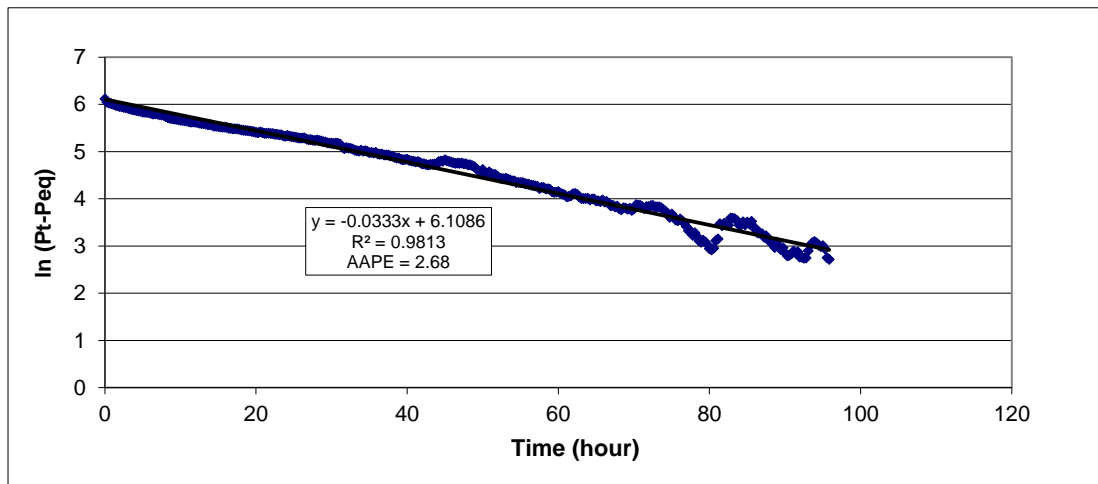


Figure 4.6: Semi-logarithmic plot of methane-Sumandak oil at initial pressure of 797 psi (Test 1)

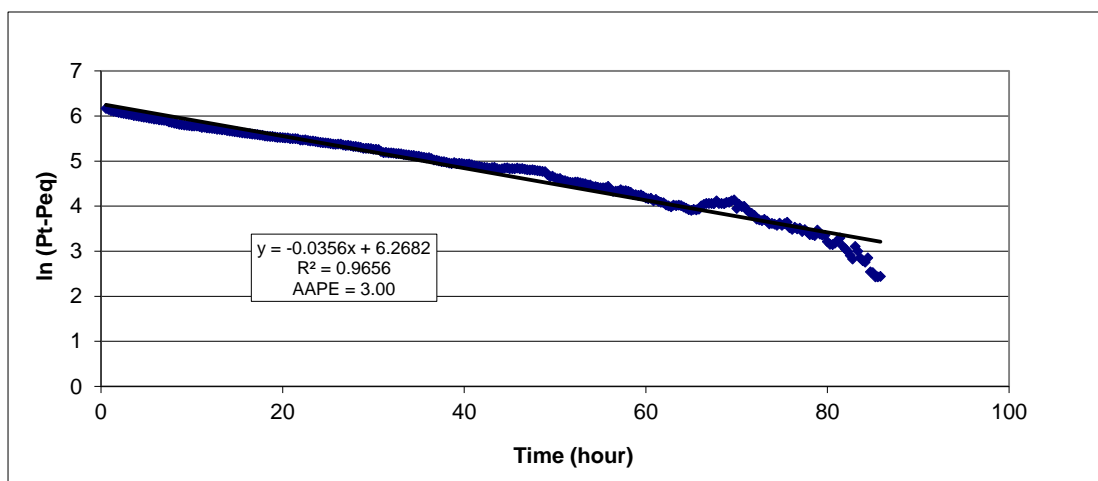


Figure 4.7: Semi-logarithmic plot of methane-Sumandak oil at initial pressure of 1035 psi (Test 2)

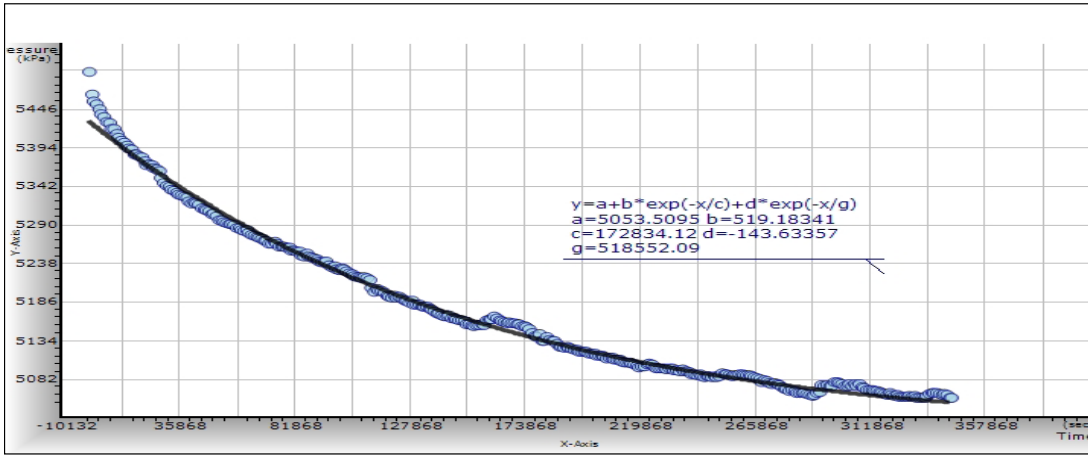


Figure 4.8: Non-linear exponential plot of methane-Sumandak oil at initial pressure of 797 psi (Test 1) (extracted from FindGraph software)

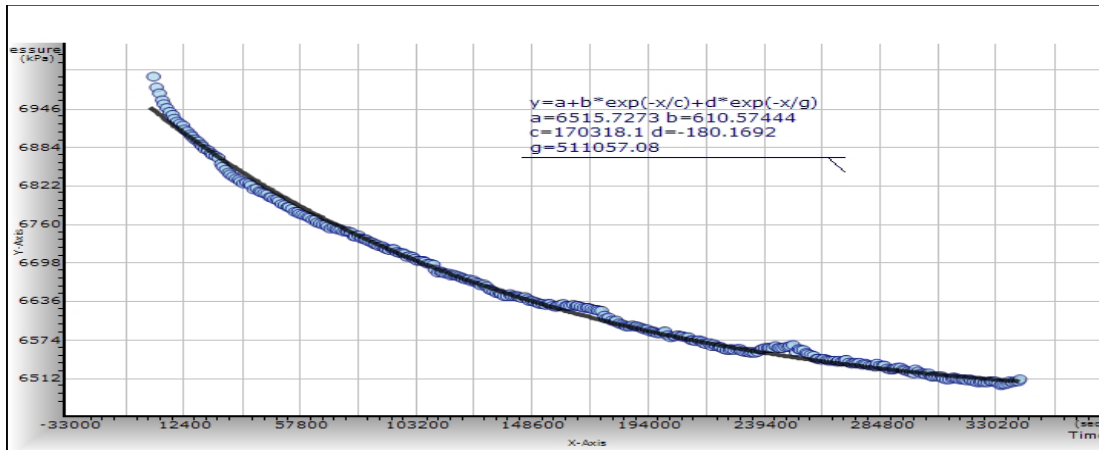


Figure 4.9: Non-linear exponential plot of methane-Sumandak oil at initial pressure of 1035 psi (Test 2) (extracted from FindGraph software)

Table 4.5 presents the diffusion coefficient results of methane-Sumandak oil systems at the test pressures and temperature. Published study by Jamialahmadi *et al.* (2006) and Schmidt (1989) were referred since these published reports have an almost similar test conditions. The test temperature between these reported studies and current work are almost the same (i.e.: between 50°C - 65°C) while the test pressures of the current work are within the range of the test pressures used in the reported studies. The major difference would be the oil viscosities. An exact temperature of 50°C as per the published reports could not be attained due to the PVT unit limitation in terms of the instability of the temperature if set lower than 60°C.

Table 4.5: Diffusion coefficient values for methane-Sumandak oil system at different pressures

Gas	Liquid	Temperature	Initial pressure	$D_{AB}$ ( $10^{-9}$ m <sup>2</sup> /s)		Reference
		(° C)	(psia)	Graphical	Numerical	
CH <sub>4</sub>	Sumandak oil (10.4 cP)	60	797	4.19	2.65	This work
CH <sub>4</sub>	Sumandak oil (10.4 cP)	60	1035	4.07	2.62	This work
CH <sub>4</sub>	Dodecane (1.34 cP)	65	580 - 5,076	10.5 to 15.0		Jamialahmadi <i>et al.</i> (2006)
CH <sub>4</sub>	Iranian crude (0.16 - 0.29 cP)	50	508 - 3,989	9.8 to 16.4		Jamialahmadi <i>et al.</i> (2006)
CH <sub>4</sub>	Oil (8,360 cP)	50	725.2	0.40 to 0.75		Schimdt (1989)

At the respective pressure range, the diffusion coefficients obtained by Schmidt (1989) was found to be very much lower while the diffusion coefficients by Jamialahmadi *et al.* (2006) was very much higher than the methane-Sumandak oil system. This might be due to the viscosity difference. The influence of viscosity in diffusivity is prominent. According to Riazi and Whitson (1993), viscosity of the solvent (liquid) is the primary parameter used in almost all theoretical and empirical correlations to estimate diffusivity in liquid system. Figure 4.10 shows comparison between the diffusion coefficients obtained from the present work to the published studies in relation to viscosity.

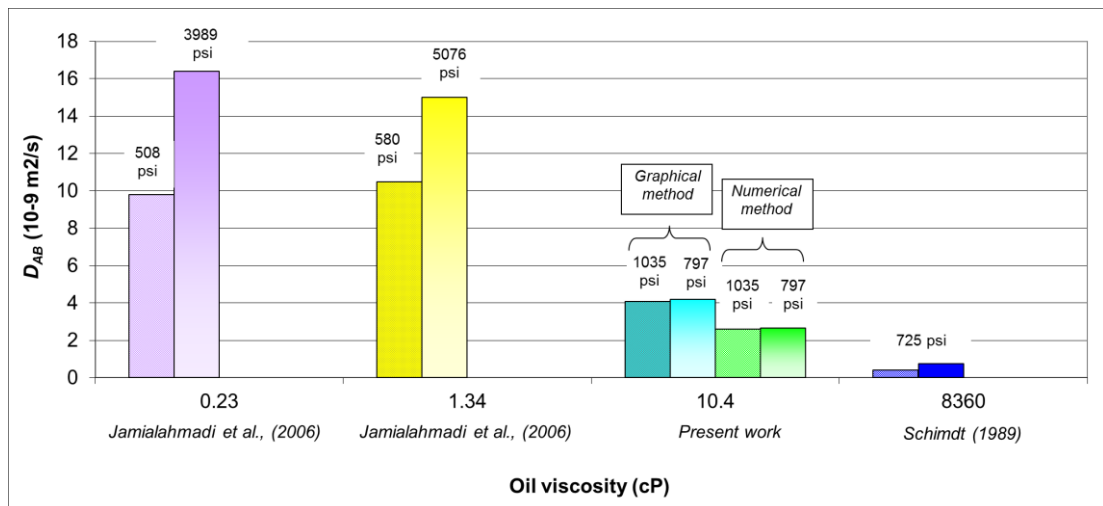


Figure 4.10: Comparison of the diffusion coefficients of methane-Sumandak oil to published reports in terms of oil viscosity difference

The Stokes-Einstein equation, based on Stokes law (Bird *et al.*, 1960) stated that diffusion coefficients in liquid systems are inversely proportional to viscosity.

Similarly, this relationship has been observed experimentally by Jamialahmadi *et al.* (2006) and Nguyen and Farouq Ali (1995). Viscosity of the solvent (liquid) is considered as a primary parameter in estimating diffusivity in liquid system (Riazi, 1996). The large difference in diffusion coefficient is therefore, mainly contributed by the large viscosity difference.

#### 4.2.2 Methane-Angsi Oil System

For the methane-Angsi oil system, the test temperature was set at 90°C but the test pressures varied. Figure 4.11 shows the experimental pressure-time profile for the methane-Angsi oil system. Similarly with the earlier methane-Sumandak oil system, the incubation period at the early part of experiment occurred due to injection of a high pressure gas into the test cell. Likewise, higher initial test pressure of 1289 psi showed faster time to reach equilibrium.

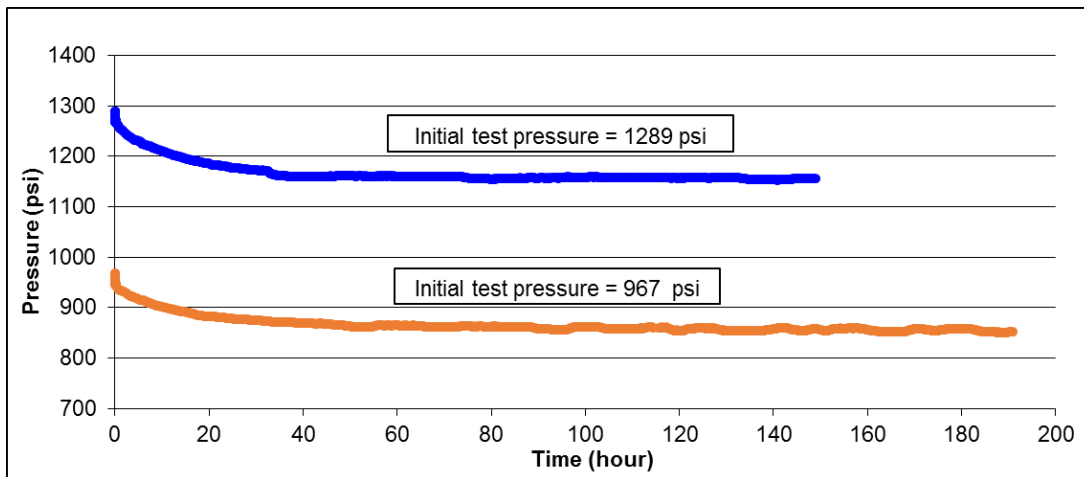


Figure 4.11: Methane-Angsi oil pressure decay profile at different initial pressures

During the experiment, it was observed that there were quite significant fluctuations on the measured pressure-time curve. The instability of the temperature transducer had affected the test temperature causing similar trend of fluctuations to the pressure profile. However, the deviation in the set temperature was minimal ( $\pm 2\%$  from the set temperature). The recorded pressure profile showed that as temperature went down, the test pressure decreased. These fluctuations were apparent when analyzing the pressure-time data in the respective semi-logarithmic and non-linear

exponential plots as per Figure 4.12 through Figure 4.15. The fluctuations of the pressure-time curve have influenced the R-squared value or the square of the correlation coefficient for the semi-logarithmic and non-linear exponential plots. It has affected the best trendline fitting to the data points. This can be observed where the methane-Angsi oil systems have a lower R-squared values as compared to the methane-Sumandak oil systems, even when the outliers (i.e.: highly deviated data points) were removed. Lower R-squared value indicates poorer line fitting. Even so, it does not greatly influence the calculation of the diffusion coefficient.

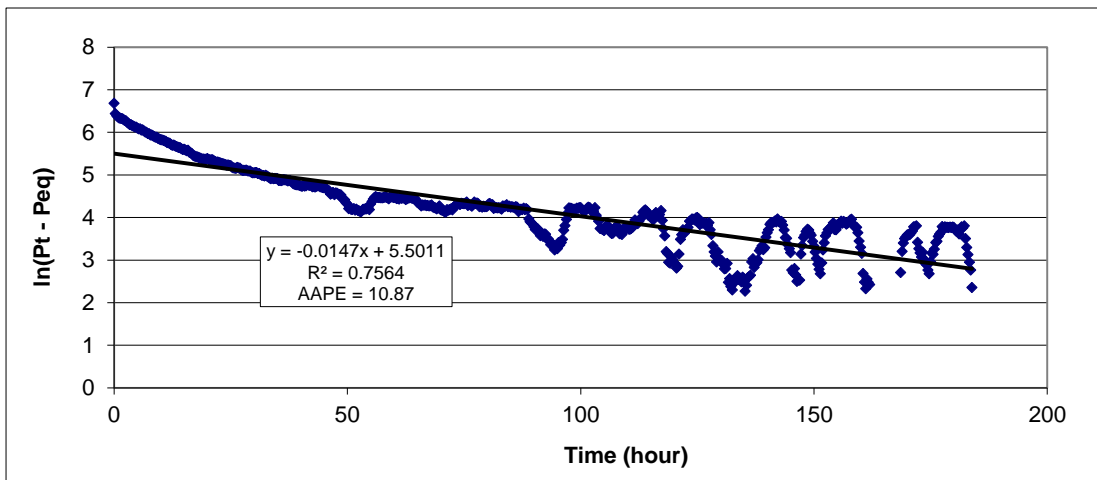


Figure 4.12: Semi-logarithmic plot of methane-Angsi oil at initial pressure of 967 psi (Test 1)

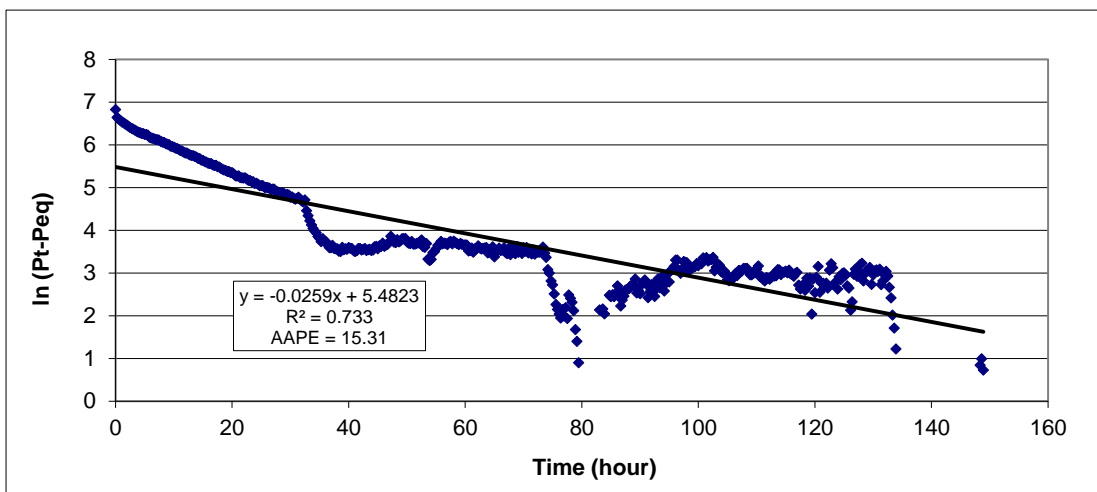


Figure 4.13: Semi-logarithmic plot of methane-Angsi oil at initial pressure of 1289 psi (Test 2)

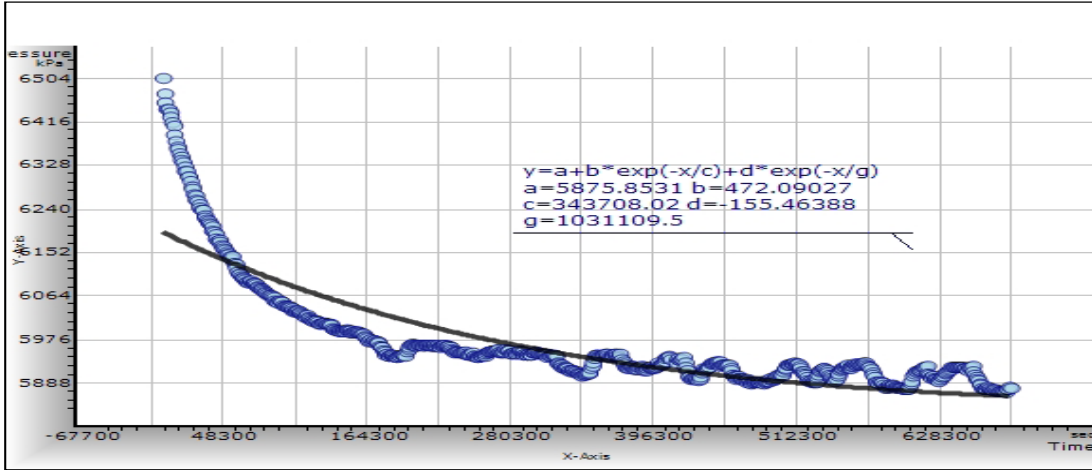


Figure 4.14: Non-linear exponential plot of methane-Angsi oil at initial pressure of 967 psi (Test 1) (extracted from FindGraph software)

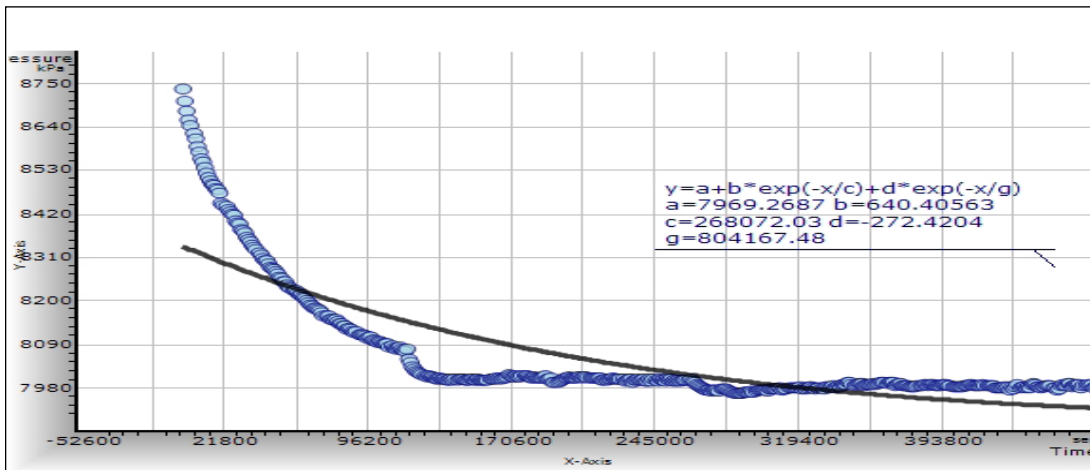


Figure 4.15: Non-linear exponential plot of methane-Angsi oil at initial pressure of 1289 psi (Test 2) (extracted from FindGraph software)

In this experiment, it was also observed that when test temperature decreased, the test pressure decreased. According to Zhang *et al.* (2000), when test pressure decreased, the equilibrium concentration on the gas-liquid interface also decreased. However, as temperature decreased, the solubility of gas increased (Zhang *et al.*, 2000). Hence, the effects of decreasing temperature compensate the effect of decreasing pressure on the equilibrium concentration of gas at the interface. The overall effect of temperature fluctuations on the test is therefore small. This counteract is explainable per the Le-Chatelier's principle which is used to predict the effect of a change in conditions on a chemical equilibrium. If a chemical system at equilibrium experiences a change in its conditions (i.e.: concentration, temperature, volume,

pressure), the equilibrium shifts to offset the imposed change and establish a new equilibrium (Atkins, 1993). Hence, it is likely that even though some fluctuations were observed in the pressure profile, the change in equilibrium concentration of gas at the interface is being offset by increase in gas solubility; thus, giving least impact to the gas diffusivity process.

The equilibrium pressures obtained from the graphical and numerical methods are also compared as per Table 4.6 to ascertain the accuracy of the estimated equilibrium pressures in the graphical method. Similarly with methane-Sumandak oil system, the equilibrium pressures from both methods of analysis closely matched each other.

Table 4.6: Comparison of equilibrium pressure for methane-Angsi oil system

Initial test pressure (psi)	Time to equilibrium		Equilibrium pressure, $P_{eq}$ (psi)	
	(sec)	(hour)	Graphical method	Numerical method
967	687,600	191.0	852.0	852.2
1289	536,040	148.9	1155.5	1155.8

Table 4.7 presents the diffusion coefficients of methane–Angsi oil systems at the test pressures. Published study by Jamialahmadi *et al.* (2006) using dodecane was referenced since it has an almost similar test temperature and pressure with the present work. None other methane-oil reported study listed in Table 4.1 earlier has closer test temperature than the present work. When compared, diffusion coefficients of methane-Angsi oil system were found to be lower than the published report since Angsi oil viscosity is much higher than the dodecane used. This finding indicated that gas diffusivity decreases at higher oil viscosity.

Table 4.7: Diffusion coefficient values for methane-Angsi oil system at different pressures

Gas	Liquid	Temperature	Initial pressure	$D_{AB}$ ( $10^{-9}$ m <sup>2</sup> /s)		Reference
		(° C)	(psia)	Graphical	Numerical	
CH <sub>4</sub>	Angsi oil (4.73 cP)	90	967	1.79	1.30	This work
CH <sub>4</sub>	Angsi oil (4.73 cP)	90	1289	3.18	1.69	This work
CH <sub>4</sub>	Dodecane (1.34 cP)	81	580 - 4,641	11.5 to 17.0		Jamialahmadi <i>et al.</i> (2006)
CH <sub>4</sub>	Dodecane (1.34 cP)	65	580 - 4,641	10.5 to 15.0		Jamialahmadi <i>et al.</i> (2006)

Figure 4.16 demonstrates the effect of oil viscosity to the diffusion coefficients between the present work and the published study. Diffusivity is shown to be lower at higher oil viscosity. This conforms to the viscosity-diffusion coefficient relationship from earlier investigations (Jamialahmadi *et al.*, 2006; Riazi, 1996; Nguyen and Farouq Ali, 1995) presented in Table 2.2. Even if the viscosity difference is relatively small, viscosity effect on diffusion coefficient is still significant.

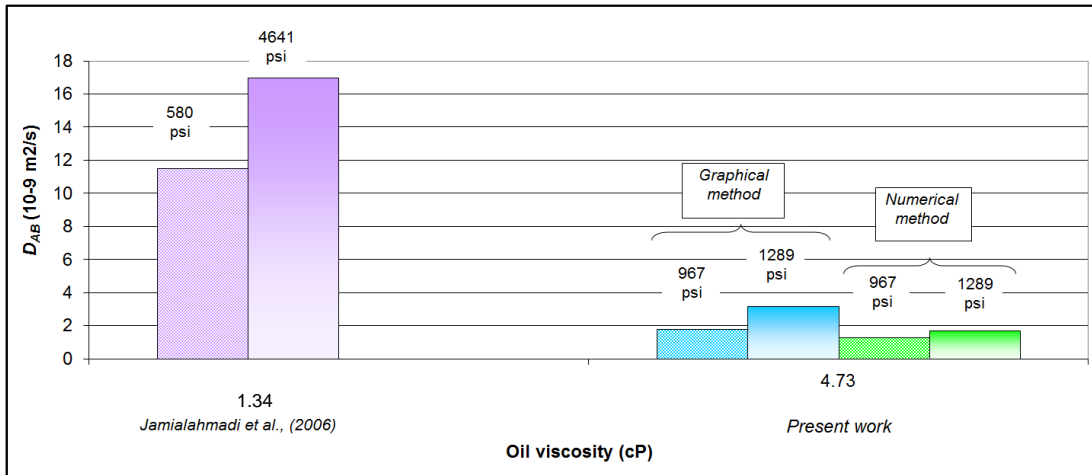


Figure 4.16: Comparison of the diffusion coefficients of methane-Angsi oil to published reports in terms of viscosity difference

### 4.2.3 Effect of Pressure

Table 4.8 presents diffusion coefficients of methane-Sumandak oil and methane-Angsi oil respectively. Pressure-diffusivity relationships however, are different for these two systems. In methane-Sumandak oil system, pressure-diffusivity relationship is inversely proportional, which means, diffusivity decreases at higher pressure. The contrary was observed for methane-Angsi oil system.



Table 4.8: Effect of pressure on diffusion coefficient values of methane-Malaysian oil system

Gas	Liquid	Temperature	Initial pressure	$D_{AB}$ ( $10^{-9}$ m <sup>2</sup> /s)			
		(° C)	(psia)	Graphical	Difference	Numerical	Difference
CH <sub>4</sub>	Sumandak oil (10.4 cP)	60	797	4.19	3%	2.65	1%
CH <sub>4</sub>	Sumandak oil (10.4 cP)	60	1035	4.07		2.62	
CH <sub>4</sub>	Angsi oil (4.73 cP)	90	967	1.79	44%	1.30	23%
CH <sub>4</sub>	Angsi oil (4.73 cP)	90	1289	3.18		1.69	

Pressure has also affected the diffusivity results in another aspect, which is the magnitude of difference in diffusivity values. Diffusion coefficients of the methane-Sumandak oil system at its two different initial test pressures deviated by merely 3% (graphical method) and 1% (numerical method) at pressure difference of 238 psi. On the other hand, diffusion coefficient results of the methane-Angsi oil system showed deviation of 44% (graphical method) and 23% (numerical method) at pressure difference of 322 psi. Pressure appeared to have quite a significant effect on diffusion coefficient of the methane-Angsi oil system, in contrast with the methane-Sumandak oil system. The effect of pressure difference in particular, is more pronounced in the system with higher test temperature and lower oil viscosity (i.e.: methane-Angsi oil).

In order to observe the effect of pressure to diffusivity, three reported studies using methane-oil system were compared ranging from low to high viscosity oil. Riazi (1996) performed its methane-n-pentane (0.23 cP) diffusivity tests at temperature of 37.8°C. Jamialahmadi *et al.* (2006) run its methane-dodecane (1.34 cP) diffusivity test at temperatures from 45°C, 65°C and 81°C. Nguyen and Farouq Ali (1995) conducted their methane-oil (1842 cP) system diffusivity test at 57.1°C. Figures 4.17, 4.18 and 4.19 show the different pressure-diffusivity relationship of these reported studies.

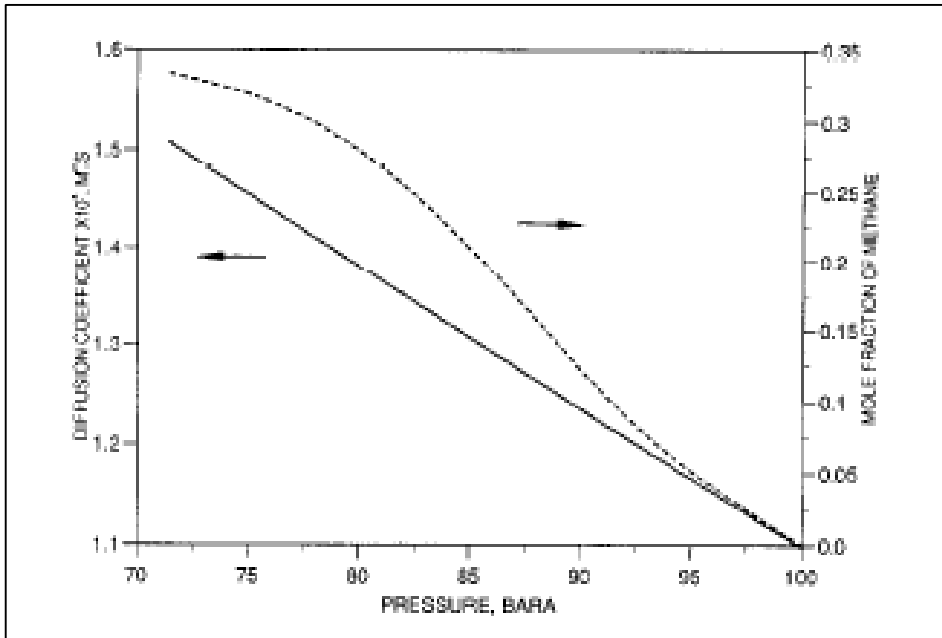


Figure 4.17: Pressure-diffusivity plot extracted from published report by Riazi (1996) on methane-n-pentane system at 37.8°C

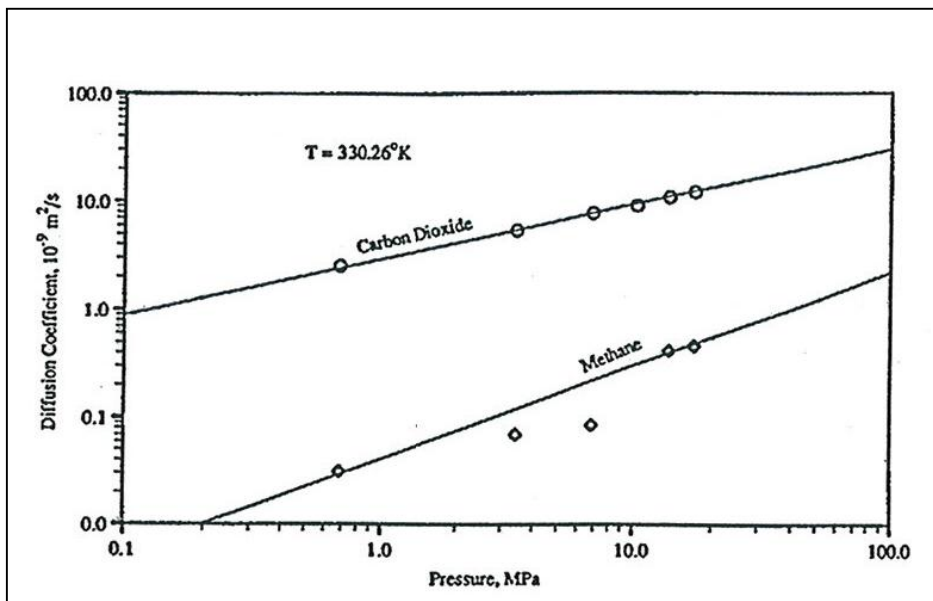


Figure 4.18: Pressure-diffusivity plot extracted from published report by Nguyen and Farouq Ali (1995) for carbon dioxide-oil and methane-oil systems at 57.1°C

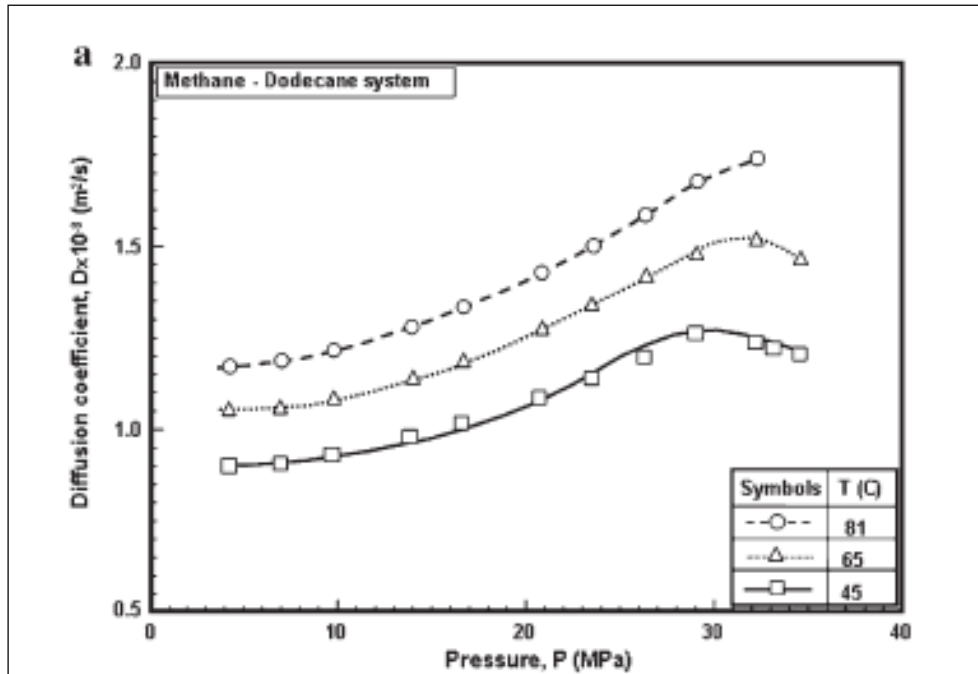


Figure 4.19: Pressure-diffusivity plot extracted from published report by Jamialahmadi *et al.* (2006) for methane-dodecane systems at 45°C, 65°C and 81°C

From above figures, Riazi (1996) reported an inverse pressure-diffusivity relationship while Nguyen and Farouq Ali (1995) and Jamialahmadi *et al.* (2006) reported proportional relationship. The contradicting pressure-diffusivity relationship was also observed from present work as reported earlier in this section. Methane-Sumandak oil system showed inverse pressure-diffusivity relationship while methane-Angsi system was contrary. In methane-Sumandak and Riazi's methane-n-pentane system where pressure-diffusivity relationship were inversed, one such explanation might be; as pressure increased, the liquid density decreased. Hence, the intermolecular friction is larger and diffusivity decreased (Rutten, 1992).

#### 4.2.4 Effect of Temperature

Temperature effect on diffusion can be observed from the diffusion coefficients of the present work involving methane-Sumandak oil system as per Table 4.9. The results suggested that temperature has some effect on diffusion coefficients. However, a fair conclusion could not be derived since the initial test pressures were different. As indicated earlier, it is a challenge to attain an exactly same initial pressure due to pressure loss as a result of initial gas ingress into oil or possibly due to the long tubing

line from the high pressure gas chamber to the inlet of the PVT unit (i.e.: 348 cm). The control systems (i.e.: valves) were all manually operated rather than automated and hence, it was quite difficult to achieve the targeted test pressure as desired.

Table 4.9: Effect of temperature on diffusion coefficient values of methane-Sumandak oil system

Gas	Liquid	Temperature	Initial pressure	$D_{AB}$ ( $10^{-9}$ m <sup>2</sup> /s)	
		(° C)	(psia)	Graphical	Numerical
CH <sub>4</sub>	Sumandak oil (10.4 cP)	60	1035	4.07	2.62
CH <sub>4</sub>	Sumandak oil (10.4 cP)	90	1348	2.98	1.44

Earlier studies (Hines and Maddox, 1985; Nguyen and Farouq Ali, 1995; Upreti & Mehrotra, 2002; Jamialahmadi *et al.*, 2006) found that diffusion coefficients increase at higher temperature; which is contradicting from results in Table 4.9. Higher temperature causes an increase in kinetic energy which accelerates the movement of the gas molecules causing higher methane diffusion (Nguyen and Farouq Ali, 1995). However, pressure may have influence this finding. Based on pressure-diffusivity results from methane-Sumandak oil, diffusivity decreases at higher pressure. Here, pressure may have more prevailing influence, hence affecting the temperature-diffusivity relationship.

#### 4.2.5 Effect of Composition

Fluid composition may have some apparent effects on gas diffusivity. Rutten (1992) however, stated that the effect of composition is complicated and only partly understood. In this aspect, viscosity is a parameter that implicates the composition of a fluid system as explained earlier in section 2.2.4. Figure 4.10 and Figure 4.16 from earlier discussions showed that the viscosity of oil has significant effect on diffusion coefficient. When diffusion coefficients of the present work were compared to published reports' at comparatively same pressure and temperature, the diffusion coefficient deviated largely due to difference in the viscosity. In particular, diffusion coefficient has an inverse relationship with viscosity of the liquid system.

Table 4.10 compares the diffusion coefficients between the Sumandak and Angsi gas-oil systems. Since diffusion coefficient is a function of pressure, temperature and composition of the system (Welty *et al.*, 1984), the only variable here is the oil composition. The test temperature and pressure are comparatively similar. Sumandak oil which is more viscous produced lower diffusion coefficients for its methane-oil system.

Table 4.10: Effect of oil viscosity on diffusion coefficient values of methane-oil system

Gas	Liquid	Temperature	Initial pressure	$D_{AB}$ ( $10^{-9}$ m <sup>2</sup> /s)	
		(° C)	(psia)	Graphical	Numerical
CH <sub>4</sub>	Sumandak oil (10.4 cP)	90	1348	2.98	1.44
CH <sub>4</sub>	Angsi oil (4.73 cP)	90	1289	3.18	1.69

A simple prediction on diffusion coefficient values for methane-oil system can be derived from this viscosity-diffusivity relationship. Data from Table 4.10 is translated into plot as in Figure 4.20 and will be used as a basis to estimate the diffusion coefficient of other methane-oil system for Malaysian oilfields. However, these sets of data are not enough to serve as a correlation. Further work is needed to acquire as much diffusion coefficient data to develop some correlations for the Malaysian methane-oil system.

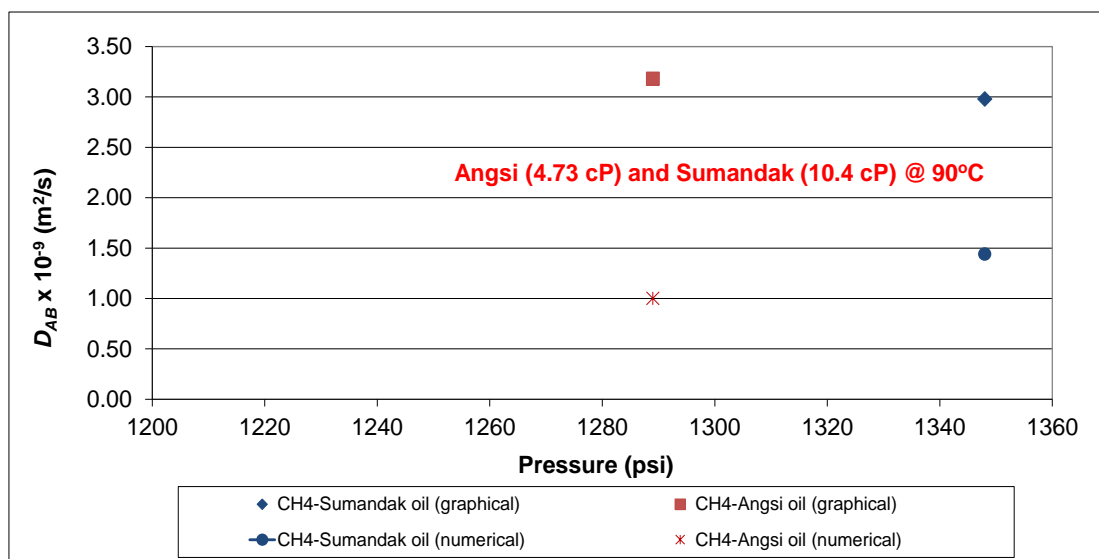


Figure 4.20: Viscosity-Diffusivity relationship of Sumandak and Angsi methane-oil systems

### 4.3 Phase 3: Diffusivity of Multicomponent Gas-Oil System

Tests were performed using the actual produced gas and crude oil sampled from Sumandak and Angsi oilfields. The same test temperatures were applied for this actual gas-oil system. Temperatures of 60°C and 90°C were used for the Sumandak and Angsi gas-oil systems respectively.

Compositions of the oil samples, shown earlier in Figures 4.2 and 4.4 and their viscosities are the same as in the methane-oil system. Compositions of the gas samples are presented in Figures 4.21 and 4.22. It can be observed that methane dominates the produced gas composition. Sumandak produced gas has 96 wt% of methane while Angsi has 75 wt%. The detail compositions of the oil and gas samples are presented in Appendix D.

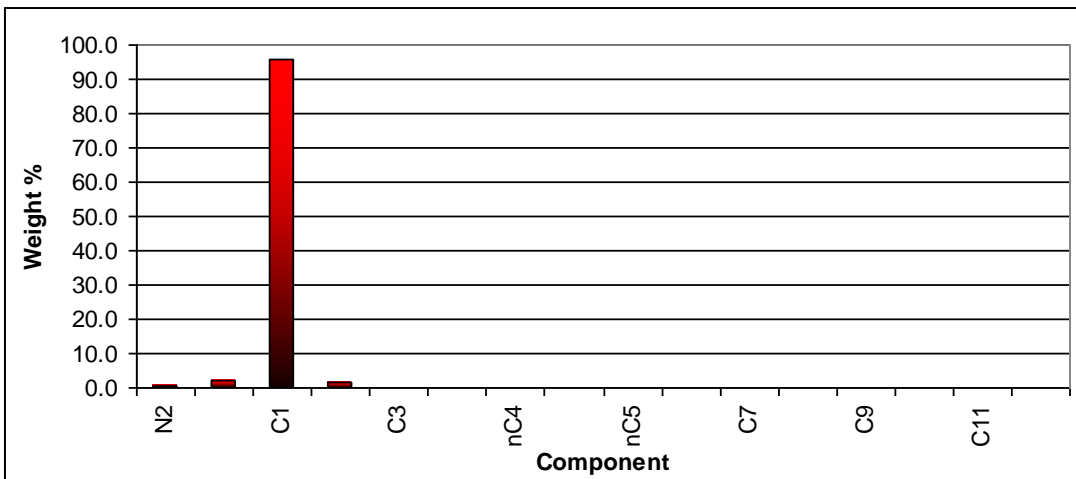


Figure 4.21: Compositions of Sumandak gas (wellhead sample)

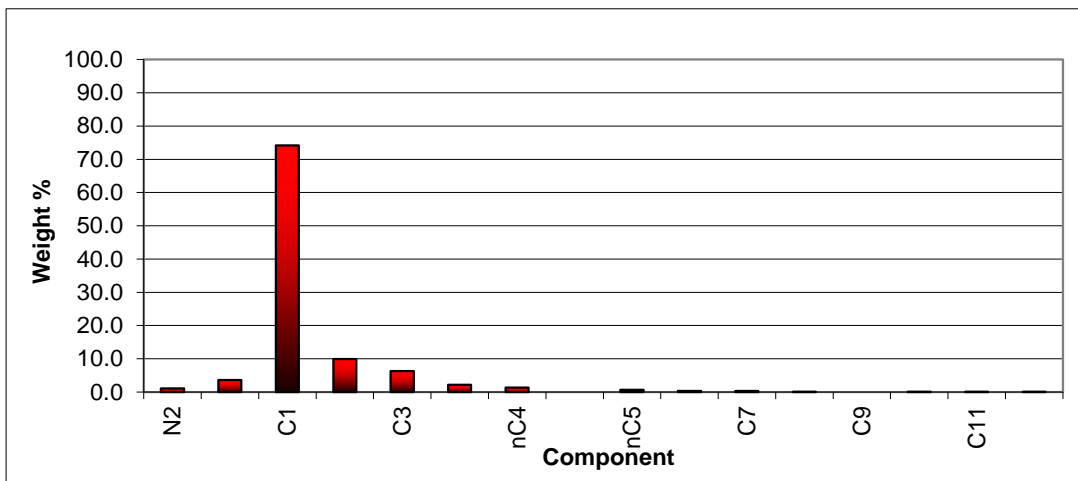


Figure 4.22: Compositions of Angsi gas (separator sample)

### 4.3.1 Sumandak Gas – Sumandak Oil System

Experiments were conducted using actual produced gas and crude oil from Sumandak's well A-14L. The mathematical model by Zhang *et al.* (2000) was used to verify whether this mathematical model designed for a pure gas-oil system could be extended to a multicomponent gas-oil system.

Figure 4.23 shows the pressure decay plots for Sumandak's multicomponent gas-oil systems. There is an obvious rapidly decreasing pressure section at the initial test period, followed by a slower decreasing pressure and finally to an almost constant pressure, indicating the system has reached equilibrium. This same trend was purposely achieved to ensure conformance to the correct molecular diffusion condition. It can be observed that earlier equilibrium is reached at higher test pressure.

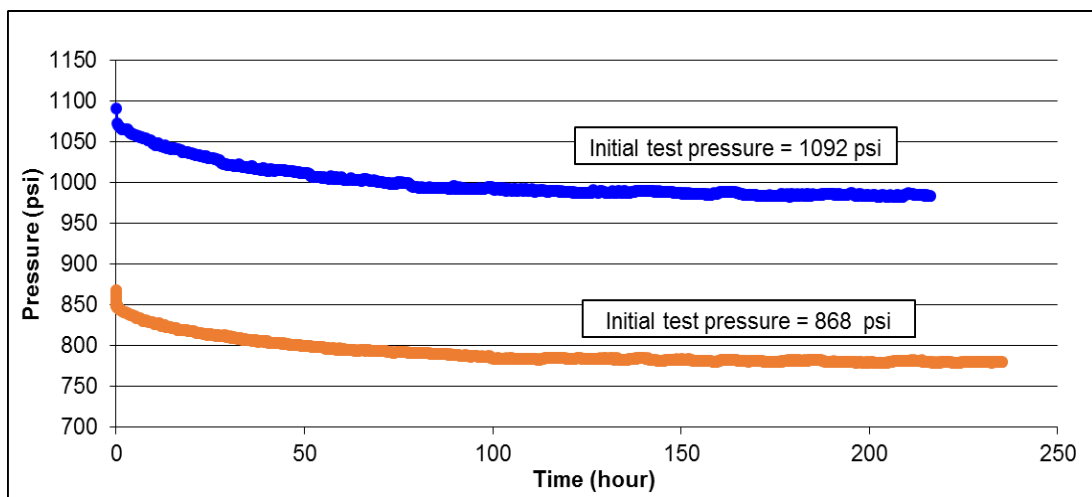


Figure 4.23: Sumandak gas-Sumandak oil pressure decay profile at different initial pressures

The semi-logarithmic plots shown in Figures 4.24 and 4.25 demonstrate large fluctuations at the middle to tail of the test period in which some highly deviated data points (i.e.: outliers) have to be discarded to better represent the general trend of the semi logarithmic plots. Only then good trendline fitting to the data points could be obtained, giving a reasonably good R-squared value for the semi-logarithmic plots for both Test 1 and 2. This is permissible considering a large number of pressure data points were gathered from the tests. In the non-linear exponential plots as in Figures 4.26 and 4.27, the trendline fitting are considered closely matched. Hence, the

interpretation on the value of constants used to calculate diffusion coefficient values and the equilibrium pressure was reliable.

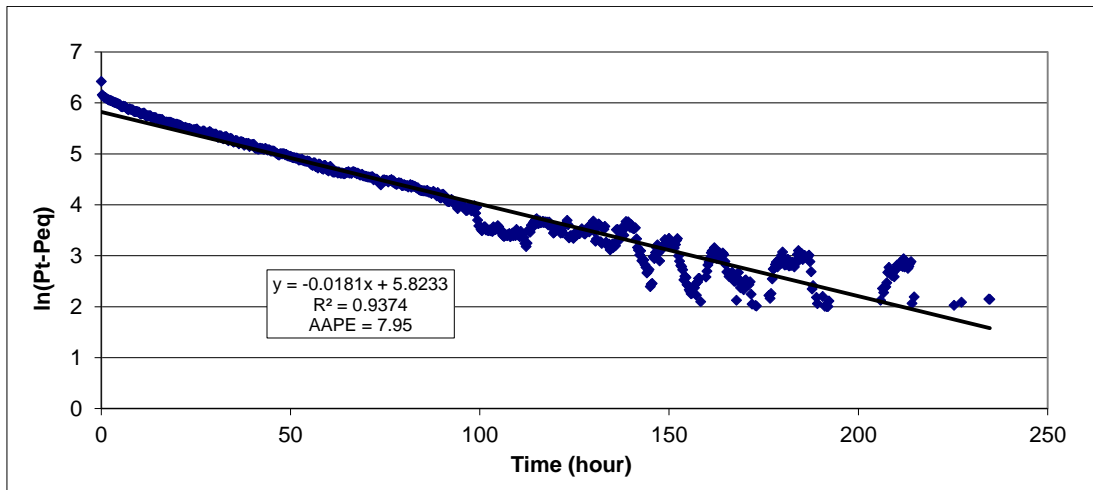


Figure 4.24: Semi-logarithmic plot of Sumandak gas-Sumandak oil at initial pressure of 868 psi (Test 1)

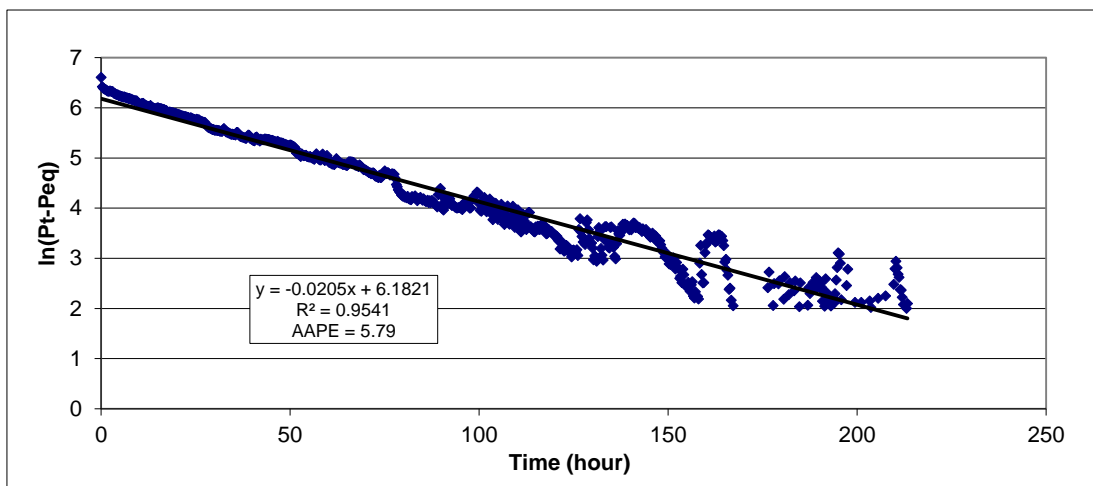


Figure 4.25: Semi-logarithmic plot of Sumandak gas-Sumandak oil at initial pressure of 1092 psi (Test 2)



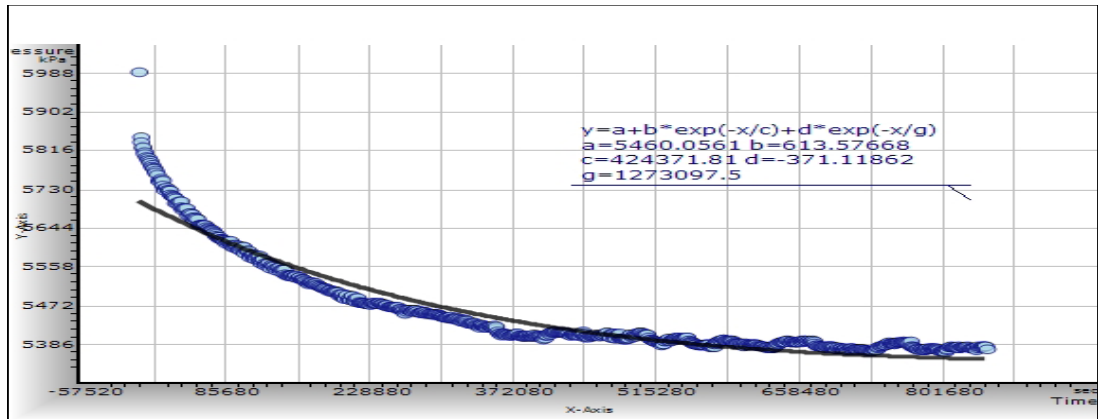


Figure 4.26: Non-linear exponential plot of Sumandak gas-Sumandak oil at initial pressure of 868 psi (Test 1) (extracted from FindGraph software)

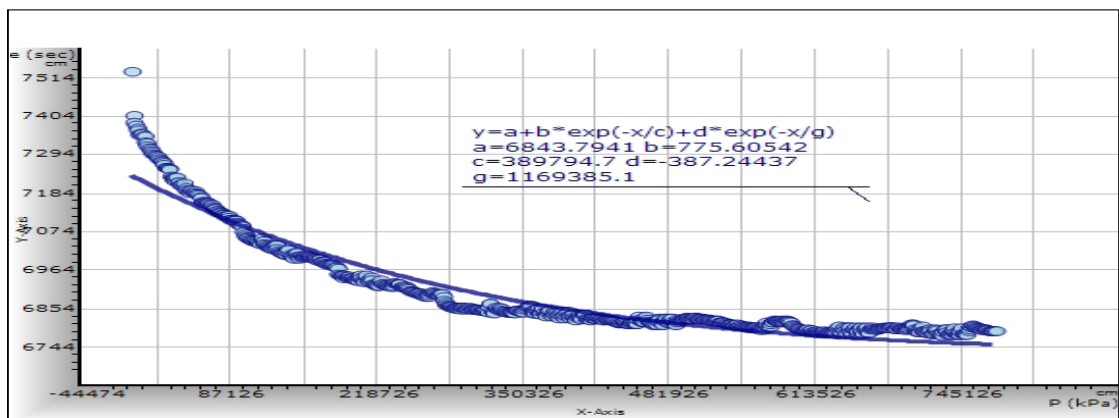


Figure 4.27: Non-linear exponential plot of Sumandak gas-Sumandak oil at initial pressure of 1092 psi (Test 2) (extracted from FindGraph software)

Table 4.11 compares the diffusion coefficients obtained from multicomponent (produced) gas and pure methane gas with Sumandak oil. It is found that there is a small difference in the diffusion coefficients between these two systems which primarily contributed by the different gas compositions. At the same temperature and almost the same pressure, the multicomponent gas-oil system produced lower diffusion coefficient values using both the graphical and numerical method of analysis. This may be attributed to the higher gas viscosity and higher molecular weight of the multicomponent gas system due to the presence of higher hydrocarbon components than  $C_1$ . The molecular weight of the Sumandak's produced gas (multicomponent) is also higher, being 16.94 g/mole while pure methane gas has molecular weight of 16.04 g/mole. Figure 4.28 demonstrates this effect of gas composition and its molecular weight to diffusion coefficient.

Table 4.11: Diffusion coefficient values for Sumandak gas-Sumandak oil system at different pressures

Gas	Liquid	Temperature	Initial pressure	$D_{AB}$ ( $10^{-9}$ m <sup>2</sup> /s)	
		(° C)	(psia)	Graphical	Numerical
Sumandak produced gas	Sumandak oil (10.4 cP)	60	868	2.06	0.97
Sumandak produced gas	Sumandak oil (10.4 cP)	60	1092	2.56	1.09
CH <sub>4</sub>	Sumandak oil (10.4 cP)	60	797	4.19	2.65
CH <sub>4</sub>	Sumandak oil (10.4 cP)	60	1035	4.07	2.62

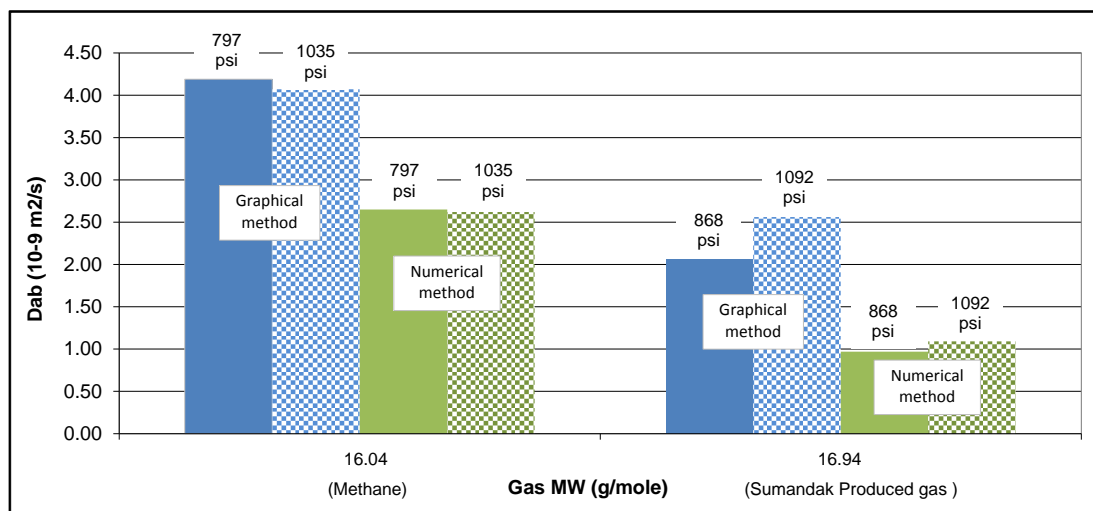


Figure 4.28: Effect of gas molecular weight to diffusivity on Sumandak gas-oil system

Sumandak produced gas having higher molecular weight may have larger solute size and longer hydrocarbon chain length. The produced gas consists of hydrocarbon gases from C<sub>1</sub> up to C<sub>3</sub>. Earlier study by Wise and Houghton (1966) reported physical explanations for the observed variation of diffusion coefficient with the solute's (gas) molecule size and hydrocarbon chain length. The study discovered an inverse relationship between diffusivity and solute molecule size during their investigation on diffusion coefficient of dissolved pure and hydrocarbon gases in water. Furthermore, the study found a linear decrease in diffusivity as chain length is increased. In their experiment on diffusivity of each methane, ethane, propane and butane diffusivity in water, the study observed that butane having the longest chain length produced the slowest diffusivity in water. These earlier findings might justify on the lower diffusion coefficient values of Sumandak's multicomponent gas-oil system as compared to pure

gas-oil system. This multicomponent gas contains more hydrocarbon component, has higher molecular weight and longer hydrocarbon chain length. As a result, its gas-oil system produced lower diffusion coefficient values than the pure methane gas-oil system.

The diffusion coefficients for Sumandak's multicomponent gas-oil systems are in the same order of magnitude ( $\sim 10^{-9}$  m<sup>2</sup>/s) as its methane-Sumandak oil system. The variations in diffusion coefficients are justifiable owing to the difference gas compositions. This suggests that Zhang's analysis methods may be applicable for a multicomponent gas-oil diffusivity measurement, in particular Sumandak's produced gas-oil system.

#### **4.3.2 Angsi Gas – Angsi Oil System**

Experiments were performed using actual produced gas and crude oil from Angsi's well A-38. The mathematical model by Zhang *et al.* (2000) is again employed to verify the model's capability in analyzing diffusion coefficient for Angsi multicomponent gas-oil system.

Figure 4.29 shows a smoother pressure decline curve for the Angsi gas-oil systems. There are not many fluctuations in terms of its pressure profile as compared to the Sumandak gas-oil systems. This smaller fluctuation is attributed to a much stable test temperatures during the experiments. There are also smaller fluctuations at the tail of the semi logarithmic plots and the non-linear exponential plots as shown in Figures 4.30 through 4.33. For the semi-logarithmic plots, some outliers were removed as they were highly diverted and not representatives of the pressure profile.

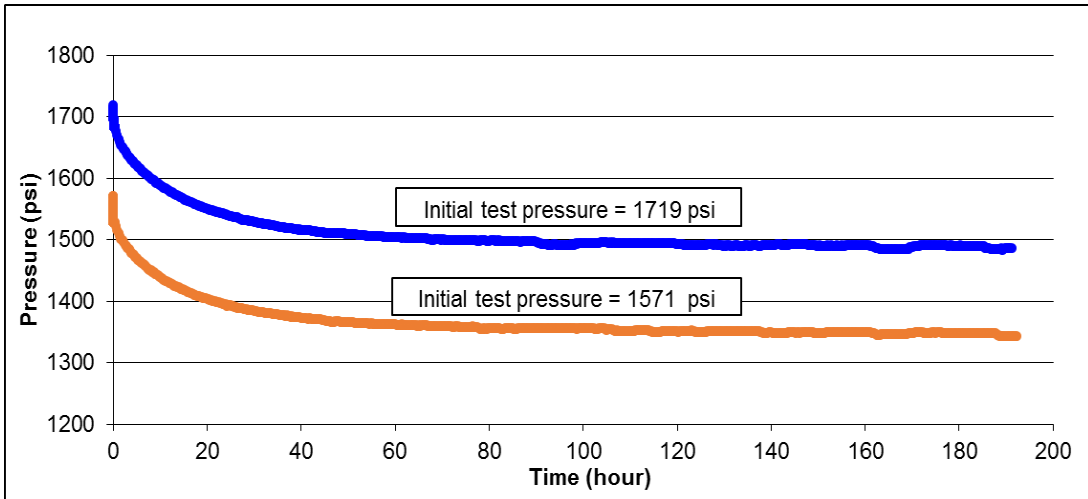


Figure 4.29: Angsi gas-Angsi oil pressure decay profile at different initial pressures

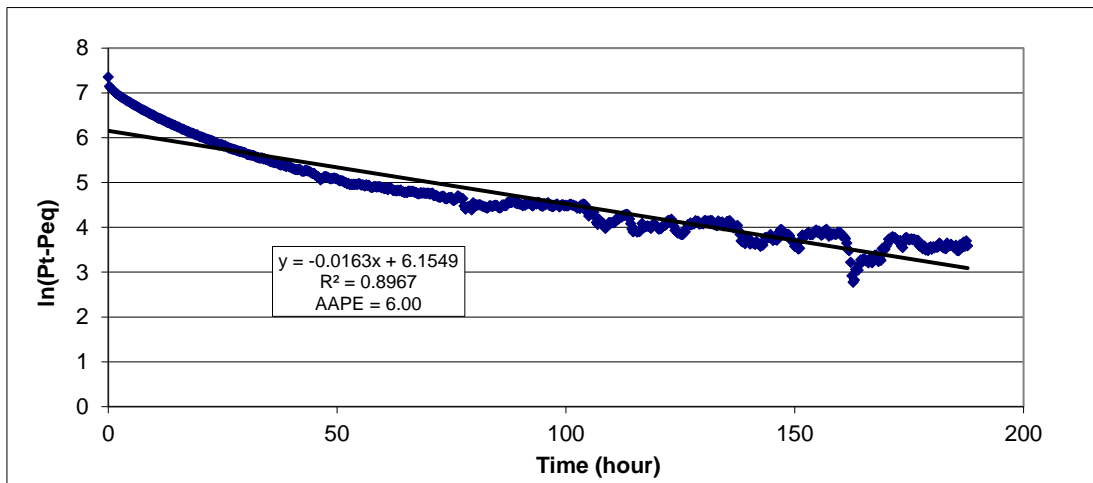


Figure 4.30: Semi-logarithmic plot of Angsi gas-Angsi oil at initial pressure of 1571 psi (Test 1)

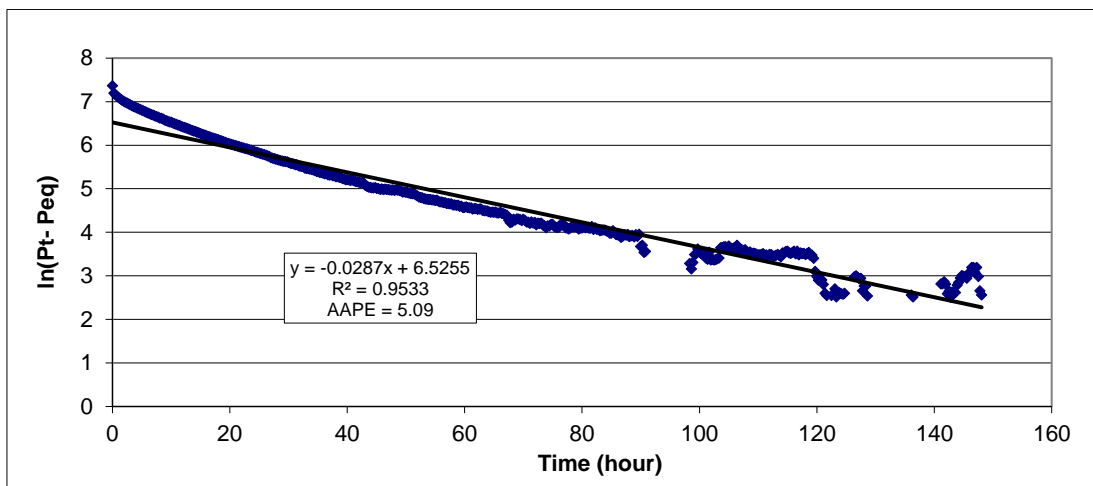


Figure 4.31: Semi-logarithmic plot of Angsi gas-Angsi oil at initial pressure of 1719 psi (Test 2)

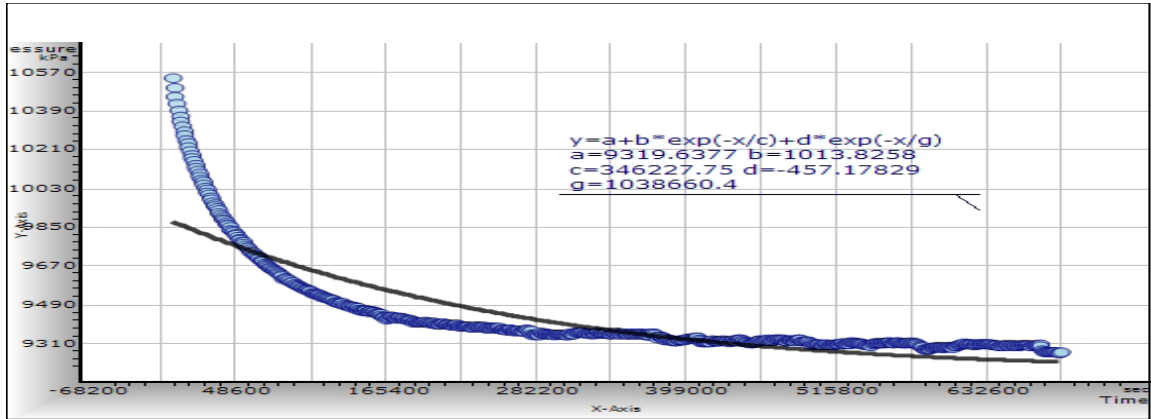


Figure 4.32: Non-linear exponential plot of Angsi gas-Angsi oil at initial pressure of 1571 psi (Test 1) (extracted from FindGraph software)

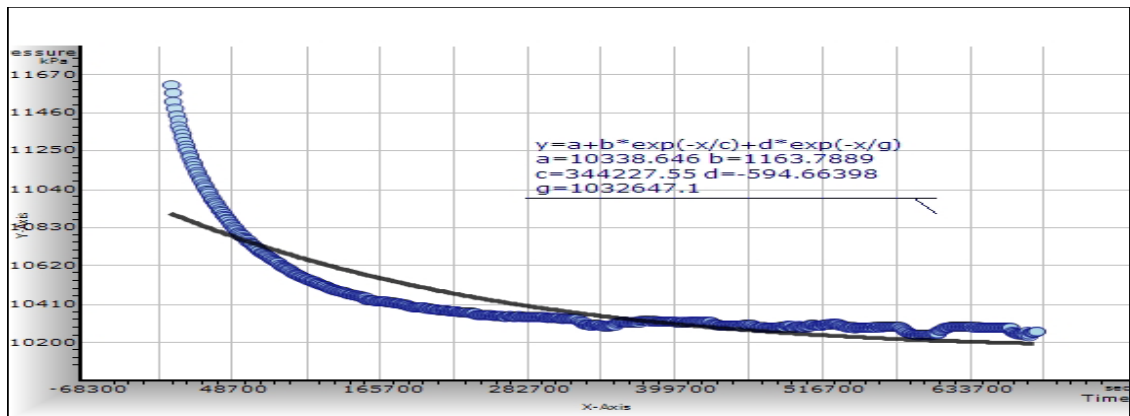


Figure 4.33: Non-linear exponential plot of Angsi gas-Angsi oil at initial pressure of 1719 psi (Test 2) (extracted from FindGraph software)

Table 4.12 compares the diffusion coefficient results from Angsi gas-Angsi oil and methane-Angsi oil systems. The test pressures are different but temperatures are the same for all the four tests. In other words, different pressure set was used for each gas-oil systems. Earlier tests on gas-oil systems from Sumandak field had demonstrated the effect of diffusion coefficient to different hydrocarbon chain length. This is achieved where the diffusion coefficient of the respective pure gas-oil and multicomponent gas-oil were compared at about the same test pressures and temperatures. The same effect was not investigated again for the gas-oil systems from Angsi.

Table 4.12: Diffusion coefficient values for Angsi gas-oil system at different pressures

Gas	Liquid	Temperature	Initial pressure	Dab ( $10^{-9}$ m <sup>2</sup> /s)	
		(° C)	(psia)	Graphical	Numerical
Angsi produced gas	Angsi oil (4.73 cP)	90	1571	2.16	1.25
Angsi produced gas	Angsi oil (4.73 cP)	90	1719	3.69	1.34
CH <sub>4</sub>	Angsi oil (4.73 cP)	90	967	1.79	1.30
CH <sub>4</sub>	Angsi oil (4.73 cP)	90	1289	3.18	1.69

For the multicomponent gas-oil systems, it is observed generally that diffusivities are higher at higher pressures. Nonetheless, when compared, the diffusivity of multicomponent gas in oil at a higher initial pressure of 1571 psia seemed to be slightly lower than the pure gas-oil system which has a lower initial pressure (1289 psia). This is amenable since diffusivity decreases as hydrocarbon chain length increased as in a multicomponent gas (Wise and Houghton, 1966). Interestingly, the diffusivity of multicomponent gas in oil at initial test pressure of 1719 psia when compared to the pure gas-oil system at 1289 psia showed some result inconsistencies. In graphical analysis, the diffusion coefficient is higher in multicomponent gas-oil system. However, using numerical analysis, the contrary is found. This inconsistency is not observed in Sumandak's results in Table 4.11 earlier.

One possible explanation on this inconsistency might be due to the higher impurities in the multicomponent gas (produced gas) from Angsi as compared to Sumandak field. Impurities here relate to the composition of methane in the multicomponent gas. Pure methane gas used in this research has an almost 99.9% purity, while in Sumandak's multicomponent gas, methane dominated the gas composition at 96 wt% which is near purity while Angsi's methane composition is only 75 wt%. Hence, Angsi is considered only slightly diverted from a pure gas. The mathematical model adopted from Zhang *et al.* (2000) assumed that the gas phase is pure (single component) gas. This model may be applicable for multicomponent gas-oil systems from Sumandak since methane dominated the gas compositions at 96 wt%, which may be considered as nearly pure gas. The deviation from the pure gas system may explain on the unsuitability of Zhang's model to the multicomponent gas-oil systems from Angsi.

## CHAPTER 5

### CONCLUSIONS AND RECOMMENDATIONS

#### 5.1 Conclusions

From the gas diffusivity experiments, conclusions that can be made are as follows:

- *Diffusivity of Pure Gas-Water System*

A pure gas that is not reactive to the water need to be chosen in the evaluation of a molecular diffusion system. A chemical reaction or turbulence condition does not agree with the concept of molecular diffusion which assumes zero convection.

- *Diffusivity of Pure Gas-Oil System*

Based on the encouraging diffusion coefficients from the methane-oil systems, it might be relevant to consider mathematical model by Zhang *et al.* (2000) for gas-oil diffusivity measurement for Malaysian oilfield with the sampled oil viscosity range from 4.73 – 10.40 cP which can be considered light to medium oil. The diffusion coefficients of both the methane-Sumandak oil and methane-Angsi oil are in the same order of magnitude (i.e.:  $10^{-9}$  m<sup>2</sup>/s) as per the published methane-oil systems. The effects of gas-liquid diffusivity to the pressure, temperature and oil compositions were also investigated. Pressure was shown to have different effect at different type of crude oil. Oil compositions which are closely linked to the oil viscosity showed the expected behavior in which gas diffusivity is lower at higher oil viscosity. Temperature, on the other hand demonstrated a contradicting behavior than the published work which may be due to stronger influence of the test pressure since the test pressures were not exactly similar.

- *Diffusivity of Multicomponent Gas-Oil System*

Based on the diffusion coefficients of the multicomponent gas-oil systems, the mathematical model by Zhang *et al.* (2000) can be considered relevant in such systems up to a certain extent. The factor of gas composition plays a role in determining the model's suitability in evaluating a multicomponent gas-oil's diffusivity. Since Zhang's model was developed based on using pure gas as the assumption, this model was found to be not suitable for a gas phase which has lower compositions of methane. Produced hydrocarbon gas from oilfields is generally methane dominated. A produced gas system which resembled a pure gas state (e.g.: more than 96 wt% methane as in Sumandak) was found to be more suited for Zhang's mathematical model. In future experiments, it is recommended to analyze the produced gas's composition prior to adopting Zhang's model in determining the diffusion coefficient of a gas-liquid system.

## **5.2 Recommendations**

The following recommendations are suggested for future research work:

- More gas-liquid diffusivity experiments using oil samples from other Malaysian oilfields to be conducted. This will provide wide range of crude oil viscosity and hence, some correlations can be made specifically for Malaysian oil systems.
- Oilfields having > 96% of methane in its gas compositions may be good candidates if the mathematical model by Zhang *et al.* (2000) is adopted.



## REFERENCES

- Abd Manap A.A., Chong M.O., Mat Sai R., Zainal S., Yahaya A.W. and Othman M.  
“Evaluation of Alkali-Surfactant Effectiveness by Single Well Pilot in a  
Malaysian Offshore Field Environment”, paper SPE 144150, presented at SPE  
Enhanced Oil Recovery Conference 2011, Kuala Lumpur, Malaysia, 19 - 21  
July 2011
- Ahmad T., *Reservoir Engineering Handbook*, 3rd Edition, Gulf Professional  
Publishing, 77-80, 2001
- Atkins P.W., *Elements of Physical Chemistry*, 3rd Edition, Oxford University Press,  
114, 1993
- Bardon C. and Denoyelle L., “CO<sub>2</sub> Injection to Enhance Heavy Oil Recovery”, In:  
Okandan, E. (Ed.), *Heavy Crude Oil Recovery*, Martinus Nijhoff Publishers,  
The Hague, 196-200, 1984
- Berry Jr. V.J. and Koeller R.C., “Diffusion in Compressed Binary Systems”, *American  
Institute of Chemical Engineers Journal*, 6(2), 274-279, 1960
- Bird R.B., Stewart W.E. and Lightfoot E.N., *Transport Phenomena*, John Wiley &  
Sons, New York, Chapter 16, 1960
- Burger J.E. and Mohanty K.K., “Mass Transfer from Bypassed Zones During Gas  
Injection”, paper SPE 30768, presented at Annual Technical Conference and  
Exhibition, Dallas, Texas, USA, October 1995
- Caudwell D.R., Trusler J. P. M., Vesovic V. and Wakeham W. A., “The Viscosity and  
Density of n-Dodecane and n-Octadecane at Pressures up to 200 MPa and  
Temperatures up to 473 K”, *International Journal of Thermophysics*, 25, 1339-  
1352, 2004
- Civan F. and Rasmussen M.L., “Improved Measurement of Gas Diffusivity for  
Miscible Gas Flooding under Non-equilibrium vs. Equilibrium Conditions”,  
paper SPE 75135 presented at Tulsa Oklahoma, 2002

- Civan F. and Rasmussen M.L., “Determination of Gas-Diffusion and Interface-Mass-Transfer Coefficients for Quiescent Reservoir Liquids”, *SPE Journal*, 71-79, 2006
- Codeon, *Technical Manual on Transient Wellbore Dynamics*, 2002
- Coulson J.M and Richardson J.F., *Fluid Flow, Heat Transfer and Mass Transfer*, Pergamon Press, Oxford, Vol 1, 4<sup>th</sup> Edition, 446-500, 1990
- Dawson R., Khoury F. and Kobayashi R., “Self Diffusion Measurements in Methane by Pulsed Nuclear Magnetic Resonance”, *American Institute of Chemical Engineers Journal*, 16(5), 725-729, 1970
- Denoyelle L. and C. Bardon C., “Influence of Diffusion on Enhanced Oil Recovery by CO<sub>2</sub> Injection”, *Proceedings International Symposium on CO<sub>2</sub> Enhanced Oil Recovery*, Budapest, Hungary, March 1983
- Denoyelle L. and Bardon C., “Diffusivity of Carbon Dioxide into Reservoir Fluids”, 86<sup>th</sup> Annual Congress, Canadian Institute of Mining and Metallurgy, Ottawa, April 9, 1984
- Dickson K.B. and Johnson J.P., “Measurement of Nitrogen Diffusion into Ekofisk Chalk”, *Philips Petroleum Company Drilling and Production Division*, Bartlesville, OK, July 1988, 34, 1988
- Dusseault M.B., “Comparing Venezuelan and Canadian Heavy Oil and Tar Sands”, *Petroleum Society’s Canadian International Petroleum Conference 2001*, June 12 -14, Calgary, Canada, 16, 2001
- Eyring H., *Journal of Chemical Physics*, Vol. 4, 283, 1936
- Firoozabadi, A., Hekim, Y., and Katz, *The Canadian Society of Chemical Engineering*, 56, 80 -85, 1978
- Fjelde I., Zuta J. and Duyilemi O.V., “Oil Recovery from Matrix during CO<sub>2</sub>-Foam Flooding of Fractured Carbonate Oil Reservoirs”, paper SPE 113880 presented at SPE Europe/EAGE Conference and Exhibition, 9 – 12 June 2008
- Gavalas G.R., Reamer H.H. and Sage B.H., “Diffusion Coefficients in Hydrocarbon System”, *Fundamentals*, 7, 306, 1968
- Halbaek M., Hafskjold B., Dysthe D.K. and Sorland G.H., “Self diffusion coefficients of methane or ethane mixtures with hydrocarbon at high pressure by NMR”, *Journal of Chem. Engineering Data*, 41, 598-603, 1996

- Hassan A.R and Kabir C.S., “Modelling Changing Storage During a Shut-In test”, paper SPE 24717 presented at SPE Formation Evaluation, 279-284, December 1994
- Hill E.S. and Lacey W.N., “Rate of Solution of Propane in Quiescent Liquid Hydrocarbons”, *Industrial Engineering Chemical*, 26(2), 1324-1327, 1934
- Hines A.L and Maddox R.N., *Mass Transfer: Fundamentals and Applications*, Prentice Hall International Series, 17-60, 1985
- Incropera F.P. and DeWitt D.P., *Fundamental of Heat and Mass Transfer*, Wiley, 784-818, 1996
- Jamialahmadi M., Emadi M. and Muller-Steinhagen H., “Diffusion Coefficients of Methane in Liquid Hydrocarbons at High Pressure and Temperature”, *Journal of Petroleum Science and Engineering*, Vol 53, No. 1-2, 46-60, 2006
- LeGallo Y., LeRomancecer J.F. and Bourbiaux B., “Mass Transfer in Fractured Reservoirs During Gas Injection: Experimental and Numerical Modeling”, paper SPE 38924, Texas, 1997
- Lo H.Y., “Diffusion Coefficients in Binary Liquid n-Alkanes Systems”, *Journal of Chemical Engineering Data*, 19 (3), 239-241, 1974
- McKay W.N., “Experiments Concerning Diffusion of Multicomponent Systems at Reservoir Conditions”, *Journal of Canadian Petroleum*, 10 (April-June), 25-32, 1971
- Morgenroth H. and Wallmann G., “Transient Well Performance Modeling - Adding the Time Dimension to Well Performance”, *Helix RDS Annual Technology Bulletin*, 2005
- Munroe N.D.H, Bravo M.C and Gill P.K.S., “Advances in Heavy Oil Recovery”, presented at 5th International Latin American and Caribbean Conference for Engineering and Technology (LACCEI), 29 May – 1 June 2007
- Nadeson G., Anua N.A., Singhal A. and Ibrahim R. “Water Alternating Gas (WAG) Pilot Implementation, A First EOR Development Project in Dulang Field, Offshore Peninsular Malaysia”, paper SPE 88499, presented at SPE Asia Pacific Oil and Gas Conference and Exhibition, Perth, Australia, 18 – 20 October 2004
- Nguyen T.A. and Farouq Ali S.M., “Role of Diffusion and Gravity Segregation in Oil Recovery by The Immiscible Carbon Dioxide WAG Process”, UNITAR

- International Conference on Heavy Crude and Tar Sands, February 12-17, Houston, TX., 393-403, 1995
- Perry, R.H., Green, D.W. and Maloney, J.O., *Perry's Chemical Engineering Handbook*, 7<sup>th</sup> Edition, McGraw-Hill, 2-40, 1997
- Ping G., Zhuohua W., Pingping S. and Jianfen D., "Molecular Diffusion Coefficients of the Multicomponent Gas-Crude Oil Systems under High Temperature and Pressure", *Industrial Engineering Chemical Res.*, 48, 9023-9027, 2009
- Reamer H.H., Duffy C.H. and Sage B.H., "Diffusion Coefficients in Hydrocarbon Systems: Methane-Pentane in Liquid Phase", *Industrial Engineering Chemical*, 3,54, 1958
- Renner, T.A., "Measurement and Correlation of Diffusion Coefficients for CO<sub>2</sub> and rich-gas applications", *SPE Reservoir Engineering*, 517-523, May 1988
- Riazi M.R. and Whitson C.H., "Estimating Diffusion Coefficients of Dense Fluids", *Industrial Engineering Chemical Res.*, 30, 3081-3088, 1993
- Riazi M.R., Whitson C.H. and da Silva F., "Modeling of Diffusional Mass Transfer in Naturally Fractured Reservoirs", *Journal of Petroleum Science Engineering*, 10, 239-253, 1994
- Riazi M.R., "A New Method for Experimental Measurement of Diffusion Coefficients in Reservoir Fluids", *Journal of Petroleum Science and Engineering*, 14, 235-250, 1996
- Rutten Ph. W. M., *Diffusion in Liquid*. Delft University Press, 27 – 31, 1992
- Sachs W., "The Diffusional Transport of Methane in Liquid Water: Method and Result of Experimental Investigation at Elevated Pressure", *Journal of Petroleum Science and Engineering*, 21, 153 – 164, 1988
- Sheng J.J., "Foamy Oil Flow in Porous Media", PhD Thesis, University of Alberta, Canada, 1996
- Schmidt T., "Mass Transfer by Diffusion", In: Hepler, L.G., His, C (Eds.), *AOSTRA Technical Handbook on Oil Sands, Bitumen and Heavy Oils*. Alberta Oil Sand Technology and Research Authority, Edmonton, Canada, 311-332, 1989
- Sigmund P.M., "Prediction of Molecular Diffusion at Reservoir Conditions. Part 1 – Measurements and Prediction of Binary Dense Gas Diffusion Coefficients", *Canada Journal Petroleum Technology*, April – June 1976
- Upreti S.R and Mehrotra A.K., "Diffusivity of CO<sub>2</sub>, CH<sub>4</sub>, C<sub>2</sub>H<sub>6</sub> and N<sub>2</sub> in Athabasca Bitumen", *Canada Journal Chemical Engineering*, 80, 116-125, 2002

- Welty J.R, Wicks C.E. and Wilson R.E., “Fundamentals of Momentum, Heat and Mass Transfer”, 3<sup>rd</sup> Edition, 472-500, 1984
- Whitson C.H. and Brule M.R., *Phase Behavior*, SPE Monograph Series, 1<sup>st</sup> Edition, 20, 4-40, 2000
- Wise D.L. and Houghton G., “The Diffusion Coefficients of Ten Slightly Soluble Gases in Water at 10 – 60°C”, *Chemical Engineering Science*, Pergamon Press, Oxford, Vol. 21, 999–1010, 1966
- Woessner E., Snowden B.S., George R.A. and Melrose J.C., “Dense Gas Diffusion Coefficients for the Methane-Propane System”, *Industrial Engineering Chemical Fund.*, 8 (4), 780-787, 1969
- Zainal S., Abd Manap A.A., Abd Hamid P., Othman M., Chong M.O., Yahya A.W.,... Mat Sai R. “Offshore Chemical EOR: The Role of an Innovative Laboratory Program in Managing Result Uncertainty to Ensure the Success of a Pilot Field Implementation”, paper SPE 113154, presented at SPE Europec/EAGE Annual Conference and Exhibition 2008, Rome, Italy, 9 – 12 June 2008
- Zainal S., Hon V.Y. and Saaid I.M., “Gas Diffusivity Measurement in Reservoir Fluid at Elevated Pressures Systems for Transient Shut-in Modeling”, paper SPE 139004, presented at Offshore Europe 2011, Aberdeen, U.K, 6 – 8 September 2011
- Zhang Y.P, Hyndman C.L and Maini B.B., “Measurement of Gas Diffusivity in Heavy Oils”, *Journal of Petroleum Science and Engineering*, 25, 37-47, 2000

APPENDIX A: SAMPLE PREPARATION, TEST PROCEDURES AND  
EQUIPMENT DESCRIPTION

**A.1 Gas Sample Preparation**

**a) Well Head Sample - Collection**

1. The wellhead gas sample is collected via 1L gas sampling cylinder. The sampling pressure and temperature during site sampling are recorded.
2. The cylinder is checked for any contamination once it reached the lab. See the Quality Check Procedure (A.3).
3. For acquiring the gas volume for the test, the gasometer is used to flash the gas sample. The gas sample will be directly transferred to a transfer cylinder before being transferred to a High Pressure Chamber located in the PVT unit. During this time, the sample has been pressurized up to the desired pressure or test pressure.

**b) Gas Separator Sample - Collection**

1. The separator gas sample is collected via 20L gas sampling cylinder.
2. The gas cylinder is checked for any contamination once it reaches the lab. See the Quality Check Procedure (A.3).
3. The gas sample in the cylinder is heated up by using a heating coil until it reached the separator temperature. The temperature varies depending on the sampling condition.
4. The gas sample is then placed into a transfer cylinder before being transferred to a high pressure gas chamber located in the PVT unit. During this time, the gas has been pressurized up to the desired pressure or test pressure.

**c) Well Head and Separator Gas Sample - Compositional tests**

After the desired gas has been collected via the above procedures, about 300 cc of the gas sample is sent to the Gas Chromatograph (GC) (i.e.: Natural Gas Analyzer) to determine the gas composition.

**A.2 Liquid/Oil Sample Preparation**

**a) Well Head Sample - Collection**

1. The liquid/oil sample is collected via polycarbonate sampling bottle (i.e.: that can withstand high temperature).
2. The oil sample for test will be directly taken from the bottle.

**b) Separator Sample - Collection**

1. The sample is collected via 629 ml or 700 ml oil cylinder.
2. The cylinder is checked for any contamination once it reaches the lab. Please refer to the Quality Check Procedure (A.3)
3. Gasometer is then used to obtain the oil sample.

**c) Well head and Separator Oil Sample – Compositional analysis, viscosity and density tests**

The compositions for the liquid/oil can be determined using the High Temperature Gas Chromatography (HTGC) (for liquid/oil sample). The viscosity of the liquid/oil can be determined by either using dynamic viscosity or kinematic viscosity method.

- Dynamic viscosity test is conducted using HAAKE Viscometer. Around 8.2 ml of sample is required when using spindle Z-20 for viscosity range up to 1000 cP.
- Kinematic Viscosity Test is conducted using ASTM D445 method.

### A.3 Quality Check Procedure for Gas and Oil Sample

1. Place the sampling cylinder in vertical upright position in which the glycol is located at the top while the sample at bottom. Leave it for 1 day.
2. Check the opening pressure by attaching the hand pump to the glycol. Note this pressure. The purpose is to check for any leakage. This is the 1st leak test.
3. Heat the sampling cylinder for 6 hours up to the sampling temperature by placing heating coil around the cylinder. The heating coil is connected to the hot water bath
4. Check the opening pressure again by comparing the opening pressure to the sampling pressure and temperature. This is the 2nd leak test.
5. Drain mud, water and any other contamination (ullage) from the sampling cylinder until only one phase sample is acquired (i.e.: either oil or gas, depends on the targeted sample type in cylinder)
6. At the sampling temperature and pressure condition, agitate the sampling cylinder (using 'rocker) for about 4 - 6 hours to acquire a homogenized sample. At this time, the cylinder is always connected to the hand pump to check for cylinder pressure. If the cylinder pressure (at any time) falls below the sampling pressure, the sample is pressurized again using the hand pump.
7. To determine the bubble point pressure ( $P_b$ ) of the sample, (applicable to oil cylinder only), pressurized the sample up to 1500 psi. Then, slowly reduce the pressure until there is no pressure change. At this point, the  $P_b$  is achieved. Note this  $P_b$  and compare it to the sampling pressure. Both pressures should be about the same to indicate that there is no leakage observed.
8. After all these steps, the best fluid sample can then be chosen for further tests (i.e.: those without contamination and leakage). The chosen sample will be flashed using the gasometer.



## A.4 Gas Diffusivity Experimental Procedure

### a) Equipment Preparation

1. The equipment that is used for Gas Diffusivity Test is PVT-2 unit.
2. Clean up the PVT cell with dichloromethane (DCM). Replace the piston O-ring with HNBR type if using corrosive sample (i.e.: CO<sub>2</sub> gas) or Viton type if other. Ensure also that the back-up ring at the top cap and bottom cap of the PVT glass are in good condition.
3. Set up the equipment as follows:

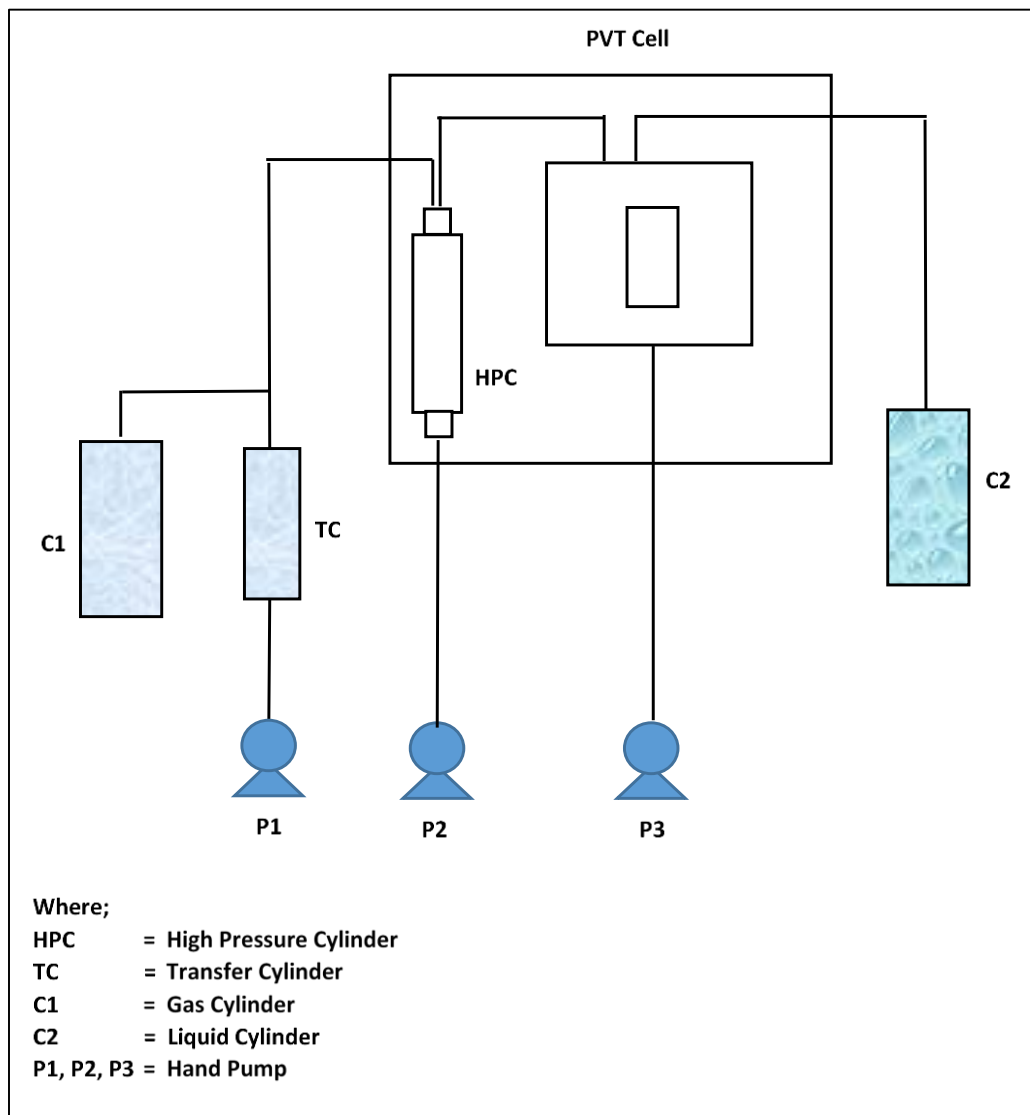


Figure A.1: Set up of the PVT-2 equipment for sample transfer

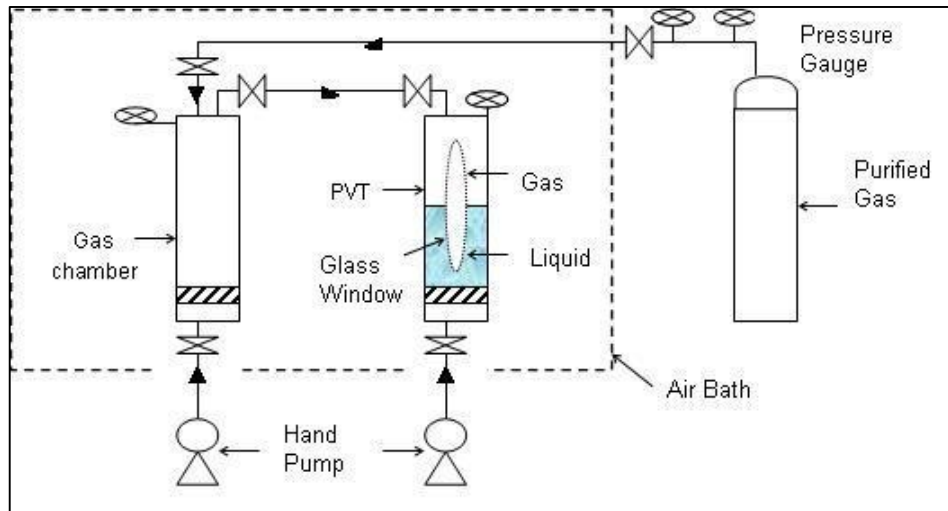


Figure A.2: Schematics of the diffusivity test set-up

4. Heat up the oven up to the test temperature.
5. Ensure the oven has reached the test temperature and this temperature is stabilized.
6. At atmospheric pressure and test temperature, by using hand pump, push the piston in PVT cell up to 0 cc mark (top most piston position).
7. Fill in gas (any type of non-flammable gas) at test pressure and pressurized the PVT cell until the position reached a level/position that gives 100 cc total volumes. Mark this piston position.
8. At this point, close the inlet valve to the PVT cell and lock the hand pump.
9. Make sure all the valves are connected. Check all the valves to avoid any leakage. Special liquid soap, ‘Snoop’ Soap is used to check the valve connection. This is important to ensure that the analysis is running smoothly.
10. Vacuum out the gas that has been injected for at least 30 minutes. Now the piston will move to the top at the 0cc mark and thus, there is no more gas sample in the PVT cell.

11. Gas sample (from transfer cylinder) is now transferred to the High Pressure Chamber that is placed inside the oven. Pressurize further the gas chamber by using the hand pump until the pressure reached the test pressure. The sample gas (in gas chamber) is now ready for the diffusion test.
12. For the oil/liquid well head sample, the sample is transferred into the PVT cell after connecting the transfer cylinder to the injection point outside the oven.
13. For the oil/liquid separator sample, the sample is heated up to the separator sample or above the bubble point temperature. The cylinder is then connected to the injection point outside the oven before being transferred into the PVT cell.

**b) Setting-up Software for Gas Diffusivity Test**

1. The software that is used is LABVIEW Software from National Instrument (NI)
2. Ensure that the software is in STOP condition. Note that, the STOP button is in green color.
3. Select <Configuration and Setting File Name>.
4. Select <Insert Descriptor> <Dev1> - for pressure device
5. Select <Insert Descriptor> <Dev2-ai0> - for temperature device
6. Choose the 'delay time' desired to capture data. For example, if the data is required in every 5 second, key in the delay time as 5 seconds.
7. Type in the file name in the <New File Path> box.
8. Set <Time> for 24 hours auto filling.
9. Select pressure and temperature units.
10. Reset the file number to "0" when <Stop data acquisition> button is in green color.

11. Go to <Chart Management Display> and put a file name under a specific file name for real time chart capturing.
12. Click (→) button to start the test. Note that, it is important to make sure that <Stop data acquisition> button is in green color.

**c) Running the Diffusivity Test**

1. Fill in the pressurized/sample gas into the PVT cell until the piston position reached the marked level of 100 cc or until the pressure indicator showed the highest pressure after gas is released. Slowly transfer this gas to avoid turbulence at the interface.
2. Close the inlet and outlet valve of the PVT cell.
3. Reset the time to zero (0).
4. Immediately, record the height of the piston bottom and interface position and observe the pressure in the PVT cell through the digital interface on the PVT-2 equipment. It is important to note the initial pressure after the sample gas has been fully released. The initial pressure is the highest pressure observed after the gas is released.
5. Continue the test as follows. Monitor and record the pressure, temperature, interface position and piston bottom position at:
  - a. Every 30 seconds for 30 minutes
  - b. Every 1 minute for 30 minutes
  - c. Every 5 minutes for 60 minutes
  - d. Every 30 minutes for 120 minutes, and
  - e. Every one (1) hour until 24 hours or more whenever  $\Delta P = 0$ .

(Note: The recording interval depends on each test requirement)

6. The test will be running until equilibrium is reached. This means that no pressure change is observed. The test period depends on each gas-liquid sample equilibrium state. The data will be taken every 5 seconds automatically by the computer. (This depends on the software settings that have been set earlier).

The data will be recorded until the end of the test period. The computer will record important information such as time, temperature and pressure data.

7. At the same time, record the data manually to observe the trend of the data. This process is continued until the test is terminated.
8. Caution: Note that, it is required to have a full 24-hour supervision of this test as it is running at high temperature and pressure.

## A.5 Equipment Description

Table A.1: Diffusivity equipment description

Equipment	PVT cell	PVT glass	Gas chamber	Hand pump	Gas cylinders
<b>Brand Name</b>	Oilphase-DBR	Pyrex	Proserve (Petrotech)	Jefri	Concoa
<b>Model No.</b>	DBR PVT 150-100-200-286-155	<i>(no information)</i>	Prolight Ti-690-64 MB	500-1-10-HB	MOX/Linde Compressed
<b>Manufacturer</b>	Schlumberger DBR	Schlumberger DBR	Proserve	Schlumberger DBR	MOX Gases Bhd
<b>Pressure Rating</b>	Max; 10000 psi (68.9 Mpa, 700 bar)	Pressure PVT cell & overburden < 10000 psi	Max: 12690 psi/875 bar g	Max: 10000 psi	Max: 1000 psi, Max: 4000 psi
<b>Temperature Rating</b>	Max: 200 °C (392 °F)	Max: 200 °C (392 °F)	<i>(no information)</i>	Operating: 0 °C to 40 °C	<i>(no information)</i>
<b>Material Specification</b>	A-286 Stainless Steel, 15% Cr, 5% Ni precipitation, hardened alloy steel	Glass Pyrex	Titanium	Cylinder: 316 SS, Piston: 316 SS, Piston Coating: Colmonoy, Cylinder Gland Nut: Plated Alloy Steel, Gland Follower: 316 SS	<i>(no information)</i>

## APPENDIX B: FINDGRAPH SOFTWARE AND SAMPLE CALCULATIONS

### B.1 FindGraph - How to take the points from the clipboard

Below are the steps:

1. In Microsoft Excel, select related cells and select menu item <Edit><Copy>.
2. In FindGraph, select menu item <Data><Paste Points.>. Make sure that the pressure unit is in kPa.
3. The Wizard of Creation starts.
4. Follow 4 steps of 4.
5. It creates new series of points with current color and marker.
6. Series, named 'Data from Clipboard', appear in list.

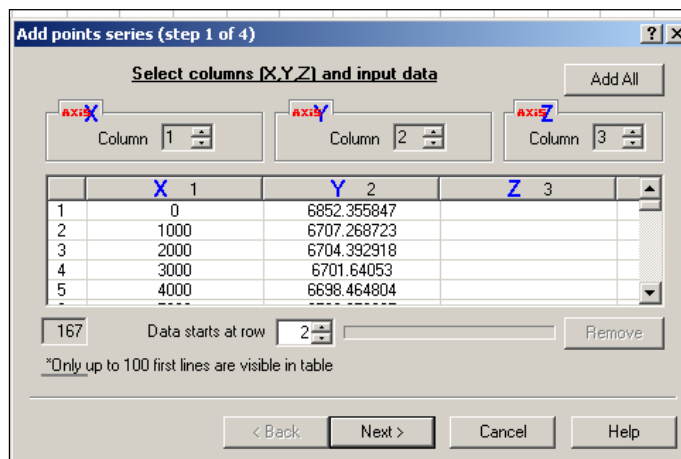


Figure B.1: Plotting in FindGraph step 1

### B.2 FindGraph - How to fit functions on series data points.

Follow these steps to fit functions on series data points:

1. To select series of points in list, click on it.
2. Select menu item <Fit><Functions on series data point>.
3. The Wizard starts (Step 1 of 6).

4. On a step 1 choose X and Y ranges. Press 'Next'.

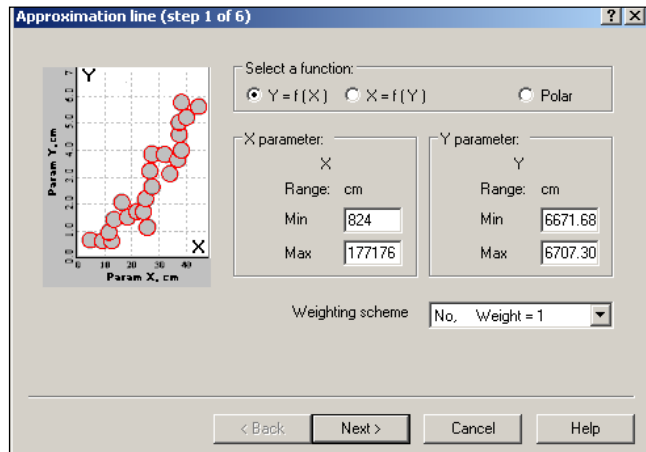


Figure B.2: Plotting in FindGraph step 2

5. On a step 2 chose functions. Select <Nonlinear>. Press 'Next'.

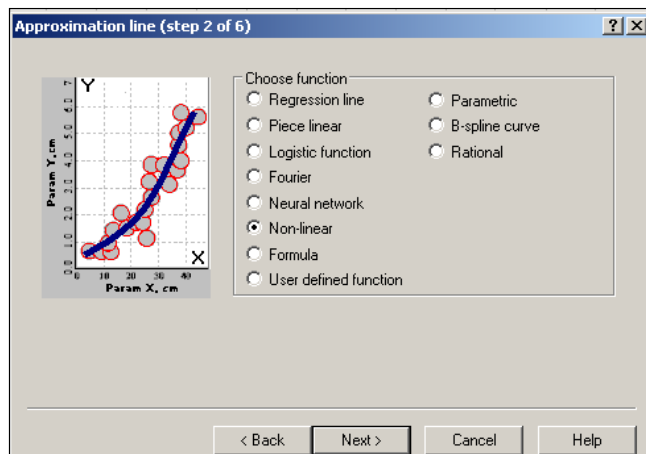


Figure B.3: Plotting in FindGraph step 3

6. On a step 3, select family <Exponential>, Functions <ExpDecay 5> and method <Simple>.

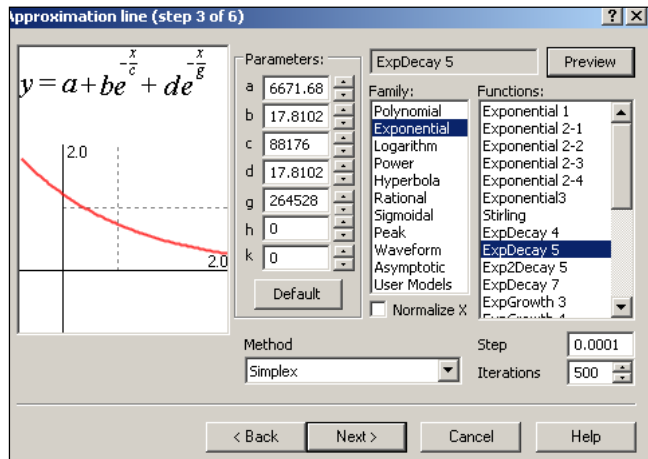


Figure B.4: Plotting in FindGraph step 4

- On a step 4, fixed the value for 'a' that is equivalent to  $P_{eq}$  from the formula that we already know from the experiment. Press <Recalc> to find a best fit on the graph and less error of the estimation.

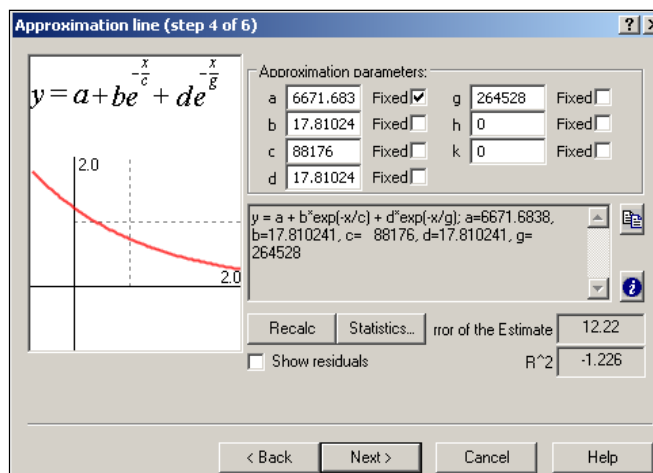


Figure B.5: Plotting in FindGraph step 5

- After recalculate, error of the estimation reduces from 12.22 to 3.77 and  $R^2$  of 0.7882. Press <Next>.



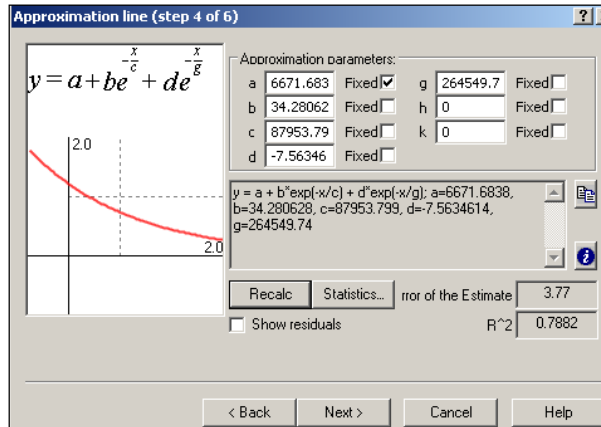


Figure B.6: Plotting in FindGraph step 6

9. On a step 5, select color and width of line. Press <Next>. Then press <Finish>.

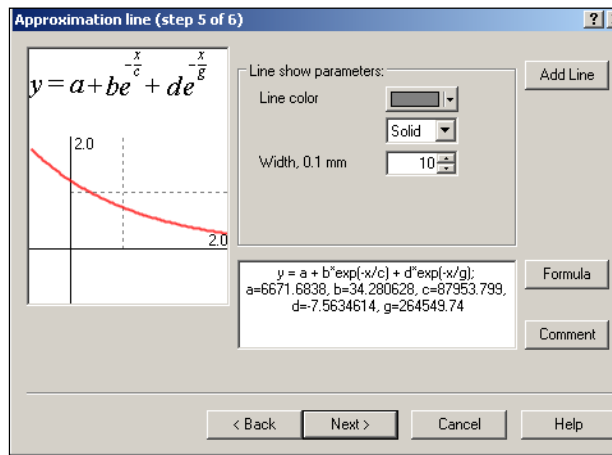


Figure B.7: Plotting in FindGraph step 7

10. Approximation line was build.

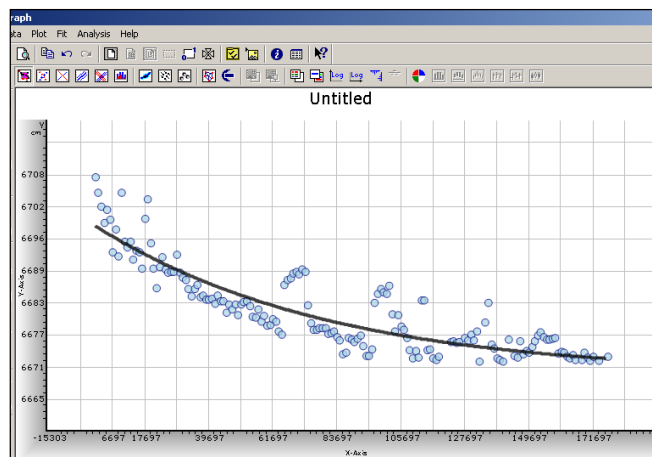


Figure B.8: Plotting in FindGraph step 8

The equation is:

$$y = a + b \exp\left(-\frac{x}{c}\right) + d \exp\left(-\frac{x}{g}\right) \quad (\text{B.1})$$

Where:  $a = 6671.6838$ ,  $b = 34.280628$ ,  $c = 87953.799$ ,  $d = -7.5634614$ ,  $g = 264549.74$

The value  $c$  is equivalent to  $k_I$  that was used to calculate  $D_{AB}$  in numerical method.

### B.3 Sample Calculation using Numerical Method

In continuation of section B.2 above, below is the sample calculation to determine the diffusion coefficient ( $D_{AB}$ ) using numerical method. Figure B.9 shows an example of a non-linear exponential plot. This plot was generated from the FindGraph software utilizing all the pressure versus time data. The unit of time is in seconds.

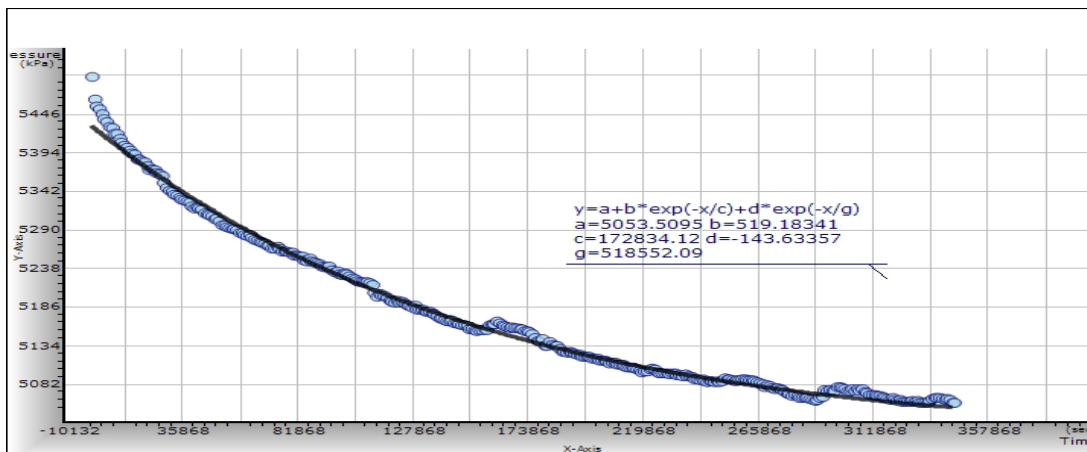


Figure B.9: Example of non-linear exponential plot

Equation B.2 (similar to Equation 3.11 in Chapter 3) was used as a basis and input to the software.

$$P(t) = m_1 \exp\left(-\frac{t}{k_1}\right) + m_2 \exp\left(-\frac{t}{k_2}\right) + P_{eq} \quad (\text{B.2})$$

An exponential function that represent Equation B.2 was then chosen from the list given in FindGraph. This chosen function is per Equation B.1. There are two values that are most important in this function which are  $a$  and  $c$  which represent  $P_{eq}$  and  $k_l$ . These values are automatically derived by the software based on the chosen exponential function. Equation B.3 is then used to calculate  $D_{AB}$ .

$$D_{AB} = \frac{4z_o^2}{k_l \pi^2} \quad (\text{B.3})$$

The value of  $z_o$  is the measured length of the liquid column in the cell and this is obtained from experimental measurement. In this example, the values of  $a = 5053.5095$ ,  $k_l = 172834.12$  and  $Z_o = 0.0334$ . Putting  $z_o$  and  $k_l$  into Equation B.3 yields  $D_{AB}$  of  $2.62 \times 10^{-9} \text{ m}^2/\text{s}$ .

#### B.4 Sample Calculation using Graphical Method

Figure B.10 shows an example of a semi-logarithmic plot. This plot was generated using the calculated  $\ln(P_t - P_{eq})$  versus time data. The unit of time is in seconds.

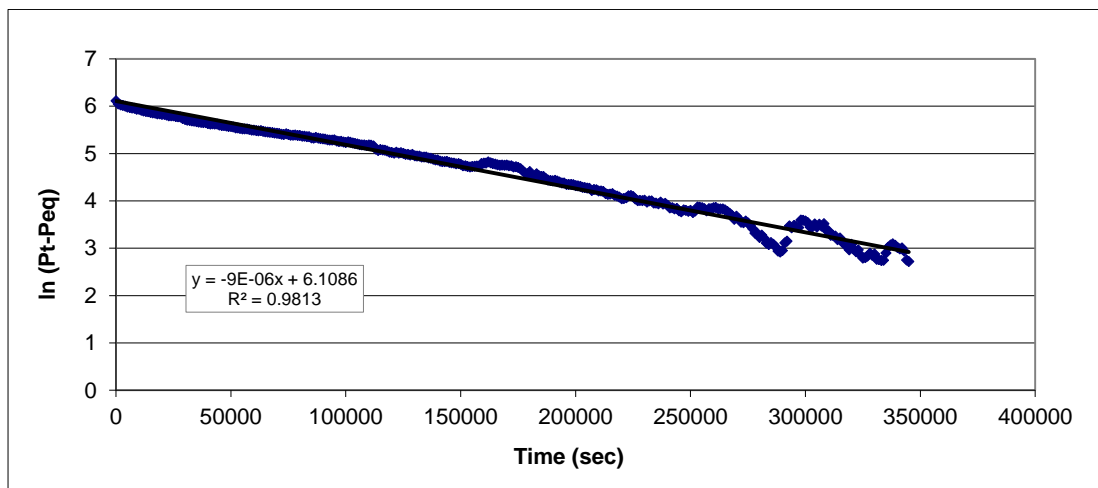


Figure B.10: Example of semi-logarithmic plot

Equations B.4 and B.5 were then used as a basis to determine the diffusion coefficient ( $D_{AB}$ ) using graphical method.

$$\ln[P(t) - P_{eq}] = \ln\left(\frac{8Bz_o x_{1,eq}(P)}{\pi^2}\right) - \frac{\pi^2 D_{AB} t}{4z_o^2} \quad (\text{B.4})$$

In Figure B.10:

$$\begin{aligned} \text{y-axis} &\equiv \ln[P(t) - P_{eq}] \\ \text{x-axis} &\equiv t \\ \text{Slope} &\equiv -\frac{\pi^2 D_{AB}}{4z_o^2} \\ \text{Intercept} &\equiv \ln\left(\frac{8Bz_o x_{1,eq}(P)}{\pi^2}\right) \end{aligned}$$

The value of  $D_{AB}$  can be directly calculated by knowing the slope of the line. From Figure B.10, the linear equation is as follows:

$$y = -9E^{-06}x + 6.1086 \quad (\text{B.5})$$

The slope of the line =  $-9 E^{-06}$  which is equivalent to:  $-\frac{\pi^2 D_{AB}}{4z_o^2}$ . The value of  $D_{AB}$  is then calculated having known the value of  $z_o$  which is 0.0334. Putting the slope value and  $z_o$  yields  $D_{AB}$  of  $4.07 \times 10^{-9} \text{ m}^2/\text{s}$ .

## APPENDIX C: DERIVATION OF MATHEMATICAL MODEL

The mathematical model by Zhang *et al.* (2000) is derived from Equation 3.8 to allow analysis from the pressure-time profile of the diffusion experiment. Following is the derivation approach by Zhang *et al.* (2000).

Equation 3.8 from ‘Section 3: Methodology’ is solved to establish molar concentration as a function of pressure and temperature. This equation becomes:

$$x_1 = x_{1,eq(P)} - \frac{4x_{1,eq(P)}}{\pi} \sum_{n=0}^{\infty} \frac{(-1)^n}{2n+1} \cos\left(\frac{(2n+1)\pi \cdot z}{2z_o}\right) \exp\left(-\frac{(2n+1)^2 \pi^2 D_{AB} t}{4z_o^2}\right) \quad (C.1)$$

In order to describe the diffusion process, material balance is used. For example, if methane is a component in the gas phase, the moles of methane removed from the gas phase must be equal to the moles of methane transferred across the interface. This is expressed in the equation below:

$$\frac{V}{Z_g RT} \frac{dP(t)}{dt} = -D_{AB} A \left( \frac{dx_1}{dz} \right)_{z=z_o} \quad (C.2)$$

Where:

- $V$       $\equiv$      Volume of gas in cell (cm<sup>3</sup>)
- $Z_g$      $\equiv$      Compressibility factor
- $R$       $\equiv$      Gas constant (8314 kPa.cm<sup>3</sup>/mol.K)
- $T$       $\equiv$      Temperature (°C)
- $A$       $\equiv$      Cross-sectional area of the cell (cm<sup>2</sup>)
- $t$       $\equiv$      Time (s)

$x_1$	$\equiv$	initial molar concentration of gas in the oil phase (component 1) (mol/cm <sup>3</sup> )
$D_{AB}$	$\equiv$	diffusion coefficient (m <sup>2</sup> /s)
$z$	$\equiv$	liquid position along the diffusion cell (cm)
$z_o$	$\equiv$	height of the liquid in the cell (cm)

Since the volume of gas in the cell and the cross-sectional area are constant, Equation C.2 is simplified as below:

$$\frac{dP(t)}{dt} = -\frac{Z_g RT}{h} D_{AB} A \left( \frac{dx_1}{dz} \right)_{z=z_o} \quad (C.3)$$

Pressure change resulting from the diffusion process is small, thus, the compressibility factor,  $Z_g$  is assumed a constant. Equation C.3 is integrated as a function of time to get:

$$\int_{P(t)}^{P_{eq}} dP(t) = -BD_{AB} \int_t^{\infty} \left( \frac{dx_1}{dz} \right)_{z=z_o} dt \quad (C.4)$$

Where:

$$B = \frac{Z_g RT}{h} = \text{constant} \quad (C.5)$$

Equation C1.1 is differentiated at  $z = z_o$  and this results in:

$$\left( \frac{dx_1}{dz} \right)_{z=z_o} = \frac{2x_{1,eq}(P)}{z_o} \times \sum_{n=0}^{\infty} \exp\left( -\frac{(2n+1)^2 \pi^2 D_{AB} t}{4z_o^2} \right) \quad (C.6)$$

Putting Equation C.6 into C.4 and integration results:

$$P(t) - P_{eq} = \frac{8Bz_o x_{1,eq(P)}}{\pi^2} \sum_{n=0}^{\infty} \frac{1}{(2n+1)^2} \exp\left(-\frac{(2n+1)^2 \pi^2 D_{AB}}{4z_o^2} t\right) \quad (C.7)$$

Equation C.7 is then rearranged and at large value of  $t$ , the infinite term converged rapidly and this equation is reduced to obtain a clear relationship between pressure and time as per below:

$$\ln[P(t) - P_{eq}] = \ln\left(\frac{8Bz_o x_{1,eq(P)}}{\pi^2}\right) - \frac{\pi^2 D_{AB} t}{4z_o^2} \quad (C.8)$$

Equation C.8 is then used to analyze by plot a semi-logarithmic plot in which:

y-axis	≡	$\ln[P(t) - P_{eq}]$
x-axis	≡	$t$
Slope	≡	$-\frac{\pi^2 D_{AB}}{4z_o^2}$
Intercept	≡	$\ln\left(\frac{8Bz_o x_{1,eq(P)}}{\pi^2}\right)$

An alternate method is to determine  $D_{AB}$  from pressure history. It is based on numerical fitting of the analytical expression that is consistent with Equation C.7. The first two terms from Equation C.7 were used in numerical technique. Based on this, Equation C.9 is derived.

$$P(t) = m_1 \exp\left(-\frac{t}{k_1}\right) + m_2 \exp\left(-\frac{t}{k_2}\right) + P_{eq} \quad (C.9)$$

The values of  $m_1$ ,  $m_2$ ,  $k_1$ ,  $k_2$  and  $P_{eq}$  are determined by the non-linear regression of the experimental pressure-time data. The value of  $D_{AB}$  is then calculated from Equation C.10.

$$D_{AB} = \frac{4z_o^2}{k_1 \pi^2} \quad (C.10)$$

## APPENDIX D: GAS AND CRUDE OIL COMPOSITIONAL ANALYSIS

Table D.1: Sumandak A-14L crude oil compositions

Component	Wt%
IC5	0
NC5	0.034
C6	0.075
C7	0.302
C8	0.643
C9	0.569
C10	1.701
C11	2.786
C12	3.240
C13	4.650
C14	4.005
C15	2.985
C16	3.054
C17	3.154
C18	3.044
C19	2.601
C20	1.968
C21	1.730
C22	2.119
C23	1.410
C24	1.921
C25	2.229
C26	1.415
C27	1.118
C28	0.169
C29	1.440
C30	1.515
C31	2.077
C32	1.487
C33	1.669
C34	2.238
C35	2.526
C36	3.239
C37	4.653
C38	4.222
C39	3.585
C40	3.746
C41	3.378
C42	2.737
C43	4.831
C44	3.968
C45	5.770
<b>Total:</b>	<b>100.000</b>
Component :	<b>C7 +</b>
MW :	313.1
Density (g/cm3) :	0.848



Table D.2: Angsi A-38 crude oil compositions

<b>Component</b>	<b>Wt%</b>
C3	0.252
IC4	0.272
NC4	0.290
IC5	0.404
NC5	0.305
C6	0.826
C7	1.363
C8	1.782
C9	1.392
C10	1.300
C11	0.889
C12	0.869
C13	0.843
C14	0.874
C15	1.118
C16	1.202
C17	1.064
C18	0.978
C19	0.835
C20	0.817
C21	0.948
C22	2.011
C23	2.568
C24	5.149
C25	6.440
C26	10.868
C27	8.649
C28	7.674
C29	9.730
C30	8.224
C31	5.118
C32	7.573
C33	7.374
<b>Total:</b>	<b>100.000</b>
Component :	<b>C7 +</b>
MW :	314.5
Density (g/cm <sup>3</sup> ) :	0.853

Table D.3: Sumandak A-14L gas compositions

Component	Mole %
N2	0.72
CO2	1.86
C1	95.69
C2	1.59
C3	0.09
iC4	0.02
nC4	0.01
iC5	0
nC5	0
C6	0
C7	0.01
C8	0
C9	0
C10	0
C11	0.01
C12+	0
<b>Total:</b>	<b>100.00</b>
Component : <b>Produced gas</b>	
MW (g/gmole) :	16.94
Density (g/cm3) :	0.315

Table D.4: Angsi A-38 gas compositions

Component	Mole %
N2	1.06
CO2	3.58
C1	74.19
C2	9.92
C3	6.35
iC4	2.15
nC4	1.36
iC5	0.00
nC5	0.64
C6	0.35
C7	0.31
C8	0.01
C9	0.00
C10	0.01
C11	0.05
C12+	0.01
<b>Total:</b>	<b>100.00</b>
Component : <b>Produced gas</b>	
MW :	22.7
Density (g/cm3) :	0.357